UNIVERSITY OF ALBERTA
LIBRARY

Regulations Regarding Theses and Dissertations

Typescript copies of theses and dissertations for Master's and Doctor's degrees deposited in the University of Alberta Library, as the official Copy of the Faculty of Graduate Studies, may be consulted in the Reference Reading Room only.

A second copy is on deposit in the Department under whose supervision the work was done. Some Departments are willing to loan their copy to libraries, through the inter-library loan service of the University of Alberta Library.

These theses and dissertations are to be used only with due regard to the rights of the author. Written permission of the author and of the Department must be obtained through the University of Alberta Library when extended passages are copied. When permission has been granted, acknowledgement must appear in the published work.

This thesis or dissertation has been used in accordance with the above regulations by the persons listed below. The borrowing library is obligated to secure the signature of each user.

Please sign below:

Date	Signature	Institution

THE UNIVERSITY OF ALBERTA

"THE DESIGN OF A DIRECT-ACTING FLOW REGULATOR"

BY

WILLIAM J. HILLIER

A THESIS

SUBMITTED TO THE FACULTY OF GRADUATE STUDIES

IN PARTIAL FULFILLMENT OF THE REQUIREMENTS FOR THE

DEGREE OF MASTER OF SCIENCE

IN CHEMICAL ENGINEERING

DEPARTMENT OF CHEMICAL AND PETROLEUM ENGINEERING

EDMONTON, ALBERTA

APRIL 1966

THE UNIVERSITY OF ALBERTA

FACULTY OF GRADUATE STUDIES

The undersigned certify that they have read, and recommend to the Faculty of Graduate Studies for acceptance, a thesis entitled "The Design of a Direct-Acting Flow Regulator" submitted by William J. Hillier, B.A.Sc. in partial fulfillment of the requirements for the Degree of Master of Science in Chemical Engineering.

Abstract

The flow rate of a fluid is normally controlled by inserting a conventional proportional reset flow control system in a pipe line. In some cases, the application does not warrant the precise control that a sophisticated feedback control loop produces. The economic justification can be very difficult for some installations.

Another method of controlling the flow rate of a fluid is by inserting a direct-acting flow regulator. A flow regulator is a self-contained control device which operates on the principle of maintaining a constant pressure drop across an adjustable orifice. Although the control limits increase from $\pm$0.5% of the span for a flow control loop to about $\pm$1.0% of maximum flow for the flow regulator, the cost of the flow regulator is approximately one fifth.

Various designs were built and tested to determine their performance. The present study discusses the development of a flow regulator that has an accuracy of $\pm$1.0% of maximum flow over a range of differential pressures from 50 psi to 150 psi, and flow rates from 1.0 to 10.0 IGPM. The design utilizes a bellows assembly which made it possible to design a regulator that has no sliding parts and is relatively simple to construct.

The flow regulator was simulated on the analog computer for the principal purpose of studying its dynamic characteristics. The frequency response and transient response indicated a very rapid recovery to disturbances of the differential pressure.

ACKNOWLEDGMENTS

The author wishes to express his appreciation for the helpful guidance and encouragement given by Dr. R. A. Ritter, under whose supervision this work was conducted. The co-operation of the Machine Shop personnel is gratefully acknowledged.

The financial support of the National Research Council and the University of Alberta was certainly appreciated.

Table of Contents

List of Tables

List of Figures

Introduction

A common method of controlling the flow of a fluid in a pipe line is to use a feedback flow control system. The flow rate is measured by a metering station which is normally an orifice. The pressure drop across the orifice, which is proportional to the square of the flow rate, is transmitted to a proportional reset controller which sends a corrective signal to a remote control valve. A control system, such as the one described, is so commonly utilized industrially that instrument engineers automatically specify their installations. Its accuracy in maintaining the flow constant is approximately $\pm$0.5% of full scale flow. If one neglects installation and maintenance costs and only considers the initial investment for the flow control loop, the cost of such a control system is approximately $1000.00. The two questions which should be answered before a sophisticated control loop is specified are:

(1) Is an accuracy of $\pm$0.5% of full scale flow required?

(2) Can an investment of more than $1000.00 be justified?

In some cases the installation of a flow control system is extremely difficult to justify.

Another method of controlling the flow rate of a fluid is by installing a self-contained direct-acting flow regulator in the pipe line. A flow regulator operates on

the simple principle that the flow through an orifice under isothermal conditions is related to the pressure differential across the orifice by the expression $Q = C_v\sqrt{\triangle P}$ and can be maintained at any desired level by regulating the pressure differential. The common method of accomplishing this can be explained with reference to Figure 1.

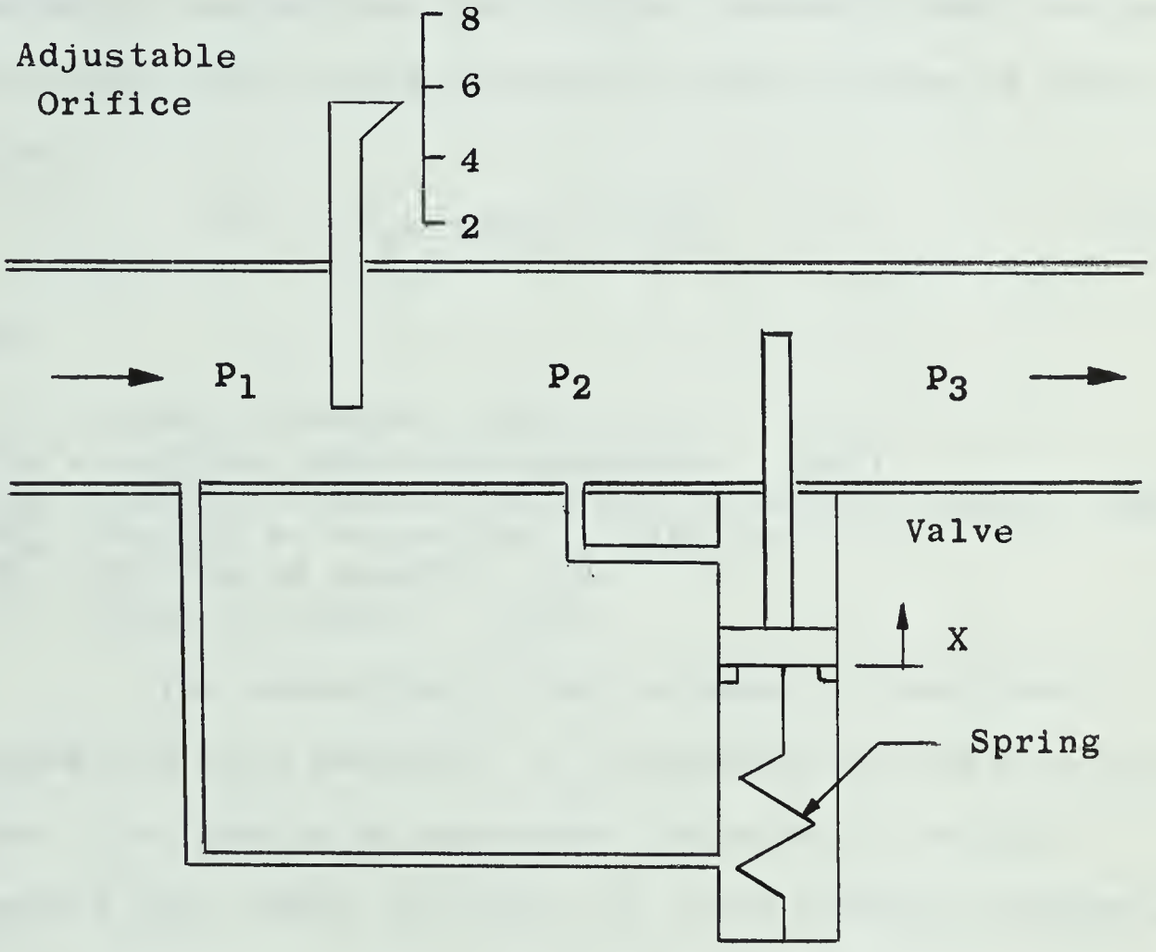

Figure 1

The fluid enters through an adjustable orifice and leaves through a regulating valve. The flow rate is set by opening or closing the orifice to expose more or less flow area.

Once the orifice area is set, variations in line

pressures P_1 and P_3 are compensated for by the regulating valve. As a result, the pressure drop $P_1 - P_2$ remains relatively constant and hence the flow rate also remains relatively constant.

The initial tension on the spring sets the approximate pressure drop that is to be maintained. Regulation begins when the orifice pressure drop reaches this value. The force balance for this system is shown below.

$$(P_1 - P_2) = \triangle P_o + \frac{K_s X}{A} \qquad (1)$$

where

P_1 = inlet pressure (psi)
P_2 = orifice downstream pressure (psi)
$\triangle P_o$ = initial pressure drop due to spring tension (psi)
K_s = spring rate constant (lb_f/in)
X = stroke of piston (in)
A = area of piston (in^2)

The operation is very simple and very fast. Suppose the line pressure, P_1, increases at the regulator inlet. The resulting momentary increase in orifice pressure drop tends to close the valve thereby increasing P_2 and immediately restoring the orifice pressure drop and flow rate to their original values. Since the movement of the valve is proportional to the error in the pressure differential across the orifice, a net change in flow rate must occur. However, this deviation from the desired value may be minimized as will be shown later. The same reasoning

applies to variations in downstream pressure P_3.

The corrective action for a device such as this is extremely fast since the control elements are directly actuated by the pressures of the fluid being controlled. Furthermore, there are no long transmission lines which increase the time lags associated with conventional control systems.

The simplicity of a flow regulator reduces the capital, installation and maintenance costs. The capital cost is about 1/5 of the cost of a flow control system.

An accuracy of about $\pm$1.0% of full scale flow can be expected from a flow regulator. This is slightly higher than the $\pm$0.5% for a flow control loop. However, in some cases this accuracy is adequate.

A survey of commercially available regulators was conducted. A regulator built by the W. A. Kates Company was purchased for evaluation, and information was received concerning a regulator built by the H. B. Franklin Company, Inc.

The aim of this research work was to design a regulator that was more economical, more accurate, and simpler than those which are available at the present time.

Evaluation of Existing Flow Regulators

Kates Flow Rate Regulator

A flow regulating valve built by the W. A. Kates Company of Deerfield, Illinois is available commercially. Information received from them indicated that their regulator would control the flow rate at $\pm 1\frac{1}{2}\%$ of the set point over a pressure differential range of 8 to 125 psi. The flow rangeability of the device was 15 to 1. The performance of the regulator appeared to be excellent and in order to justify the present work, a regulator was purchased for evaluation.

A type MF Kates Flow Rate Regulator, as shown in Figure 2, was the device that was obtained. It has the following specifications:

1) Minimum Flow Rate.....0.2 USGPM
2) Maximum Flow Rate.....3.0 USGPM
3) Maximum Operating Differential Pressure....125 psi
4) Threshold Pressure Differential..... 8 psi
5) Accuracy (based on set flow).....$\pm 1\frac{1}{2}\%$

The threshold pressure differential is that required for the valve to start regulating. The flow rate increases through the regulator with the valve port wide open until the desired flow rate is attained at the threshold differential pressure. Further increases in pressure differential actuate the valve which in turn tends to keep the orifice pressure drop constant. The

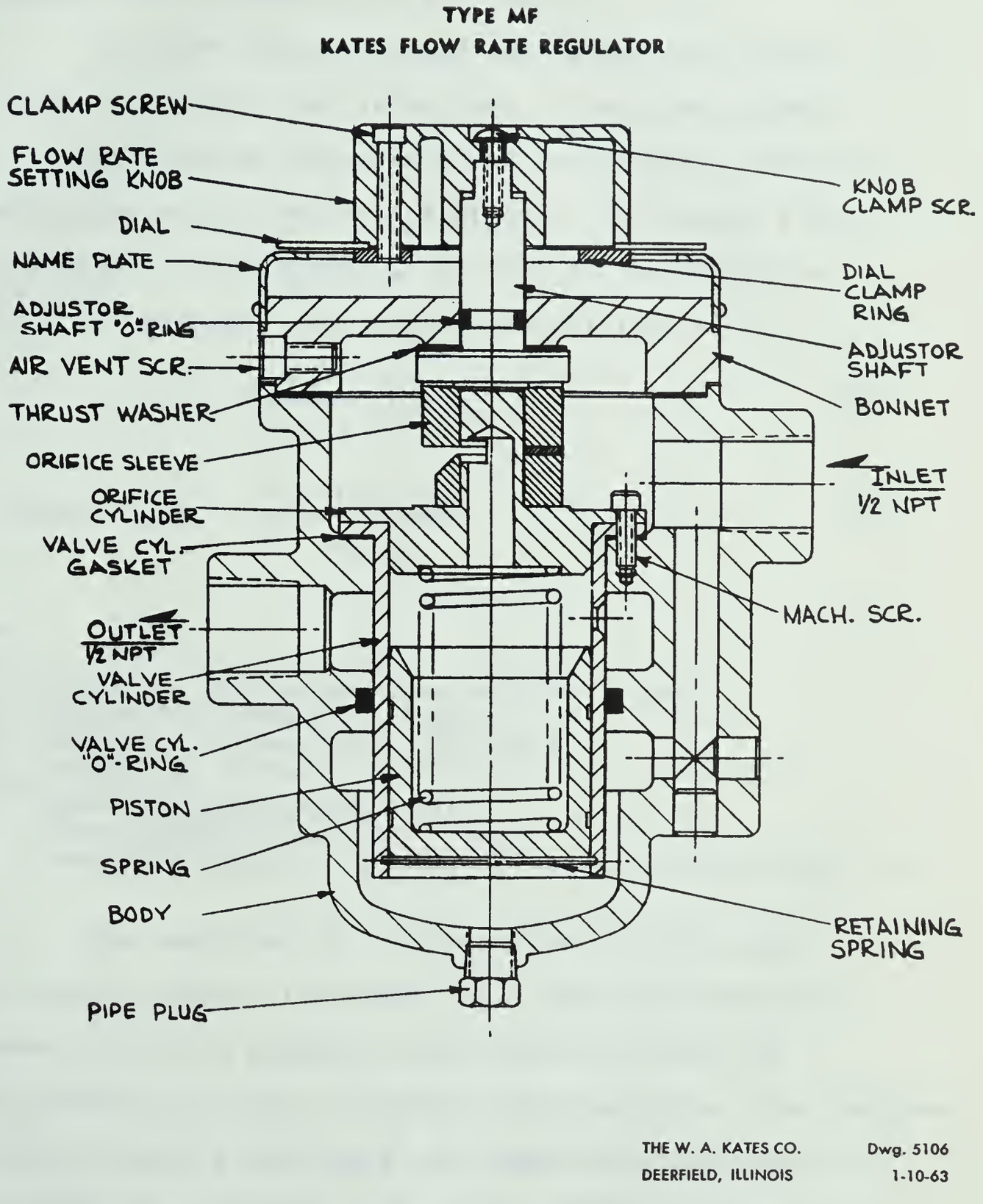
TYPE MF
KATES FLOW RATE REGULATOR
CLAMP SCREW
FLOW RATE SETTING KNOB
DIAL
NAME PLATE
ADJUSTOR SHAFT "O" RING
AIR VENT SCR.
THRUST WASHER
ORIFICE SLEEVE
ORIFICE CYLINDER
VALVE CYL. GASKET
OUTLET 1/2 NPT
VALVE CYLINDER
VALVE CYL. "O" RING
PISTON
SPRING
BODY
PIPE PLUG
KNOB CLAMP SCR.
DIAL CLAMP RING
ADJUSTOR SHAFT
BONNET
INLET 1/2 NPT
MACH. SCR.
RETAINING SPRING
THE W. A. KATES CO.
DEERFIELD, ILLINOIS
Dwg. 5106
1-10-63

Figure 2

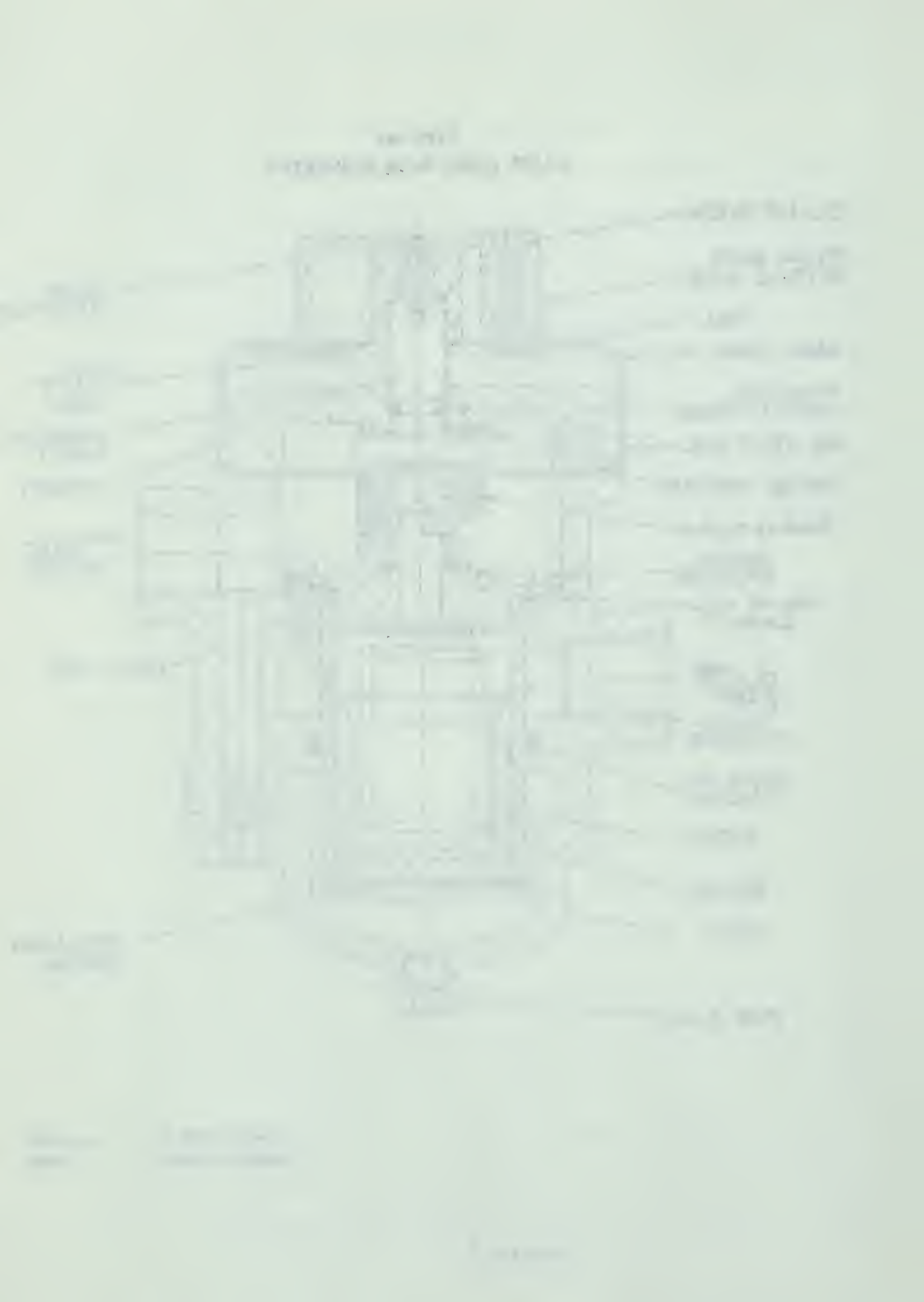

threshold pressure is determined by the initial force that the spring exerts downward on the piston.

The flow enters through the adjustable orifice and flows out through the valve port. The inlet pressure acts on the bottom of the piston and the orifice downstream pressure acts on the top of the piston. The steady state force balance on the piston gives rise to the following equation for pressure drop across the orifice:

$$\triangle P_{or} = \frac{K_s X}{A_{pist}} + \triangle P_o \qquad (2)$$

$$\text{where} \quad \triangle P_o = \frac{K_s (L_f - L_o)}{A_{pist}} \qquad (3)$$

where

$\triangle P_{or}$ = pressure drop across the orifice (psi)
$\triangle P_o$ = threshold pressure (psi)
K_s = spring rate constant (lb_f/in)
A_{pist} = area of piston (in^2)
X = piston displacement (in)
L_f = free length of spring (in)
L_o = extended length of spring in the neutral position (in)

The operation of the regulator is very simple. If the inlet pressure increases, the resulting momentary increase in orifice pressure drop instantly moves the piston upwards, partially closing the valve ports. The orifice downstream pressure increases and immediately restores the orifice pressure drop to a value only slightly higher than before. Theoretically the slope of the $\triangle P_{or}$ line, K_s/A_{pist}, determines the increase in pressure drop. If the magnitude

of K_s is kept low, and the area of the piston is made as large as is feasible, then this factor multiplied by a small $\triangle X$ will tend to keep $\triangle P_{or}$ relatively constant.

There is one undesirable feature of the design that is of particular interest. The piston slides up and down in a closely machined cylinder. Clearly, these two sliding metal parts experience considerable friction or even seizure during operation especially if the fluid contains any small particles of dirt or scale. In any case, the frictional forces would contribute significantly to the overall force balance and therefore affect the accuracy of the regulator. The regulator would then exhibit an undesirable hysteresis effect.

The Kates regulator was tested over its specified pressure drop and flow ranges. The flow was metered through a calibrated integral orifice differential pressure cell. The regulator was tested by both increasing the pressure from zero and decreasing the pressure from 125 psig. This was necessary due to the problem of not obtaining the same flow rate at a given differential pressure when that differential pressure was approached from above and below. In some cases, an average of three readings was recorded. The performance of the regulator is shown in Figure 3. The flow versus pressure drop curve display the erratic behavior of the device. On two of the curves, the lowest flow rate, highest flow rate and their average is shown for a given

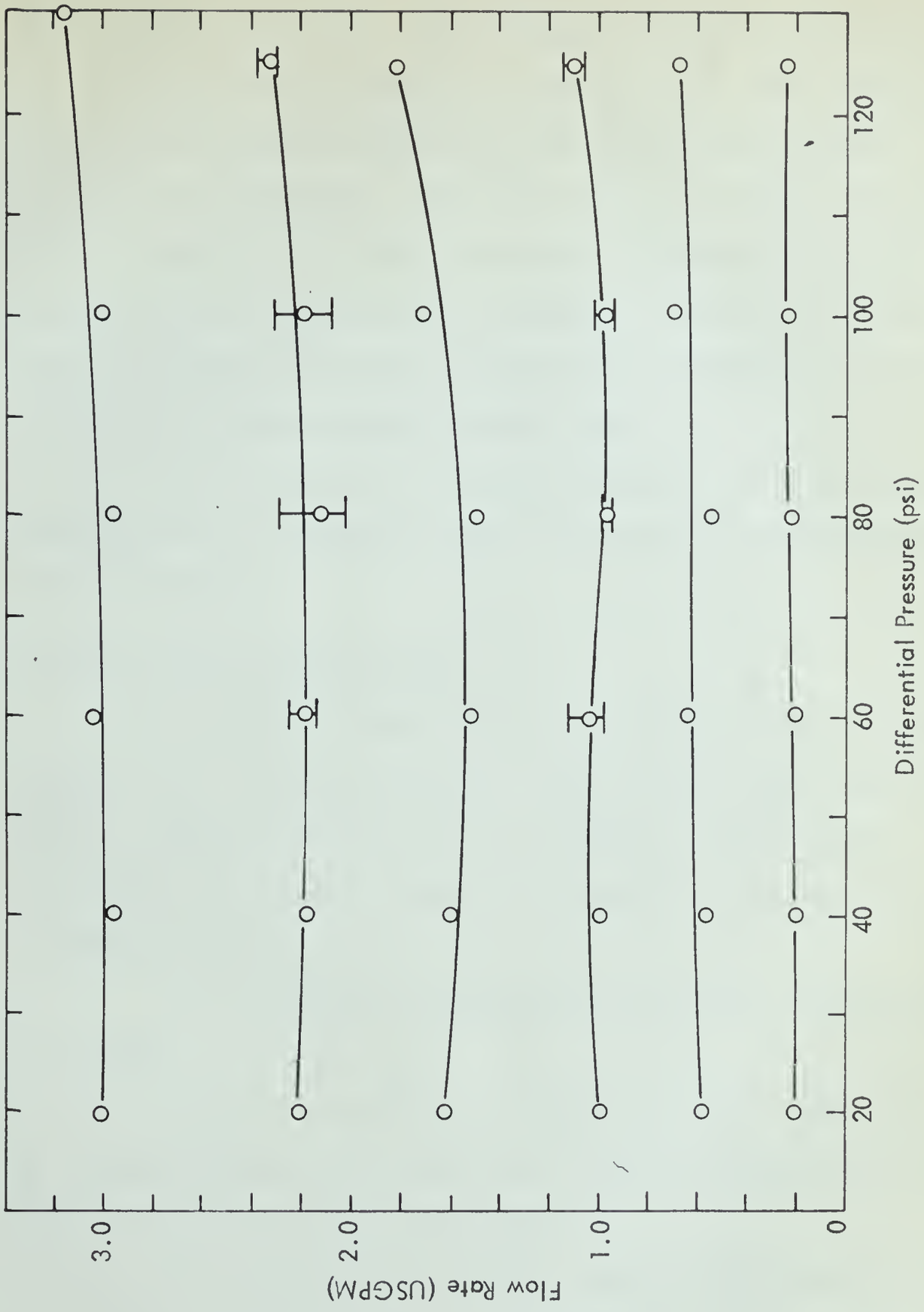

KATES TYPE MF FLOW RATE REGULATOR
FLOW RATE VS DIFFERENTIAL PRESSURE

Figure 3

differential pressure. The results definitely indicate that the friction of the piston on the valve cylinder is quite significant causing different flow rates for a given differential pressure. The flow varies much more than the $\pm 1\frac{1}{2}\%$ claimed by the Kates Company. Although the graphs terminate at a differential pressure of 20 psi, the regulator functioned down to 15 psi. Below this pressure, the flow tended to decrease below its set value.

On the basis of these results, it was felt that development of a flow regulator that had no sliding parts was justified.

Franklin Flow Control Valve

Information was received from the H. B. Franklin Company, Inc. concerning their Model KA 200 HBF, Flow Control Valve. Although some of the information received was difficult to interpret, the Flow Control Valve has the following features:

(1) The flow rangeability is from 0.0000433 to 6.0 USGPM.

(2) It was stated in the August 30, 1965 issue of Chemical Engineering that the reported accuracy of this device is $\pm 0.5\%$ of the flow setting.

(3) A constant pressure drop is maintained across a tubular coil rather than an orifice.

(4) The valve handles pressure differentials of

from 5 psi to 150 psi.

(5) The time required for the flow regulator to fully correct for a given change in upstream or downstream pressure is less than 1/25 of a second.

(6) A diaphragm is used to facilitate the movement of the valve stem.

It appears as though the flow rate is adjusted by setting a flow selector knob and a flow adjusting knob. A spring-loaded valve, actuated by a diaphragm, opens and closes to keep a constant flow rate in response to pressure changes on either the upstream or downstream side. Additional information concerning the operation of the device was requested but was not received. Features (1) and (2), as listed on the previous page, were of extreme interest. The control valve has a tremendous rangeability and the accuracy is better than a flow control loop. However, no further evaluation of the device was carried out, and work proceeded on the design of another flow regulator.

Design Specifications

The design of a self-regulating valve is simple in theory, but very difficult in practice. Before seriously attempting to design a control device, three factors must be considered:

(1) Economics - The design must be capable of competing with the devices that are presently available. In this respect, the simplicity of the design is important in order that construction and maintenance costs are low.

(2) Reliability - From a users standpoint, the operation of the regulator must be dependable. The regulator's construction must be durable to withstand normal, as well as severe operating conditions.

(3) Accuracy - This factor enters into a design problem, since the design is greatly affected by the accuracy that is required of it.

During the development of the regulator, attention was initially focused on accuracy while later on in the development simplicity and economics gained in importance. It was determined quite quickly that the regulator exhibited a fast response. Therefore, the dynamic response of the regulator did not affect its mechanical design.

The performance goals that were set were:

(1) The regulator must have an adjustable orifice. It was to operate in the general flow range 0.5 IGPM to 10.0

IGPM, and have a rangeability of 10 or 15 to 1. Furthermore, the adjustment of the orifice must be possible during operation.

(2) The regulator must handle line pressure variations of approximately 125 psi, and as low a threshold pressure as possible. The actual static pressure that the device could withstand was not of importance since the testing was only carried out over the differential pressure range. In any event, only the thickness of the outer shell of the regulator would have to be increased for increasing static pressure.

(3) The regulator was to be simple and have no moving or sliding parts. This restriction was to eliminate the hysteresis effects that were evident in the Kates Regulator. It would also permit the use of this device in a service where the fluid contained small particles or sediment.

(4) The accuracy of the regulator was to be based on its maximum flow. This was done to have a comparison between this device and a flow control loop. The accuracy of a flow control loop is $\pm$0.5% of the flow span. The accuracy that was set for the regulator was $\pm$1.0% of maximum flow.

Design Procedures

Since the regulator had so many unknown properties, it was impossible to precisely calculate the values of all the variables. Therefore, a simple construction that facilitated convenient removal of the principal parts was used as much as possible. This feature was extremely useful since the design of some of the parts turned out to be a trial and error proposition.

The major components of the flow regulator are the adjustable orifice, the valve stem and port, the bellows, and the spring. In the first design, the fluid entered through the adjustable orifice, flowed into the bellows and left through the valve port. See Figures 4 and 5 for detailed assembly drawings of this design. In later designs, the flow configuration was reversed and the fluid entered through the valve port and flowed out through the adjustable orifice. This type of construction is shown in Figures 6 to 9. The valve stem, which was attached to the orifice plate, moved in the valve port to regulate the flow. The spring supplied an initial force to the orifice plate in the opposite direction to the flow.

The methods of designing the major components of the regulator will be discussed in turn. A more detailed description will be given in the section which discusses the various designs.

Orifice Design

The size of the orifice that would give a specified flow was determined as accurately as possible by using the standard orifice equation

$$Q = C_1 C_d A_{eff} \sqrt{\triangle P} \qquad (3)$$

Q = flow rate (IGPM)
C_1= constant (38.1)
A_{eff}= effective area of flow (in^2)
$\triangle P$ = pressure drop (lb/in^2)
C_d= discharge coefficient of orifice

An adjustable orifice that could be opened or closed while the regulator is in operation could be designed in a number of ways. One method is to cut two circular slots in opposite quadrants through a flat circular plate. These slots are then exposed or covered by a two-winged circular plate that has opposite quadrants cut away. Another method is to closely fit one cylinder into another. The outer cylinder, which is the orifice, has two slots cut in opposite quadrants. When the inner cylinder is rotated, it exposes or covers the orifice. In both cases, the actual rotation of the orifice cover is accomplished by turning an external handle.

The actual size of the orifice required for a given flow is a function of the discharge coefficient and the pressure drop across the orifice. Since the orifice is a slot rather than a circular hole, it was questionable how well the orifice equation would predict the actual size required. A value of 0.70 for C_d was used initially. The

value of $\triangle P$ for the maximum flow rate was not known exactly since it depended upon the size of spring, the initial force exerted by the spring, and the support force due to the inlet pressure. However, once the size of the spring was determined, a reasonable estimate of $\triangle P$ could be calculated. This was possible because at the maximum flow rate, the orifice pressure drop would be only slightly higher than the initiation pressure drop,

$$\triangle P_o = \frac{K_s}{A_b} (L_f - L_i) \tag{4}$$

K_s = spring constant (#/in)
L_f = free length of spring (in)
L_i = initial length after compression to operating region (in)
A_b = area of bellows (in^2)

Therefore, for a certain maximum flow rate, the effective area of flow could be determined.

$$A_{eff} = \frac{Q}{C_1 C_d \sqrt{\triangle P_o}} \tag{5}$$

It was now necessary to determine the width of the circular slot assuming that the diameter was known. If one assumed that the effective area was actually the area exposed to flow then:

$$A_{eff} = \frac{\pi}{2} DW \tag{6}$$

D = mean diameter of circular slot (in)
W = width of circular slot (in)

$$W = \frac{2 A_{eff}}{\pi D} \tag{7}$$

Another method of calculating the width of the slot was used. The hydraulic radius of the orifice is defined by the following equation:

$$R_h = \frac{\text{Area of Flowing Fluid}}{\text{Wetted Perimeter}} = \frac{A_f}{S} \tag{8}$$

R_h = hydraulic radius of orifice slot (in)
A_f = cross-sectional area of orifice slot (in^2)
S = wetted perimeter of orifice slot (in)

The hydraulic diameter is 4 times the hydraulic radius.

$$D_h = \frac{4\ A_f}{S} \tag{9}$$

$$= \frac{2\ DW}{D + 2W} \tag{10}$$

Therefore

$$A_{eff} = \frac{\pi D_h^2}{4} \tag{11}$$

$$A_{eff} = \frac{\pi}{4}\left(\frac{2\ DW}{D + 2W}\right)^2 \tag{12}$$

By solving the resulting quadratic equation, the expression for W becomes

$$W = \frac{2DA_{eff} \pm \sqrt{(A_{eff}D)^2 + (\pi D^2 - 4\ A_{eff})\ A_{eff}D^2}}{(\pi D^2 - 4\ A_{eff})}$$

The actual orifice area was substituted into equations (7) and (13) and the width of the slot calculated. The hydraulic radius approach gave an orifice slot width that was much too large. Therefore, the best estimate of the width of the slot is to use the simple flow area approach.

Spring Design

The design of the spring involved specifying the spring rate constant, the free length, and its initial compressed length. The initial compressed length was fixed by the physical dimensions of the regulator. However, it was much more difficult to specify the spring rate constant and the free length of the spring. The spring rate constant can be estimated by utilizing the steady state force balance equation. Reference to Figure 12 in the discussion of the analog simulation will be helpful in understanding the equation.

$$F_o + K_c X = A_x(P_1 - P_2) + A_b(P_2 - P_3) + A_o P_3 \qquad (13a)$$

Assume that $P_3 \cong 0.0$. Since the magnitude of A_o is small, then the term $A_o P_3$ is negligible. Also, since there is some uncertainty in the force balance, especially the term $A_x(P_1 - P_2)$, this term is multiplied by a factor ϕ which should be approximately 1.0.

$$P_2 = \frac{F_o}{A_b} + \frac{K_c X}{A_b} - \frac{\phi A_x (P_1 - P_2)}{A_b} \qquad (14)$$

$$P_2 = \frac{F_o}{A_b - \phi A_x} + \frac{K_c X}{A_b - \phi A_x} - \frac{\phi A_x P_1}{A_b - \phi A_x} \qquad (16)$$

F_o = initial force exerted by spring at X = 0. (lb_f)
= $K_s(L_f - L_i)$
A_b = area of bellows (in^2)
K_c = combined spring constant of bellows and spring (lb_f/in)
X = stroke (in)
ϕ = factor which will satisfy the force balance equation
A_x = area of stem at a stroke X (in^2)
P_1 = inlet pressure (psi)
P_2 = bellows pressure (psi)

Since P_2 must remain essentially constant, the magnitude of the second term must equal the magnitude of the third term for all Q and P_1. The third term which is the support pressure could not be predicted theoretically because of the odd flow configuration around the valve stem. Consequently, it was necessary to try a number of springs of different spring constants.

There was a lower limit for the value of the spring constant. The lower the spring constant, the longer the spring that was required to give the initial force. If the spring was too long, then there were problems with buckling.

An approximate value of the combined spring constant can be determined by rearranging equation (14) and setting $\phi = 1.0$ to give

$$K_c = \frac{(A_b - A_x)P_2 + A_xP_1 - F_o}{X} \qquad (17)$$

Choose P_2 slightly greater than $\triangle P_o$, and assume at the minimum flow rate and maximum differential pressure that the value of X is at its maximum. An approximate value of K_c can be determined by assuming that A_x is a value slightly smaller than the area of the valve port. Therefore, the value of the spring constant, K_s, is

$$K_s = K_c - K_b \qquad (18)$$

Once the spring constant was determined, it was relatively easy to specify its free length from equation (4).

$$L_f = L_i + \frac{\triangle P_o A_b}{K_s} \tag{19}$$

Valve Design

Valve Stem

The design of the shape of the valve stem proved to be extremely difficult since the shape of the stem affected the support force. The support force is the term, $\phi A_x(P_1 - P_2)$, in the force balance equation (equation 14), which results from the inlet pressure acting upon the valve stem.

Referring to equation (16), the first term is essentially a constant. It is apparent that the following relationship must hold for all P_1 and Q if P_2 is to remain constant.

$$\left| \frac{K_c X}{A_b - \phi A_x} \right| = \left| \frac{\phi A_x (P_1)}{A_b - \phi A_x} \right| \tag{20}$$

The accuracy of the regulator is determined by the error, , that exists.

$$\left| \frac{K_c X}{A_b - \phi A_x} \right| = \left| \frac{\phi A_x P_1}{A_b - \phi A_x} \right| \pm \epsilon \tag{21}$$

It is impossible to predict the value of ϵ for all Q and P_1 because of the factor ϕ. The factor ϕ was inserted to make the results satisfy the force balance. The value of ϕ would be 1.0 if the force balance were an exact representation of the system. It is difficult to write a more accurate

force balance without studying in detail the pressure drop gradients along the valve stem for all flow rates. It became apparent that the design of the valve stem would be essentially a trial and error proposition. It is possible to predict the shape of the stem for a given flow rate by using the following equations and assuming $\phi = 1.0$, and assuming that the port size, A_p, is known.

$$Q = C_1 C_d (A_p - A_x) \sqrt{P_1 - P_2} \tag{22}$$

$$P_2 = \frac{F_o}{(A_b - A_x)} + \frac{K_c X}{(A_b - A_x)} - \frac{A_x P_1}{(A_b - A_x)} \tag{23}$$

The procedure is as follows:

(1) Set the flow rate Q.

(2) Choose a value of C_d. A value of 0.7 for C_d is a good approximation.

(3) Choose some constant desired value for P_2.

(4) For all values of P_1 calculate A_x.

$$A_x = A_p - \frac{Q}{C_1 C_d \sqrt{P_1 - P_2}} \tag{24}$$

(5) For each of the above points calculate X using the equation (23).

$$X = \frac{(A_b - A_x)P_2 + A_x P_1 - F_o}{K_c} \tag{25}$$

The value of K_c may have to be altered if the final

X value, for the highest P_1, is greater than the allowable stroke.

The above procedure gives a first approximation of the shape of the stem for that flow rate. However, for another flow rate, the shape of the stem would be different. The size of the stem for a given X would be slightly different. Therefore, it is inevitable for this large pressure differential range that the working stroke for two different flow rates will overlap.

It was found that the valve stem should be shaped for the maximum flow. If the desired accuracy could be attained at this flow rate, then this accuracy could also be attained at the lower flow rates. The taper of the valve stem appeared to be quite important. By changing the half angle slope by only 2^{o}, the accuracy was affected considerably. For example, changing the slope from 12^{o} to 10^{o} improved the accuracy from about $\pm 3.0\%$ to $\pm 2.0\%$ of maximum flow. The accuracy could be reduced to about ± 2 percent of maximum flow relatively quickly, but it was found that to reduce this to ± 1 percent involved a tremendous amount of trial and error experimentation. The difficulty in attaining the $\pm 1\%$ accuracy can be attributed to the lack of knowledge concerning the fluid dynamic characteristics of the device.

Valve Port

The size of the port was initially calculated based

on the fact that when the valve was wide open, the stem would be completely removed from the port. (See Figures 4 and 5.) The initial design was for flow rates of 0.5 IGPM to 7.5 IGPM. The port size was calculated using the orifice equations for an arbitrarily chosen pressure drop of 1.0 psi and a flow rate of 3.0 IGPM. The reason for this choice of flow rate was that it was near the middle of the range of flow rates. The low pressure differential guaranteed that the port was sufficiently large to provide the desired flow. The calculated size of the orifice was approximately 3/8 of an inch.

During the development, the flow configuration was reversed. The fluid entered through the valve port and flowed out through the orifice. Since the valve stem was attached to the orifice plate, there had to be some portion of the stem in the port at all times. (See Figures 6 and 7.) In addition, the flow range was increased to 10 IGPM. These changes increased the pressure drop across the wide open valve, but it was felt that it would not be necessary to increase the size of the port.

The port design became extremely important during the development. Initially, the port was simply a 3/8 inch diameter hole drilled in a 1/8 inch plate. This simple design caused problems when the regulator was being tested. The regulator would develop a high frequency noise. The vibration was observed at all flow rates and pressure

differentials but was most evident at a certain flow rate and pressure differential. It was obvious that it could not be ignored. It was theorized that the sharp edge of the port set up adverse pressure gradients and eddy currents which resulted in cavitation. High frequency vibration is generally associated with the phenomenon of cavitation. In order to eliminate this problem, the upstream and downstream edges of the 3/8 inch diameter port were chamfered at an angle of 45 degrees. A 1/32 inch parallel hole was left in the middle of the 1/8 inch plate. At the same time, some attempt was made to streamline the valve stem and also the parts downstream from the valve port. No further vibration was encountered following these alterations.

Design #1

Design #1 was built to determine whether the idea was feasible, and to obtain more knowledge of the operation of the regulator. Since it was important to obtain this information as soon as possible, some mechanical features of the design were overlooked.

The flow entered the top of the regulator, passed through an adjustable orifice, and into the bellows. The fluid flowed out through the valve port.

The major elements of this preliminary design will be discussed in turn. The cut-away drawing is shown in Figure 4, while the assembly drawing is shown in Figure 5.

Bellows (4)

The bellows was a single ply brass bellows with 14 convolutions. It had the following properties:

(1) Outside diameter (in)..... 2
(2) Inside diameter (in)..... 1 3/8
(3) Free length (in)..... 2 1/2
(4) Maximum internal pressure (psi).....40
(5) Spring rate constant (lb/in).....12.5
(6) Maximum deflection (in)..... 0.80
(7) Effective area (in^2)..... 2.24

The bellows was soft soldered to the bottom plate (13) and the supporting ring (3).

Orifice Plate (9)

The orifice plate was 3/16 inch thick brass fastened to the supporting ring (3) by three screws. Two circular slots were cut in opposite quadrants. The bottom

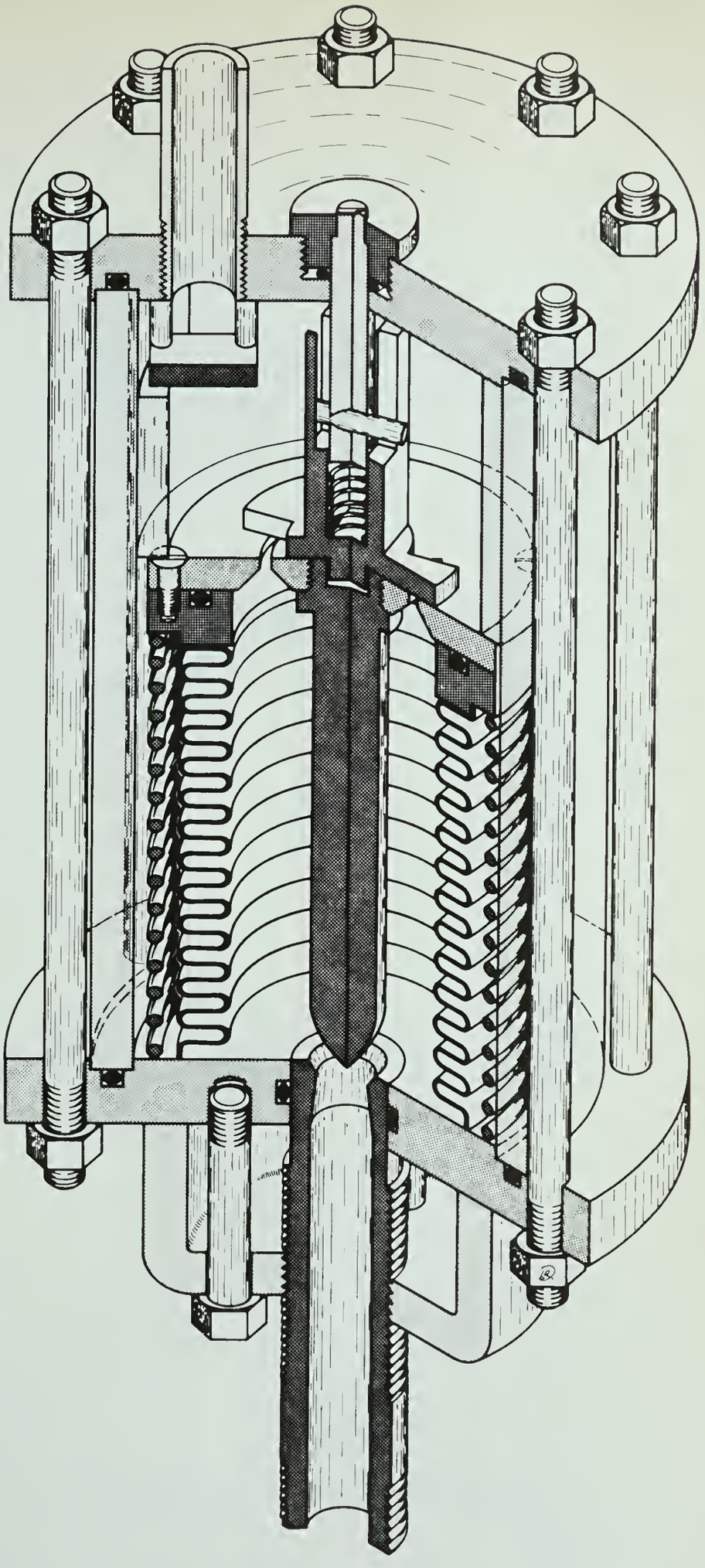

FIGURE 4

TECHNICAL ILLUSTRATION OF CONTROL VALVE NO. 1

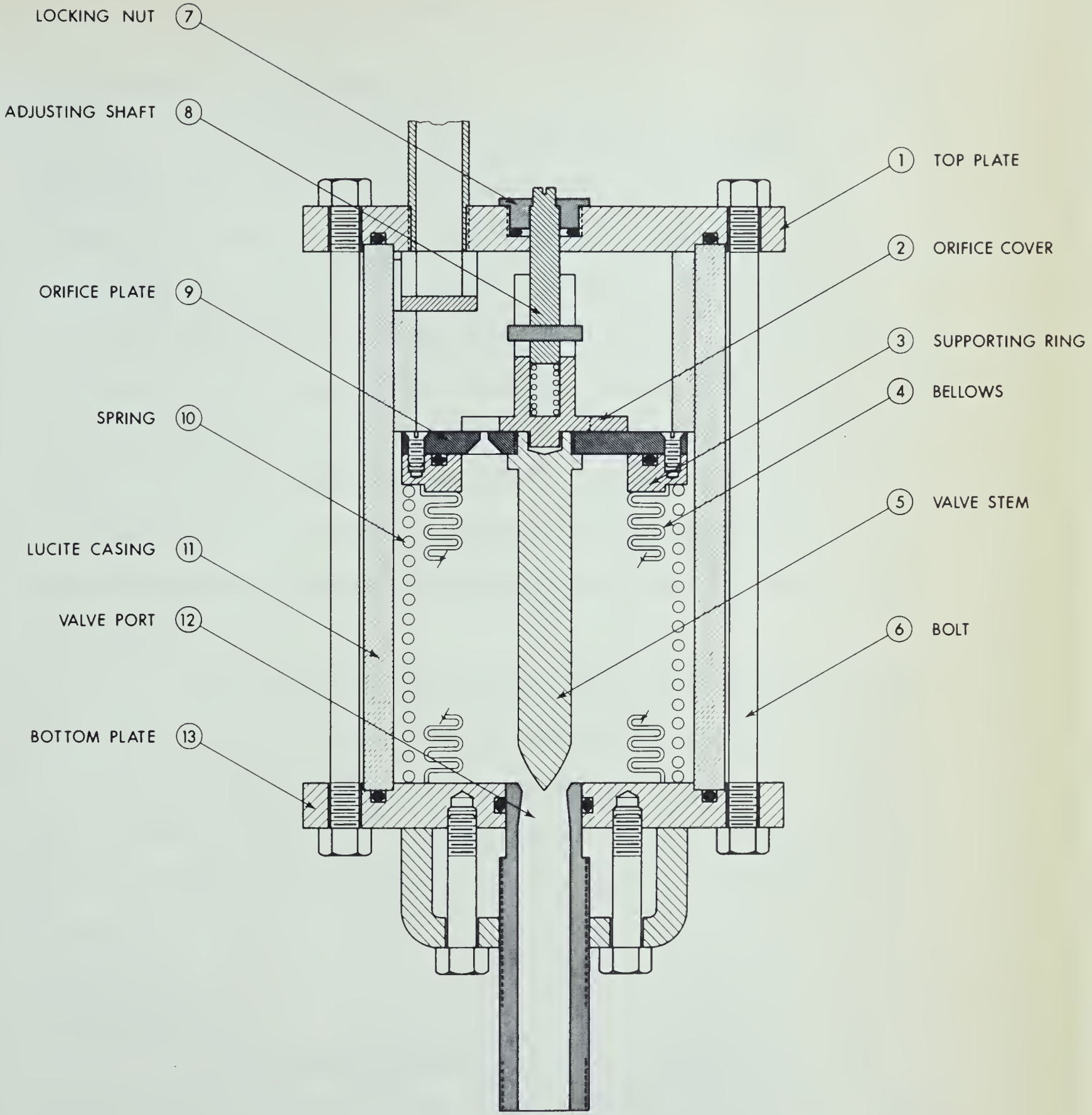

FIGURE 5

ASSEMBLY OF CONTROL VALVE NO. 1

of the slot was beveled at 45° and a 1/16 inch parallel section was retained at the top.

Valve Stem (5) and Port (12)

Initially, the valve stem was 0.40 inches in diameter and threaded into the orifice plate (9). In order to remove the valve stem, it was necessary to dismantle the entire regulator. Subsequently, the size of the valve stem was reduced to 0.26 inches with a 0.25 inch port. This was done to reduce the difference in area upon which the inlet pressure and bellows pressure acted. The principal result of the change was that it reduced the flow range of the valve since there was a greater pressure drop through the port with the valve wide open.

The vertical position of the valve port was made adjustable so that the relative location of port and stem could be altered. This allowed some latitude in setting the maximum stroke. The port simply threaded through a bottom flange and was sealed in the bottom plate by an O ring.

Spring (10)

The helical spring, which was made of 1/8 inch inconel wire, was 2 1/8 inch inside diameter and had a free length of about $8\frac{1}{4}$ inches. The spring rate constant was approximately 4 lbs/in. It had 9 active coils and was

compressed to 2½ inches initially.

The spring fit between the bottom plate (13) and the supporting ring (3). The initial extension on the spring was restrained by a lucite retaining ring which fit between the orifice plate (9) and the top plate (1). A serious problem with this type of construction was that when the regulator was dismantled, the spring would extend the bellows until the bellows force balanced the spring force. The bellows was extended beyond its maximum allowable stroke. Another problem was that the spring could not be replaced without loosening the soldered connection to the supporting ring.

Adjusting Shaft (8) and Orifice Cover (2)

The orifice area was adjusted by turning the adjusting shaft that extended through the top plate (1). The adjusting shaft had a 1/8 inch pin through it which moved up and down in slots cut in the cylindrical portion of the orifice cover plate. Since it was important that there be no friction between these parts, the fit was very loose. The orifice cover plate was centralized by fitting a hub into a hole drilled into the top of the valve stem (5). Any tendency for the orifice cover plate to lift off the orifice plate (9) was overcome by a very light spring that fit between the adjusting shaft and orifice covering plate. The pressure drop across the orifice would, of course, tend to

keep the cover plate in position.

The portion of the orifice covering plate that increased or decreased the orifice area was constructed in the following manner. The circular cover plate had two opposite quadrants cut away leaving two wings that would completely close the orifice if revolved to coincide with the orifice slots. There was no problem with the fluid passing between the orifice plate and the covering plate.

Other Features of Design #1

The material used in this design was brass except for the outer casing which was made of lucite. Brass was chosen since it was easy to machine and the casing was made of lucite to allow visual observation of the regulator operation.

The lucite casing (11) was fit into recesses in the top and bottom plate and O rings sealed the connection. The lucite and end plates were held together by $\frac{1}{4}$ inch tie rods (6). A baffle was connected to the top plate at the regulator inlet to eliminate any kinetic effects of the incoming fluid on the operation of the regulator. A fitting was provided in the top plate to bleed trapped air during start-up and also to provide a location for pressure measurement. A $\frac{1}{4}$ inch tube was inserted through the bottom plate to the inside of the bellows. This connection made it possible to obtain the pressure on the inside of the bellows.

The differential pressure across the orifice was then obtained by utilizing the connections through the top and bottom plates.

It became evident that there were many features of Design #1 that were not desirable. The reasons for changing the design are as follows:

(1) There was a serious problem concerning the practical operation of the regulator. For example, suppose the regulator were being put into service with the bellows full of air. Suppose also that the pressure of the entering fluid was greater than the bellows could withstand. With the orifice closed, the incoming fluid would crush or damage the bellows. The problem could be alleviated somewhat by ensuring that the orifice could never be closed completely. However, it takes a finite time to fill the bellows and the possibility of damaging the bellows dictated a design change.

(2) The second undesirable feature was that the spring, being trapped between the bottom plate and the supporting ring, over-extended the bellows when the regulator was disassembled. Primitive methods were used to minimize the extension, but these were not very satisfactory. The spring also could not be replaced without breaking the soldered connection between the bellows and the supporting ring.

(3) Another very annoying feature of the design

was that the regulator had to be almost completely disassembled to remove the valve stem. The valve stem was removed many times for revisions.

For these reasons, Design #2 was executed and tested.

Design #2

All the undesirable features of Design #1 were eliminated in Design #2. This was accomplished by changing the flow configuration. The fluid entered the bottom through the valve port, through the adjustable orifice, and out the top outlet. The basic principle of operation remained the same.

The major components of the second regulator are discussed below. There are some parts that have not changed from Design #1 so that they will not be included in this discussion. The cut-away drawing is shown in Figure 6 and the assembly drawing in Figure 7.

Bellows (11)

Initially, a brass bellows was used but it was subsequently replaced by a stainless steel bellows which could withstand higher pressures. The range of differential pressures to which the regulator was subjected was increased. The stainless steel bellows had the following characteristics:

(1) Outside diameter (in)..... 2.015
(2) Inside diameter (in)..... 1.562
(3) Free length (in)..... 2.50
(4) Maximum internal pressure (psi).....65
(5) Spring rate constant (lb_f/in).....63.7
(6) Maximum deflection (in)..... 0.53
(7) Effective area (in^2)..... 2.50
(8) Number of convolutions.....14

Various methods were used to fasten the stainless steel bellows to the brass plates. Soft solder was not very effective since it did not adhere properly to the stainless

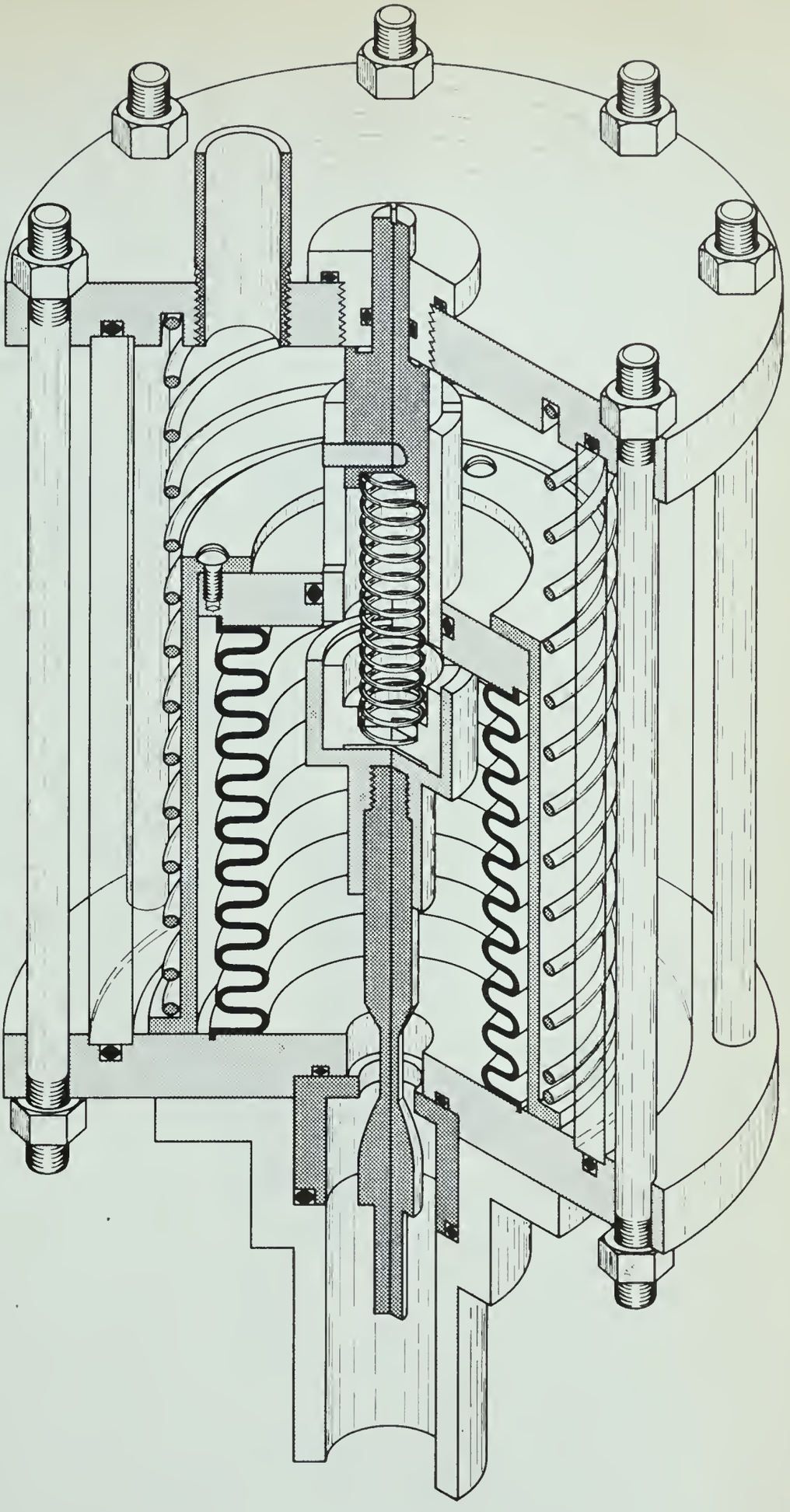

FIGURE 6

TECHNICAL ILLUSTRATION OF CONTROL VALVE NO. 2

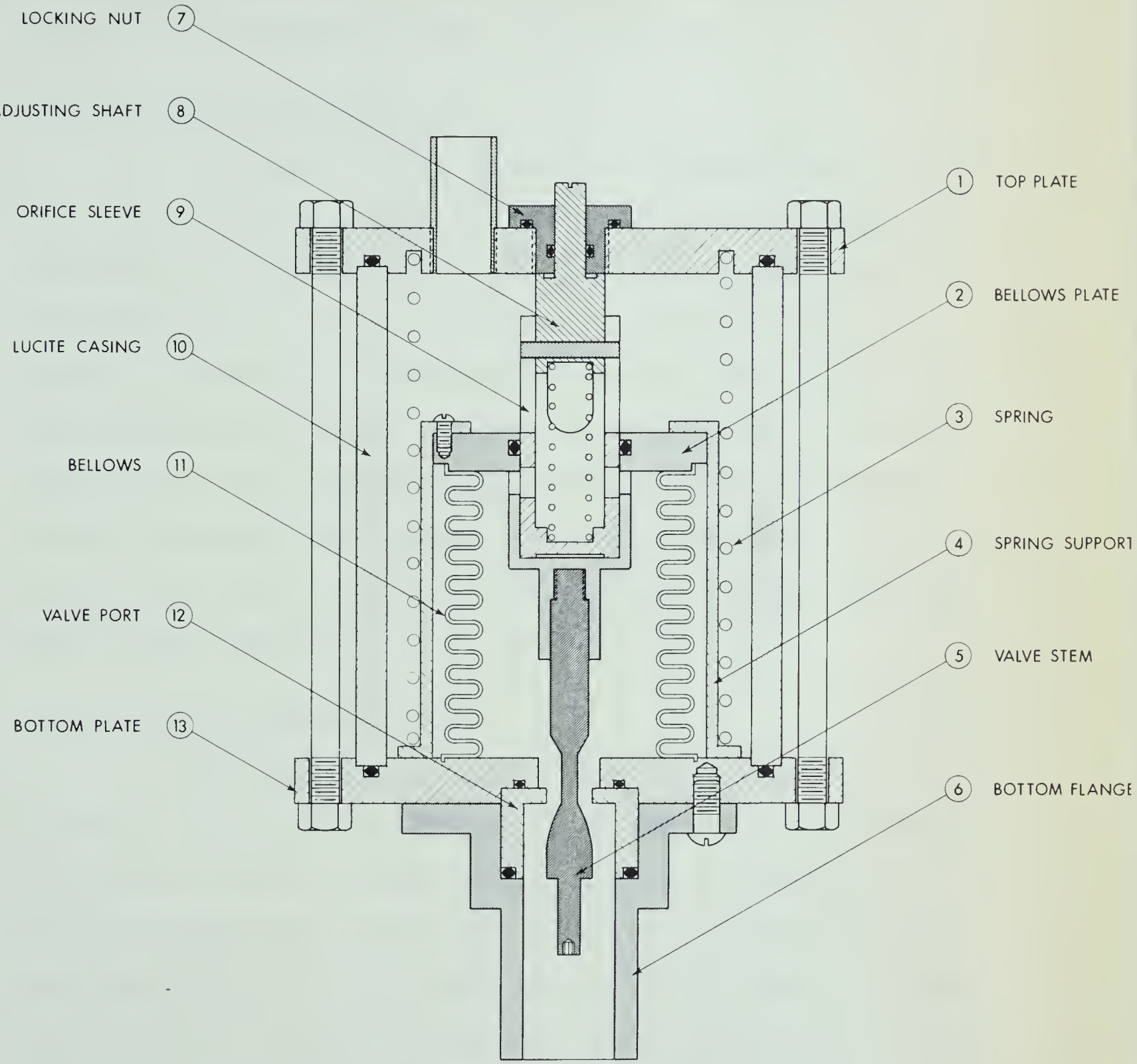

FIGURE 7

ASSEMBLY OF CONTROL VALVE NO. 2

steel. The most effective method involved the use of silver solder. However, this required heating of the end of the bellows to a relatively high temperature, which affected some of the properties of the stainless steel.

Bellows Plate (Orifice) (2)

The design of the orifice was changed from Design #1. The orifice was comprised of two slots cut in opposite quadrants of a cylindrical shell that was actually part of the plate fastened to the bellows. It was felt that the orifice arrangement of Design #1 would not work because now the pressure drop across the orifice would tend to separate the orifice cover plate and the orifice plate. The forces in the new design were radial and always balanced. The orifice was simply a 3/16 inch slot milled through the 3/32 wall of the cylinder.

Valve Stem (5) and Port (12)

The valve stem slipped through the 3/8 inch diameter valve port and threaded into the bellows top plate. The size of the stem within the port when the valve was completely open was approximately 1/8 inch in diameter and increased to 0.385 inch in diameter at the bottom end. The small shaft on the end of the stem had a socket for an Allen wrench which made it possible to remove the stem quite easily. The stem could be removed without dismantling the entire regulator.

In this design the valve port was removable and was held in place by the bottom flange (6), which in turn was bolted to the bottom plate (13). Although different sized ports were not examined, the construction was not complicated to any great extent by making it removable. No provisions were made to adjust the relative position of the valve port and the valve stem since it was felt that this was not necessary.

Spring (3)

The spring was supported by a cylindrical sleeve (4) that slipped over the bellows plate and rested on the bottom plate (13) when the valve was wide open. It was possible to replace the spring quite easily. When the regulator was dismantled, the initial force on the spring simply forced the top plate upwards, leaving the bellows in its neutral position. The spring rate of the spring was 17.8 lb_f/inch, and an initial force of about 18 lb_f was developed by the spring. The spring was made from 3/16 inch inconel wire.

Orifice Sleeve (9)

The size of the orifice was externally adjusted as in Design #1. An orifice sleeve fit into the bellows plate (2). Slots were cut in opposite quadrants of the cylinder at a level which coincided with the orifice. By turning the adjuster, more or less orifice area could be

exposed. Any tendency for the cylinder to move upwards was prevented by inserting a small spring.

During the testing of Design #2, a very serious phenomenon was observed. The bellows assembly would vibrate at quite a high audible frequency. This vibration was especially evident at one flow rate and a certain differential pressure. This was discussed previously in connection with the design procedures for the valve port. Initially, it was thought that the valve stem was simply vibrating against the valve port due to fluid flowing at a high velocity passed the stem. Since the valve stem was quite long, it was relatively easy for the stem to be displaced from its central location. It was thought that an unbalanced radial force set up by an irregular pressure gradient around the stem could displace the stem and cause the vibrations.

Since the vibrations could not be tolerated, design changes were considered to eliminate the problem. Design #2 was altered to Design #3.

Design #3

The flow configuration of Design #3 did not change from Design #2. The fluid entered through the valve port, flowed into the bellows, and out through the adjustable orifice.

The design of the major components will be discussed. The cut-away drawing is shown in Figure 8 and the assembly drawing in Figure 9.

Bellows (5)

The stainless steel bellows was the same type as that used in Design #2. The bellows had the following properties:

(1) Outside diameter (in)..... 2.015
(2) Inside diameter (in)..... 1.562
(3) Free length (in)..... 2.50
(4) Maximum internal pressure (psi).....65
(5) Spring rate constant (lb_f/in).....63.7
(6) Maximum deflection (in)..... 0.53
(7) Effective area (in^2)..... 2.50
(8) Number of convolutions.....14

The type of material was 321 stainless steel. The bellows was fabricated from tubing having a fusion butt welded longitudinal seam. The bellows was silver soldered to the brass end plates. The recommended range of temperatures for this bellows is -65 to 160 degrees Fahrenheit.

Orifice Plate (2)

The orifice arrangement was similar to that of

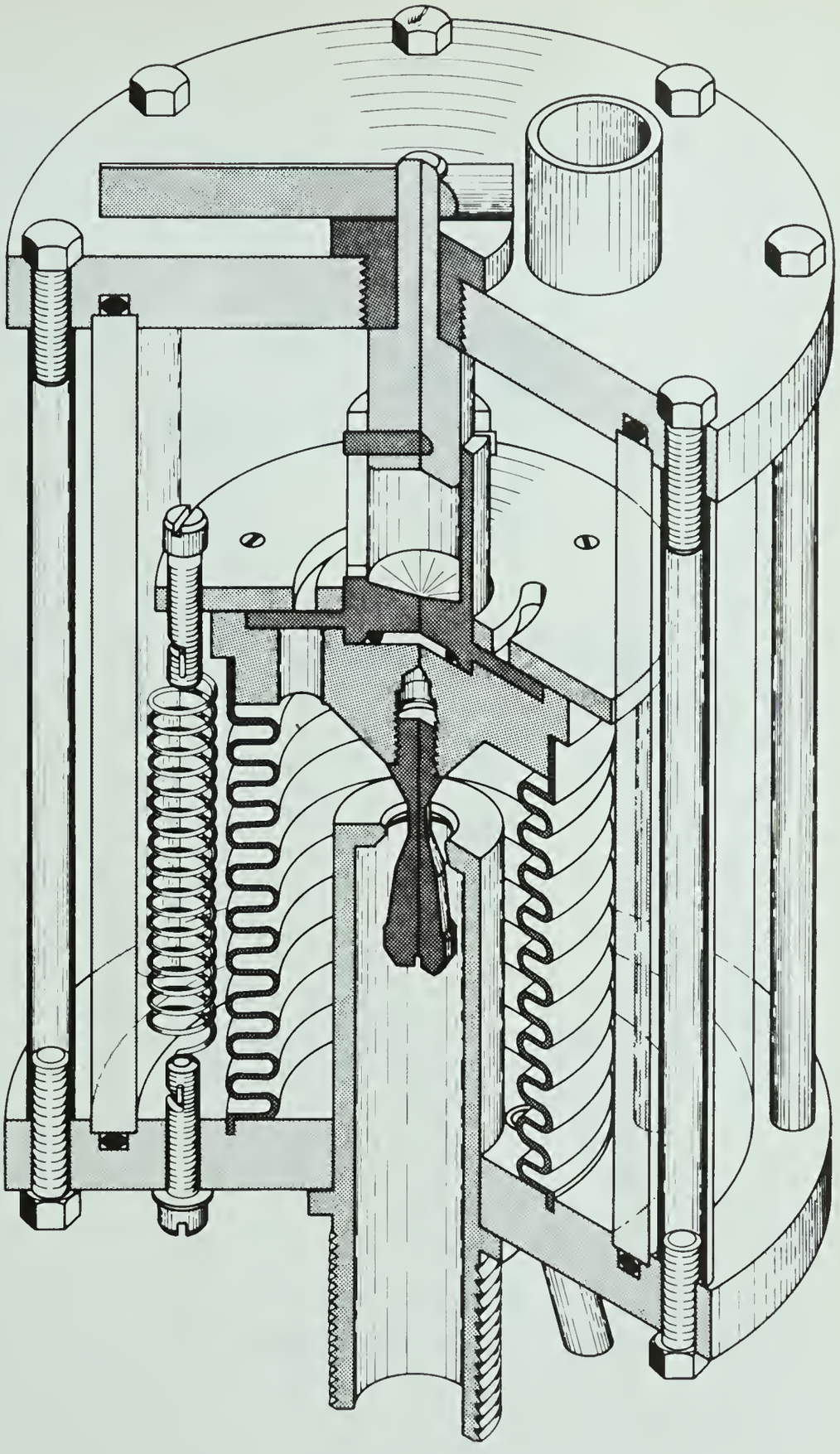

FIGURE 8

TECHNICAL ILLUSTRATION OF CONTROL VALVE NO. 3

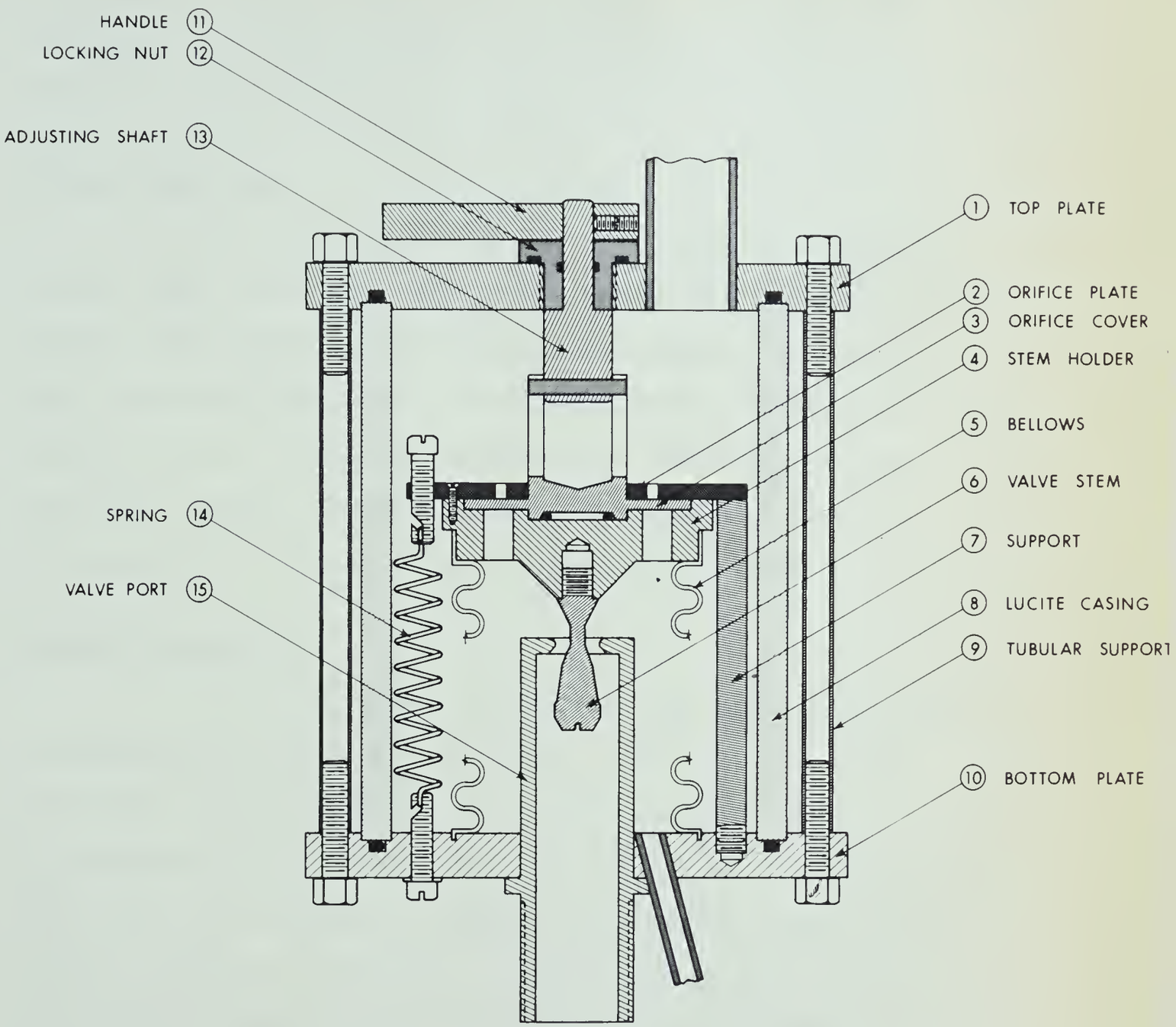

FIGURE 9

ASSEMBLY OF CONTROL VALVE NO. 3

Design #1. Two 3/32 inch wide circular slots were cut in opposite quadrants of a 1/8 inch thick plate. The mean diameter of the orifice was $1\frac{1}{4}$ inches. The plate was screwed to the stem holder (4) and also supported the extension springs (14).

Stem Holder (4)

The stem holder was the most difficult part to build. The valve stem (6) screwed into the bottom of the plate. The plate was beveled in this region to ensure that the operation would not be affected by flow over sharp corners. This was particularly important at the high flow rates. Wide free flow slots were milled to correspond to the location of the orifice slots.

Orifice Cover (3)

The adjustment mechanism of the orifice was not changed appreciably from Design #1. The orifice cover plate was located between the stem holder (4) and the orifice plate (2). An O ring inserted under the adjusting plate held the adjusting plate firmly against the orifice plate to ensure no leakage. A small screw was inserted in the orifice plate to act as a stop or a zero point. The adjusting plate was prevented from completely closing the orifice. This gave a positive starting point for testing as well as preventing the bellows from being subjected to any high inlet pressures that momentarily could be

established during start-up. The actual external adjustment was done by rotating a lever.

Valve Stem (6) and Port (15)

The changes that were made in the valve stem and valve port were extremely significant to the development of the regulator. It was hoped that by shortening the length of the valve stem that the problem of vibration would be eliminated. With the valve stem much shorter, there would be less tendency for the valve stem to move from the center of the port and there would be no whipping of the valve stem. The valve port was initially a 3/8 inch diameter hole in a 1/8 inch thick plate.

When the design was tested, the regulator vibrated as before which, of course, was very distressing. It was then postulated that the vibration was caused by cavitation of the fluid around the valve port. Since the valve port had sharp edges, adverse pressure gradients and high turbulent eddies could be developed which could cause the cavitation and vibration. As it turned out, this theorizing was correct. A 45 degree bevel on the inlet and outlet of the port completely eliminated the high frequency vibration. The port had a 1/32 inch parallel central section at a diameter of 3/8 inch.

Since this small change produced such good results, more changes were made to eliminate sharp edges. The valve

stem itself was made more streamlined. Sharp edges and corners on the stem holder (4) were replaced with a gently sloping cone. All these changes greatly improved the fluid dynamic characteristics of the regulator. A detailed drawing of the valve stem is shown in Figure 10.

Springs (14)

When this design was tested initially, the same helical spring used in Design #2 was tried. After the vibrations were eliminated, there was another problem that required solution. There was a small amount of hysteresis evident. In other words, the flow would be slightly different if one increased the differential pressure to a certain point than if one decreased the differential to the same point. After some investigation, it was found that the orifice plate (2) and stem holder (4) were tilting as the bellows extended causing some friction in the adjustment mechanism. At first it was felt that a new helical spring was required, but later it was concluded that unguided helical compression springs always have a tendency to deflect in this manner.

It was decided to use three smaller extension springs located 120 degrees apart. The springs were attached to screws in the bottom plate (10), and also to adjusting screws in the orifice plate. Since the springs were cut to approximately the same length from $\frac{1}{4}$ extension spring stock,

DETAIL DRAWING OF STEM

Figure 10

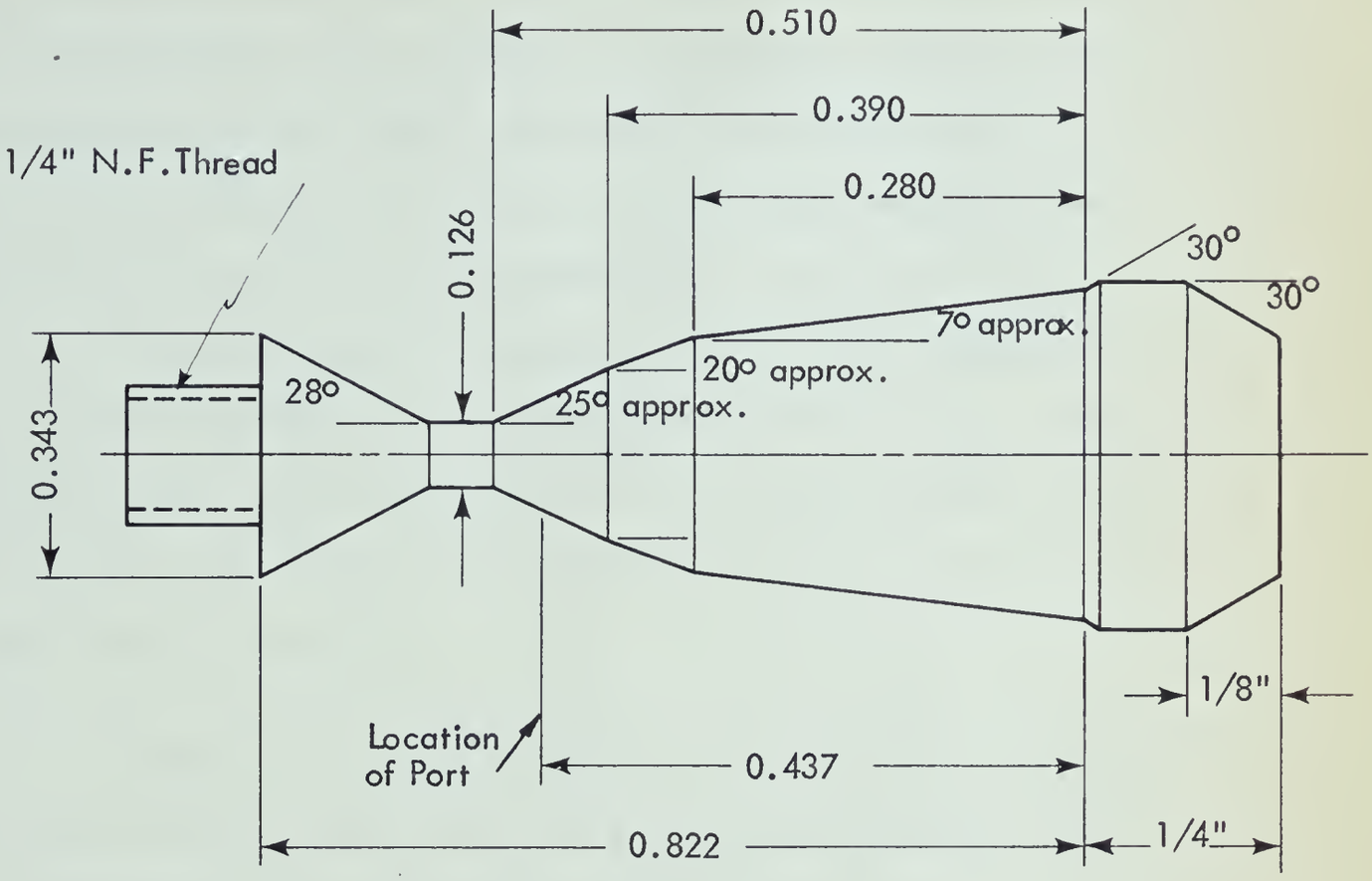

ACTUAL DIMENSIONS

Stroke(inches)	Diameter(inches)	Area(inches^2)
0.000	0.193	0.0293
0.007	0.200	0.0314
0.027	0.220	0.0380
0.047	0.240	0.0452
0.067	0.254	0.0507
0.087	0.268	0.0564
0.107	0.282	0.0625
0.127	0.294	0.0679
0.147	0.300	0.0707
0.167	0.304	0.0726
0.247	0.324	0.0824
0.327	0.344	0.0929
0.437	0.371	0.1081

the adjusting screws were quite useful. It was possible to adjust the initial tension on the springs to ensure that the stem holder and orifice plate stroked uniformly. When the regulator was tested, no hysteresis was evident. Three small rods (7) were inserted to balance the initial force of the springs and also to give some definite starting point for stroke measurement during testing.

The springs were made of 0.034 inch diameter spring steel and had an outside diameter of $\frac{1}{4}$ inch. The combined spring rate constant of the three springs was 16.8 lb_f/in. and the initial force exerted by the three springs was 16.0 lb_f.

Design #3 produced results that essentially met the initial goals that were set for the development of a flow regulator and no further designs were built.

Experimentation

A considerable amount of experimentation was required since part of the design was based upon trial and error procedures. The experimental work consisted mainly of determining the accuracy of the regulator over the desired pressure drop and flow rate ranges. The testing set-up is shown in Figure 11.

Water from the city water main at a pressure of about 75 psig was pumped by a centrifugal pump through the testing system. The pump was capable of pumping in excess of 10 IGPM at a differential pressure of about 80 psi. This made it possible to test the regulator up to 150 psi differential pressure since the outlet of the regulator was essentially at 0 psig. The gate valve on the pump discharge was adjusted to give the inlet pressure on pressure indicator number one (PI-1). The water flowed into the regulator and through the rotameters. The smaller capacity rotameter handled flows up to 1.6 IGPM and the larger rotameter had a capacity of about 8 IGPM. The rotameters were used to get an estimation of the accuracy. If more accurate results were required or effects of flow rates greater than 8 IGPM were required, it was necessary to weigh the water delivered during a measured time interval.

The differential pressure across the orifice was measured by a differential pressure cell and recorded on a recorder. Pressure indicators PI-2 and PI-3 gave an

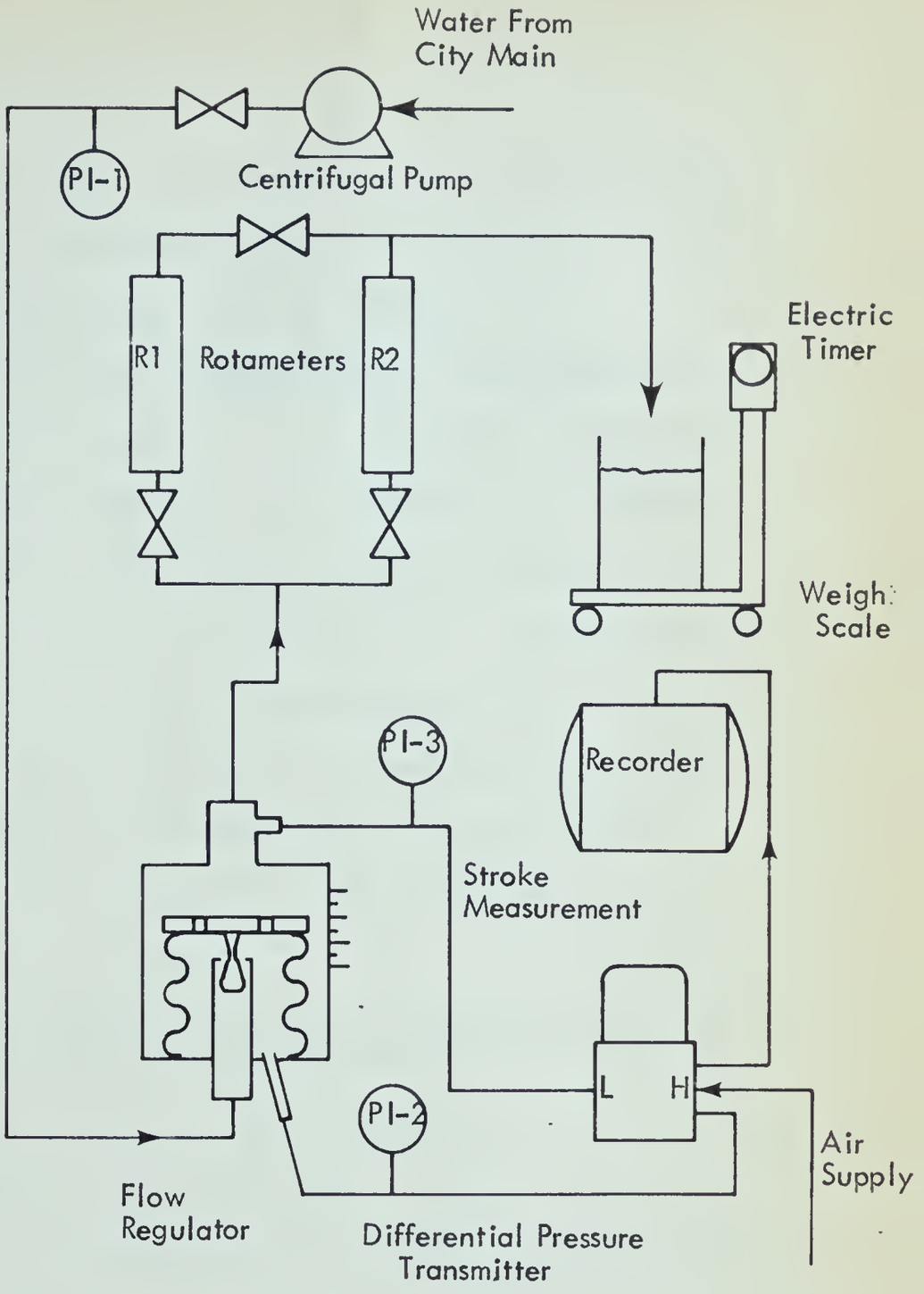

SCHEMATIC OF FLOW TESTING SET-UP

Figure 11

indication of the static pressure of the bellows and the outlet respectively.

The distance that the orifice plate moved or the stroke of the stem was determined by reading the stroke on a graduated scale on the outer lucite casing.

The value of all of the pertinent variables was recorded for each set of results. The regulator was tested at four or five different flow rates throughout the flow range. At each set flow rate, the data were obtained for approximately six different inlet pressures as measured on PI-1. Since the outlet pressure was essentially 0 psig, as measured by PI-3, the inlet pressure corresponded to the differential pressure of the regulator. At each inlet pressure setting, the following data were obtained:

(1) Flow rate, IGPM

(2) Bellows pressure (PI-2). This was actually a check on the orifice differential pressure.

(3) Orifice differential pressure

(4) Stroke of the valve stem

From this information and utilizing the experience of previous sets of results, revisions were made to the stem as discussed in the section concerning the design of the valve stem.

A list of equipment used in the testing is shown in Appendix A.

Analog Simulation of Flow Regulator

The principal purpose of simulating the flow regulator on the analog computer was to study some of the dynamic characteristics of the device. It was not possible to do this experimentally because the response was too fast to observe. Consequently, by time scaling on the analog computer, the transient and frequency response characteristics of the device could be studied.

The differential equations describing the flow regulator will now be derived based on the variables as shown in Figure 12. The nomenclature is shown below the figure.

The force balance equation can be written as follows:

$$\frac{M}{12g_c}\frac{d^2x}{dt^2} + K_d\frac{dx}{dt} = (A_b-A_o)(P_2-P_3) + P_1A_x - K_cx - P_2(A_x-A_o) - F_o \tag{26}$$

$$= A_b(P_2-P_3) + A_x(P_1-P_2) - K_cx - F_o + A_oP_3 \tag{27}$$

Assume that $P_3 \cong 0.0$ psig. This makes the term A_oP_3 negligible since the magnitude of A_o is small.

$$\frac{M}{12g_c}\frac{d^2x}{dt^2} + K_d\frac{dx}{dt} = A_bP_2 + A_x(P_1-P_2) - K_cx - F_o \tag{28}$$

In order for the force balance to be satisfied,

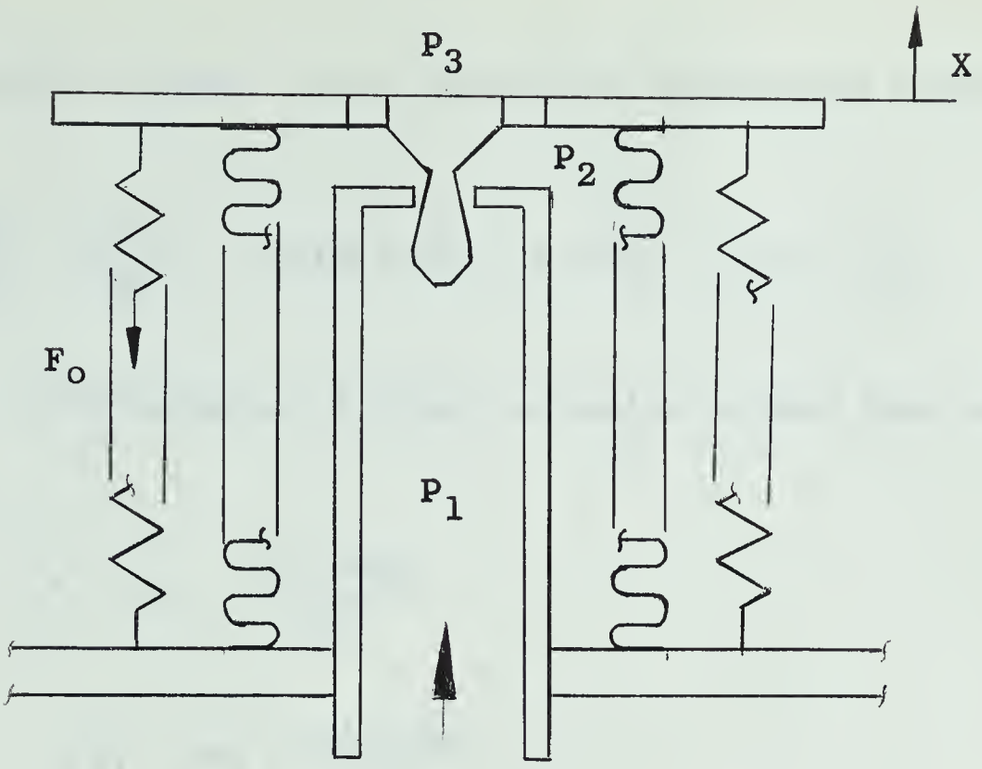

Figure 12

A_p = area of port (in^2)
A_o = area of neck of stem (in^2)
T = time (min)
t = time (sec)
X = stroke (ft)
x = stroke (in)
A_x = area of stem at a stroke x (in^2)
K_s = spring rate constant (lb_f/in)
K_c = combined spring rate constant of bellows and springs (lb_f/in)
F_o = initial force on the orifice plate at x = 0 (lb_f)
A_b = effective area of bellows (in^2)
a_b = effective area of bellows (ft^2)
V_o = volume of bellows at x = 0 (ft^3)
V_b = volume of bellows at time t (ft)
V = volumetric flow rate of fluid (ft^3/min)
W = mass flow rate of fluid (lb_m/min)
Q = flow rate (IGAL/min)
M = mass of moving parts of system (lb_m)
g_c = Newtons Law conversion factor $(lb_f\text{-}sec^2)/(ft\text{-}lb_m)$
ϕ = experimental constant that makes the force balance exact (dimensionless)
P_1 = inlet pressure to regulator (psig)
P_2 = bellows pressure (psig)
P_3 = outlet pressure (psig)
K_d = damping coefficient

a factor ϕ is added. This factor is determined experimentally.

$$\frac{M}{12g_c}\frac{d^2x}{dt^2} + K_d\frac{dx}{dt} = A_bP_2 + \phi A_x(P_1-P_2) - K_cx - F_o \qquad (29)$$

The material balance equation around the bellows is

$$W_i - W_o = \frac{d(\rho V_b)}{dT} \qquad (30)$$

$$\rho V_i - \rho V_o = \frac{d(\rho V_b)}{dT} \qquad (31)$$

Assume ρ is constant since the fluid is liquid.

$$Q_i - Q_o = 6.23\frac{dV_b}{dT} \qquad (32)$$

$$V_b = V_o + a_bx \qquad (33)$$

$$V_b = V_o + \frac{A_bx}{1728} \qquad (34)$$

$$T = \frac{t}{60} \qquad (35)$$

Substitute and simplify

$$Q_i - Q_o = 0.216\ A_b\frac{dx}{dt} \qquad (36)$$

The orifice equation was used to describe Q_i and Q_o,

$$Q_i = 38.1\ C_{dv}(A_p - A_x)\ \sqrt{P_1 - P_2} \tag{37}$$

$$Q_o = 38.1\ C_{do}\ A_{or}\ \sqrt{P_2} \tag{38}$$

where C_{dv} and C_{do} are the discharge coefficients of the valve and orifice respectively.

Let $C_v = 38.1\ C_{do} A_{or}$. The value of C_v is a constant for any flow rate.

$$Q_o = C_v\ \sqrt{P_2} \tag{39}$$

These equations were scaled for the analog computer. The solution was slowed down by a factor of 60 which means that the computer simulated 1 second of real time in 60 seconds.

The actual simulation was done in the following manner:

(1) Integrate equation (29) and generate dx/dt and x.

(2) From equation (36) and equation (39) generate Q_i.

$$Q_i = 0.216\ a_b \frac{dx}{dt} + C_v\ \sqrt{P_2} \tag{40}$$

(3) From equation (37) generate P_2

$$Q_i^2 = \left[38.1\ C_{dv}(A_p - A_x)\right]^2\ (P_1 - P_2) \tag{41}$$

$$P_2 = P_1 - \left[\frac{Q_i}{38.1\ C_{dv}(A_p - A_x)}\right]^2 \tag{42}$$

(4) Insert shape of stem in function generator.

The value of C_{dv} was determined experimentally and was found to be constant for a set flow rate. The value of C_v was determined experimentally and also was found to be relatively constant.

The analog circuit used for the simulation is shown in Figure 13.

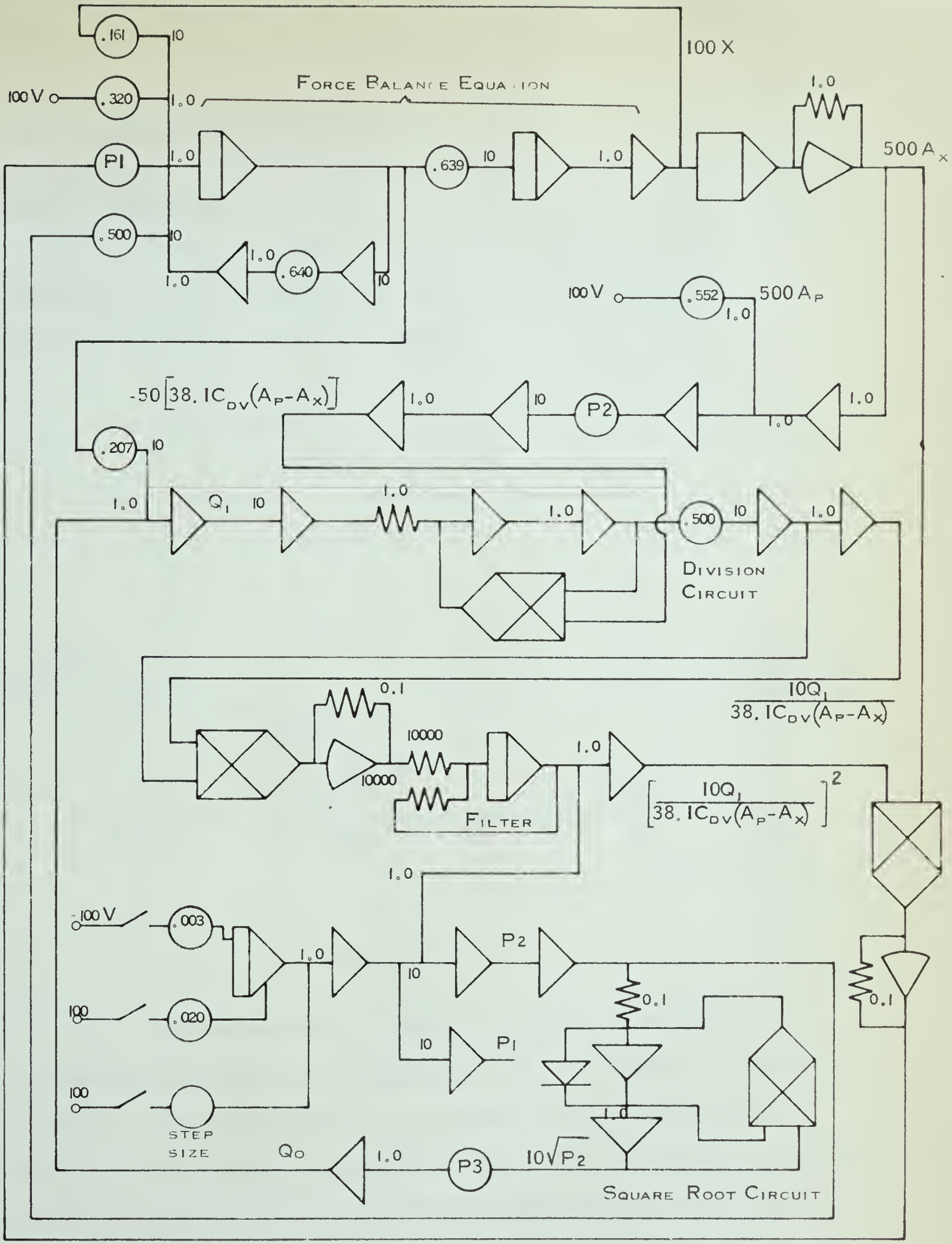

Set Flow	P1	P2	P3
0.94	0.30	0.236	0.0232
2.42	0.404	0.263	0.0635
4.72	0.448	0.263	0.138
7.42	0.532	0.263	0.252
9.94	0.608	0.274	0.393

ANALOG CIRCUIT
FLOW REGULATOR

Figure 13

Analysis of a Flow Control Loop

General Analysis

Figure 14 shows a schematic drawing of the feedback control system that is commonly utilized to regulate the flow rate of a fluid.

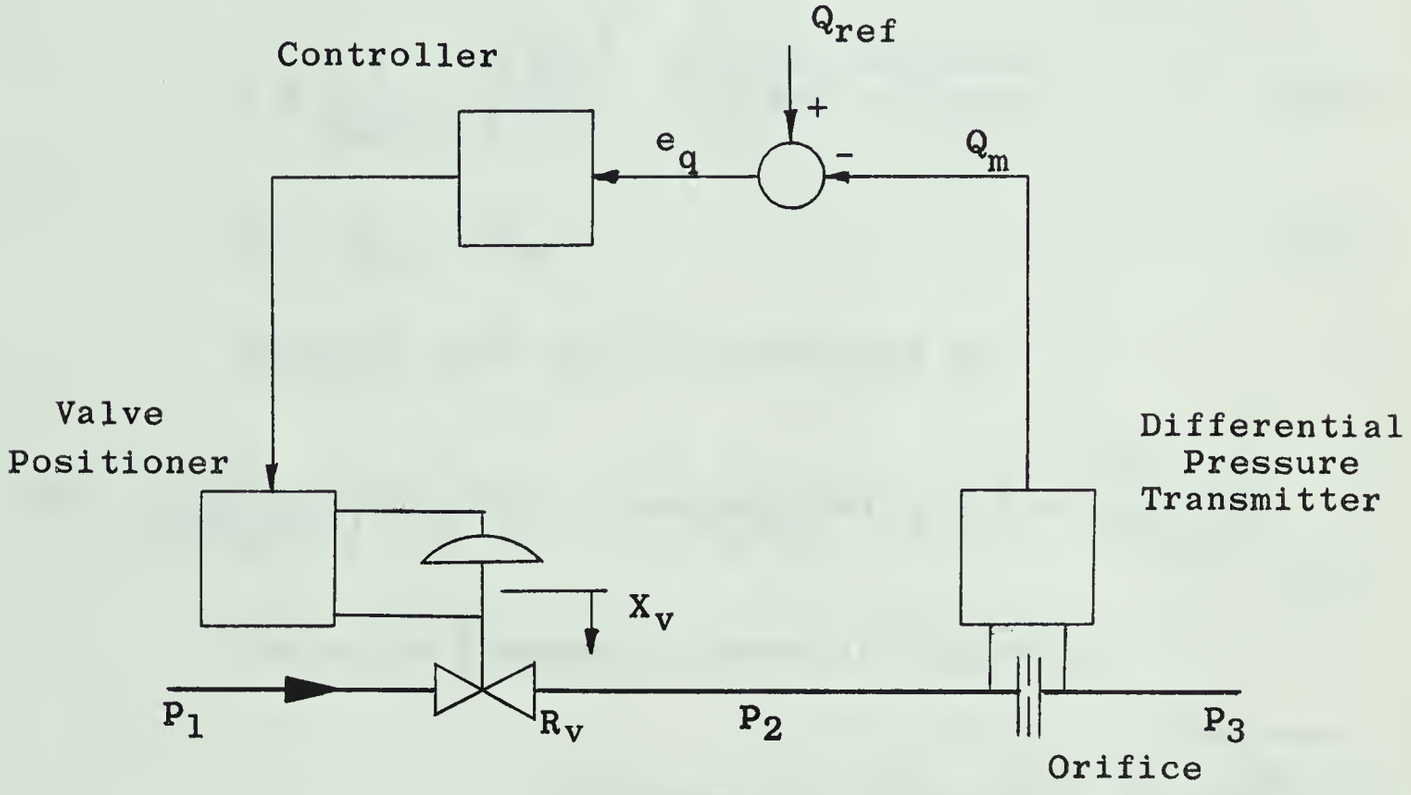

Figure 14

Disturbances of either P_1 or P_3 cause flow disturbances which are compensated for by the flow control system. The valve setting X_v determines the resistance R_v which in turn causes a pressure drop P_1-P_2 which is deducted from the total hydraulic driving force to bring about the flow Q.

To regulate the flow Q, an orifice or some other flow measuring means is located in the pipe. The differential pressure P_2-P_3 generates the measured flow Q_m. The measured flow Q_m is compared with a reference value Q_{ref} and the error e_q is used to adjust the position of the control valve.

Two equations for the system are shown below.

$$Q = \frac{1}{R_v(x_v)} \left(\frac{2g}{\rho}\right)^{\frac{1}{2}} \sqrt{(P_1-P_3) - (P_2-P_3)} \tag{43}$$

$$e_q = Q_{ref} - Q_m \tag{44}$$

Equation (43) can be linearized by

$$dQ = \left(\frac{\partial Q}{\partial (P_1-P_3)}\right) d(P_1-P_3) + \left(\frac{\partial Q}{\partial P_2-P_3}\right) d(P_2-P_3) + \left(\frac{\partial Q}{\partial X_v}\right) dX_v \tag{45}$$

The block diagram is shown in Figure 15.

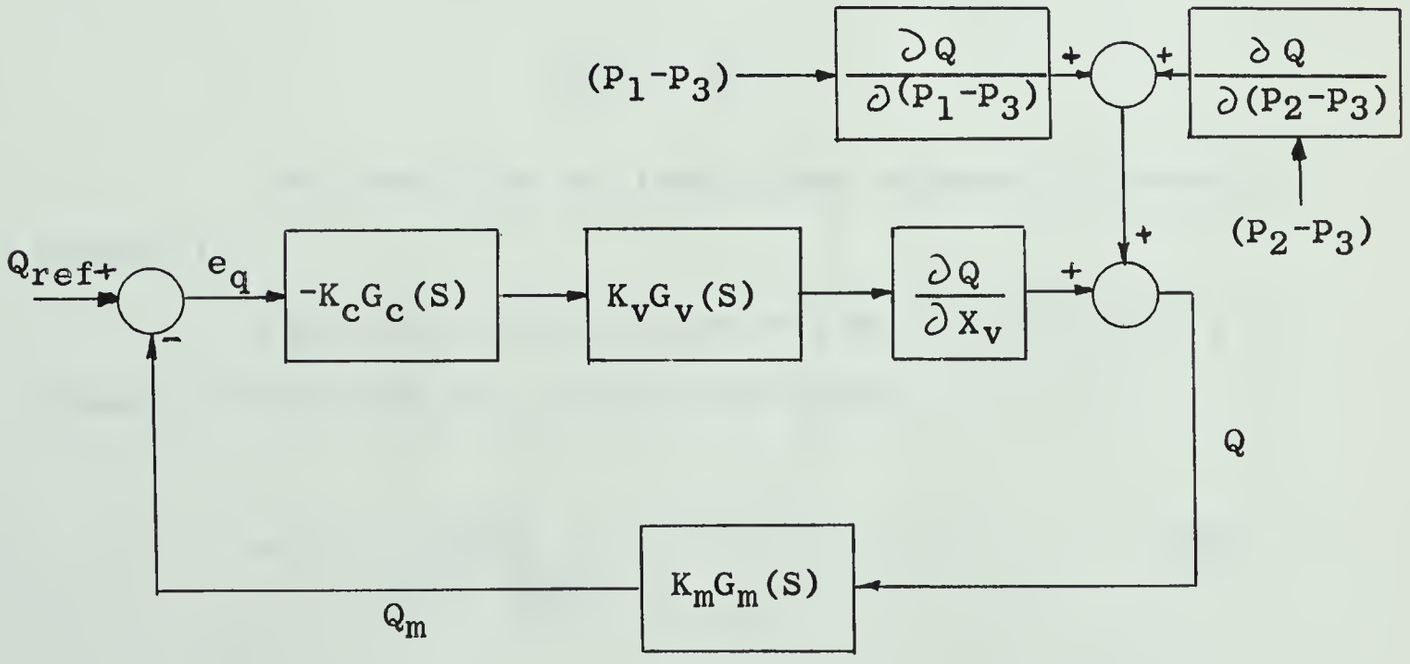

Figure 15

Suppose the disturbance is only (P_1-P_3) and that there are lags in the transmission of the signal to and from the controller which have a transfer function $G_L(S)$. Figure 16 indicates the resulting block diagram.

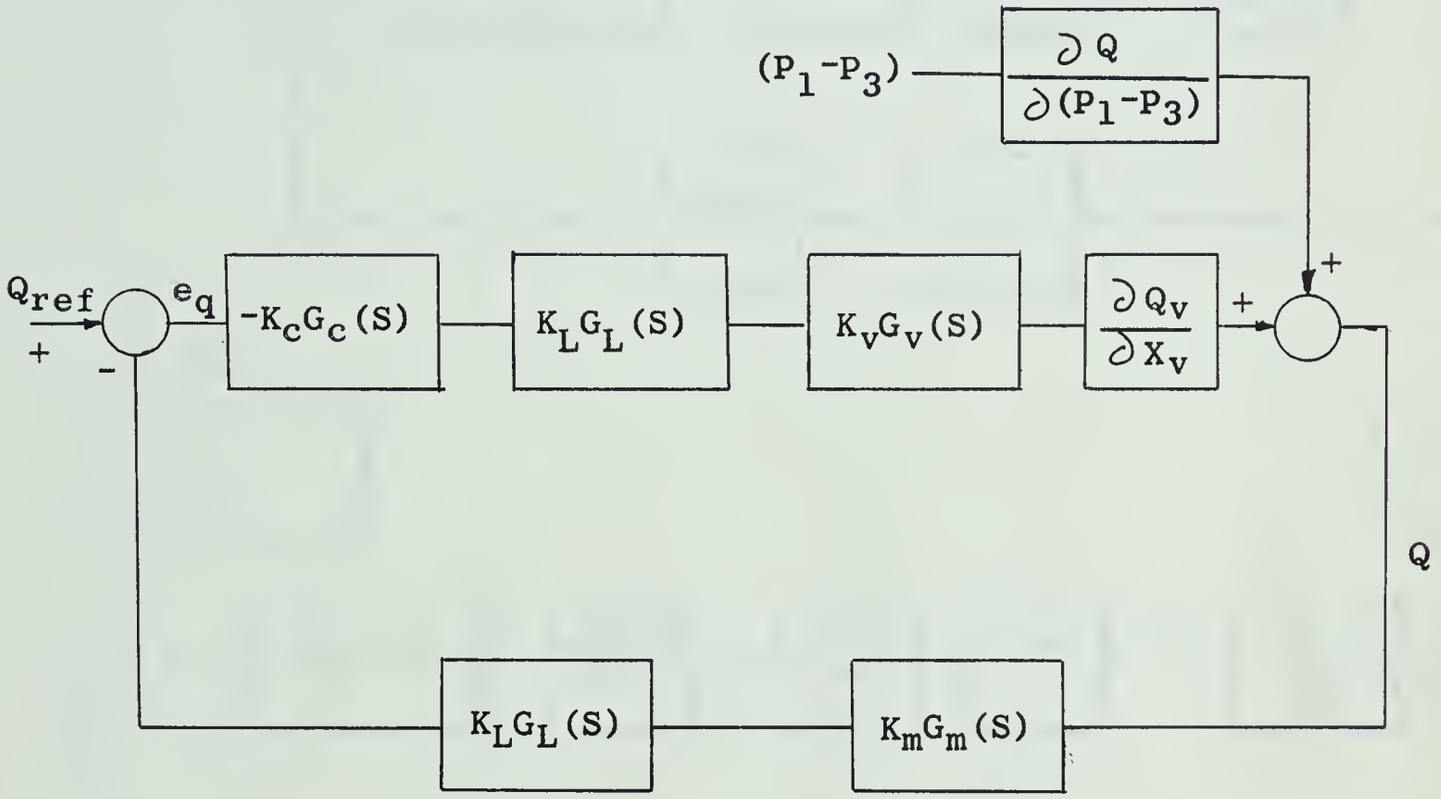

Figure 16

The reduction of this block diagram is shown in Figure 17.

The closed loop transfer function of Q for a change in load (P_1-P_3) is derived below.

$$e_1 = \frac{Qref}{G_L(S)\ G_m(S)} - Q \qquad (46)$$

BLOCK DIAGRAM REDUCTION

Figure 17

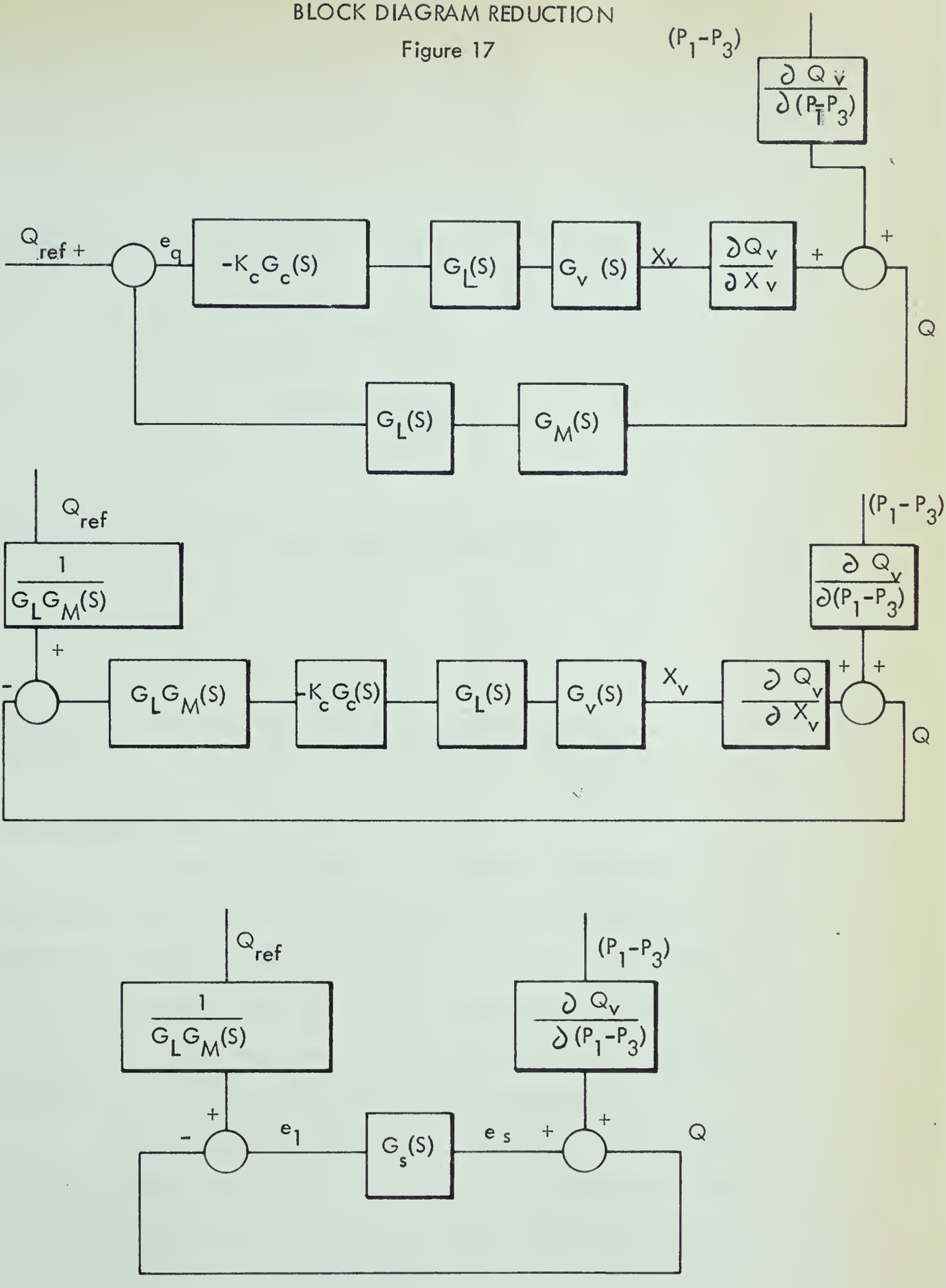

$$e_s = G_s(S)\left(\frac{Q_{ref}}{G_L(S)\ G_m(S)} - Q\right) \tag{47}$$

$$Q = -G_s(S)Q + \frac{G_s(S)\ Q_{ref}}{G_L(S)\ G_m(S)} + (P_1-P_3)\ \frac{\partial Q_v}{\partial(P_1-P_3)} \tag{48}$$

Assume Q_{ref} is constant

$$\frac{Q}{(P_1-P_3)} = \frac{\partial Q/\partial(P_1-P_3)}{1 + G_s(S)} \tag{49}$$

$$G_s(S) = -K_c G_c(S)\ \ G_L(S)\ G_m(S)\ G_v(S)\ \frac{\partial Q_v}{\partial x_v}\ G_L(S) \tag{50}$$

$$\frac{Q}{(P_1-P_3)} = \frac{\dfrac{\partial Q_v}{\partial(P_1-P_3)}}{1 - KK_c\ G_c(S)\ G_L{}^2(S)\ G_m(S)\ G_v(S)\ \dfrac{\partial Q_v}{\partial x_v}} \tag{51}$$

Detailed Analysis

In order to compare the dynamic response of the regulator with that of a flow control loop, the flow control loop was simulated on the analog computer. Some realistic transfer functions for the valve, measuring device, and transmission lags were required. A proportional integral controller was used as a basis for comparison.

Sections of an analysis of a flow loop in reference (5) were used in the simulation since the reference gave open loop frequency response plots for the flow loop components.

The following items will be discussed and the approximate transfer functions of the open loop frequency response plots will be derived:

(1) Metering

(2) Differential Pressure Transmitter

(3) Transmission lines

(4) Valve and Valve Positioner

Metering Section

If the density of the fluid was assumed constant, then the square-root relationship between flow and differential pressure will hold.

$$Q = K \sqrt{P_2 - P_3} \tag{52}$$

$$Q = K \sqrt{\Delta P_{2-3}} \tag{53}$$

$\Delta P_{2-3} = P_2 - P_3$

K = constant

When $Q = Q_{max}$ $\Delta P_{2-3} = (\Delta P_{2-3})_{max}$

$$Q_{max} = K \sqrt{(\Delta P_{2-3})_{max}} \tag{54}$$

Divide (53) by (54) and define

$$\beta = \frac{Q}{Q_{max}} \qquad \gamma = \frac{\Delta P_{2-3}}{\Delta (P_{2-3})_{max}} \tag{55}$$

$$\beta = \sqrt{\gamma} \tag{56}$$

The gain of the metering section is equal to the derivative of the percentage differential with respect to percentage flow

$$\frac{d\gamma}{d\beta} = 2\beta \qquad (57)$$

Inasmuch as the differential pressure is developed only because the fluid is experiencing a velocity change as it passes through the restriction, there is no phase lag. Instead, the flow change and resulting differential-pressure change are simultaneous effects.

Differential Pressure Transmitter

The response of the differential pressure transmitter to a change of flow is a function of a number of variables.

(1) Length and diameter of connecting pipe between instrument and pressure taps.

(2) Physical properties of fluid in connecting pipe.

(a) Liquid or gas
(b) Viscosity (if liquid)
(c) Specific gravity (if liquid)

(3) Volume transferred through connecting pipe for full differential change (cu. in./unit differential).

(4) Type of differential-pressure instrument,

(a) Diaphragm type
(b) Bellows type
(c) Mercury type
(d) U-tube type

The gain of the instrument can be determined as

follows:

$$\sigma = P_t - 3 \tag{58}$$

where P_t is the transmitter output

When $P_t = P_{t\ max}$ $\sigma = \sigma_{max}$

$$\frac{\sigma}{\sigma_{max}} = \frac{P_t - 3}{P_{t\ max} - 3} = \frac{\triangle P_{2-3}}{(\triangle P_{2-3})_{max}} \tag{59}$$

$$\frac{\sigma}{\sigma_{max}} = \frac{\triangle P_{2-3}}{(\triangle P_{2-3})_{max}} \tag{60}$$

The gain is determined by differentiating equation (60).

$$d\left(\frac{\sigma}{\sigma_{max}}\right) = d\left(\frac{(\triangle P_{2-3})}{(\triangle P_{2-3})_{max}}\right) \tag{61}$$

$$\text{Gain} = \frac{d\left(\sigma / \sigma_{max}\right)}{d\left((\triangle P_{2-3})/(\triangle P_{2-3})_{max}\right)} \tag{62}$$

Only the diaphragm type differential-pressure transmitter will be considered. It may be assumed to exhibit the following behavior:

(1) A volume change of 0.05 cubic inches is encountered during a full range change of outlet pressure.

(2) A period of 0.92 seconds is required for the output to reach 63% of its final value.

The open loop frequency response curve can be represented by a quadratic lag (Figure 29.3, Reference 5). The resonant peak occurs at a frequency of 350 cycles per minute (CPM). The height of the resonant peak, M_p, is 1.6. The value of the damping constant, ζ, can be determined from the following equation:

$$M_p = \frac{1}{2\zeta\sqrt{1-\zeta^2}} \tag{63}$$

The undamped natural frequency, f_n, is related to the resonant frequency, f, by the relation

$$\frac{f}{f_n} = \sqrt{1-\zeta^2} \tag{64}$$

In this particular case, f_n = 371 CPM or 38.9 radians per second.

The general transfer function for a quadratic lag is:

$$G_m(S) = \frac{W_n^2}{S^2 + 2\zeta W_n S + W_n^2} \tag{65}$$

Substituting

$$G_m(S) = \frac{1512}{S^2 + 25.8S + 1512} \tag{66}$$

The gain and phase angle curves for the differential pressure transmitter are shown in Figures 18 and 19. These curves were generated on the digital computer.

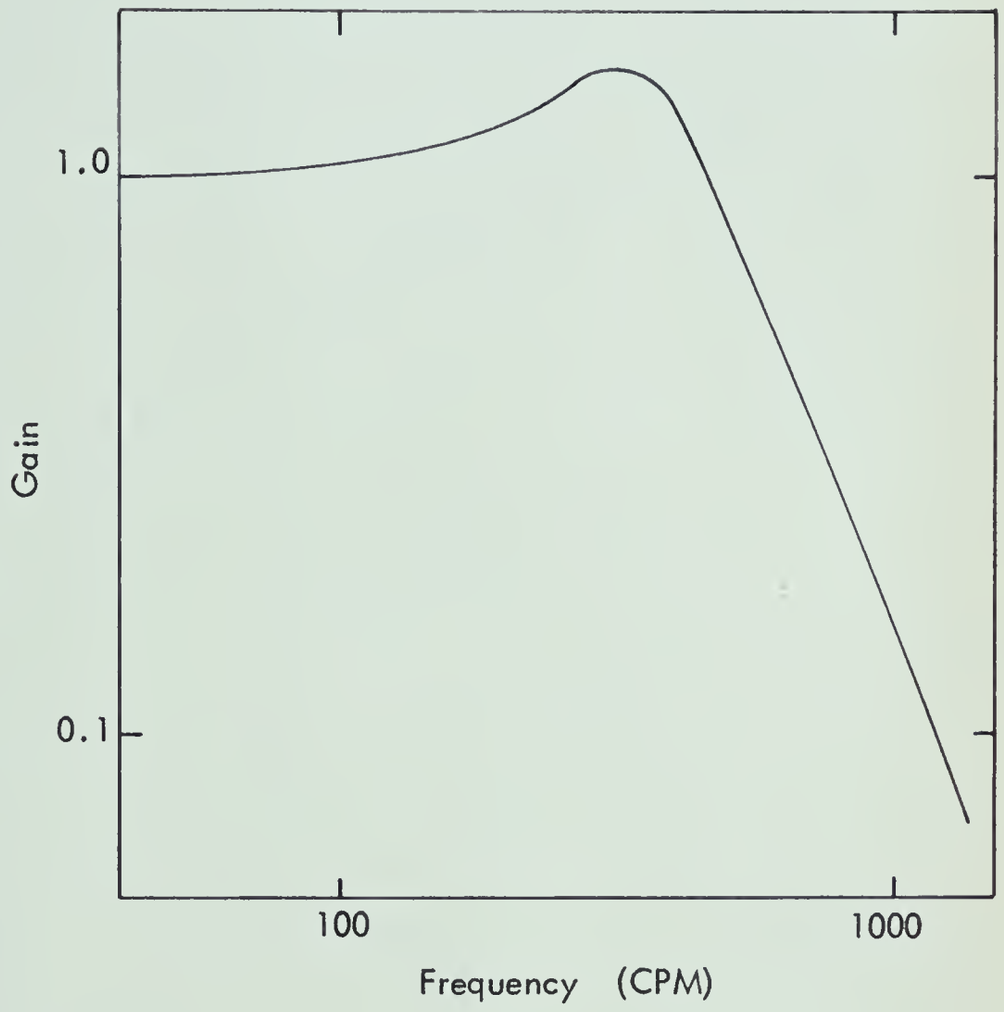

DIFFERENTIAL PRESSURE TRANSMITTER
GAIN VS FREQUENCY
Figure 18

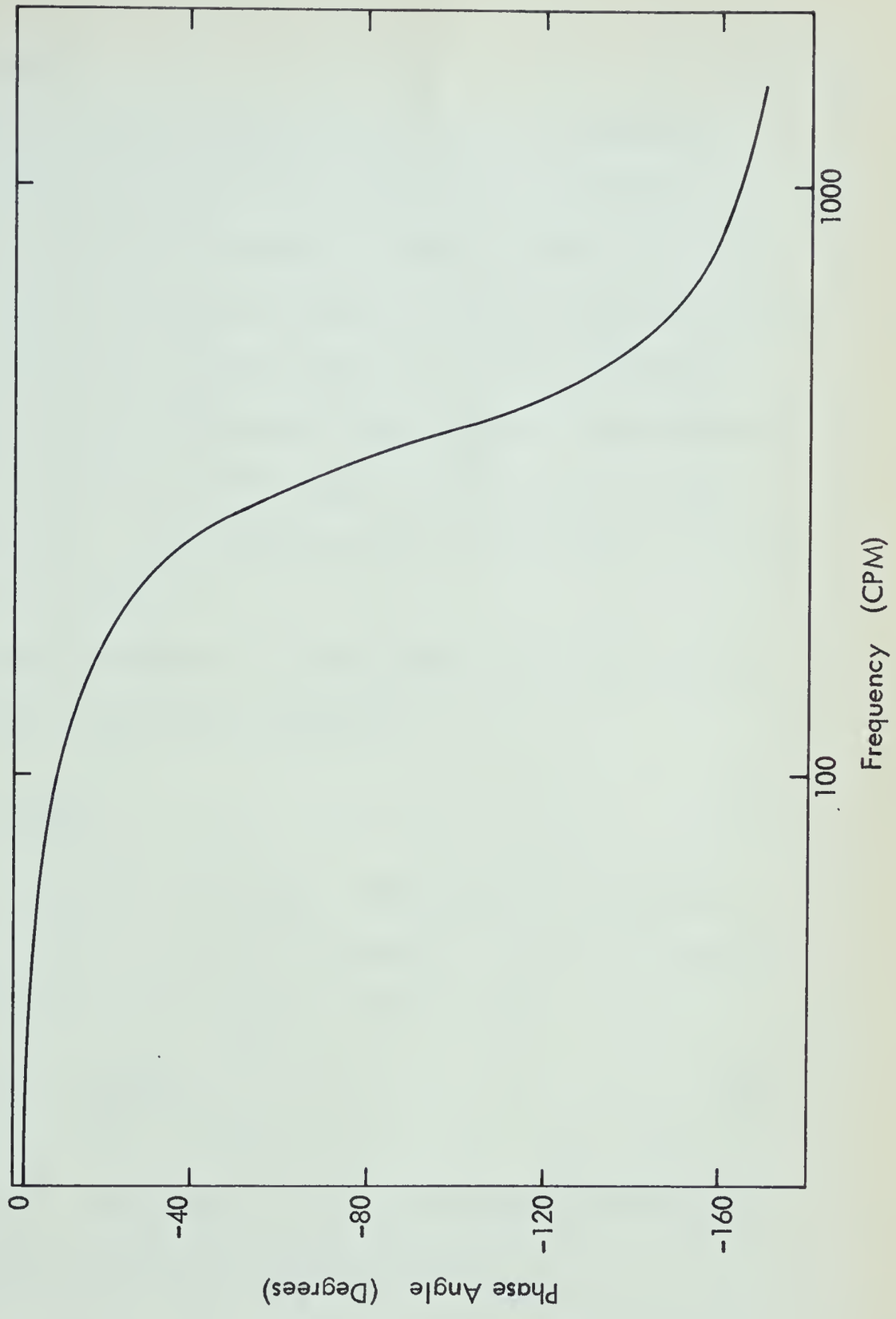

DIFFERENTIAL PRESSURE TRANSMITTER
PHASE VS FREQUENCY
Figure 19

Transmission Lines

In some cases, especially if the transmission lines to and from the controller are long, the effect of the lag of the transmitted signal is significant. In this analysis, 100 feet of $\frac{1}{4}$ inch outside diameter copper tubing, which terminates in a 2 cubic inch volume is considered.

The frequency response curve can be approximated by a first-order lag and a distance velocity lag (Figure 29.4, Reference 5). This analysis only considered it to be a first-order lag process.

The time constant of the first-order lag can be determined by the following equation:

$$T_L = \frac{1}{2\pi f_c} \tag{67}$$

where f_c is the corner frequency. The corner frequency is 95 cycles per minute. The time constant, T_L, is 0.1 second.

Therefore, the transfer function is

$$G_L(S) = \frac{1.0}{0.1S + 1} \tag{68}$$

The gain and phase of this transfer function is plotted in Figures 20 and 21 respectively.

Valve and Valve Positioner

Quite frequently, a valve positioner is added to a control valve to overcome friction from packing glands. This device ensures valve-stem motion in accordance with

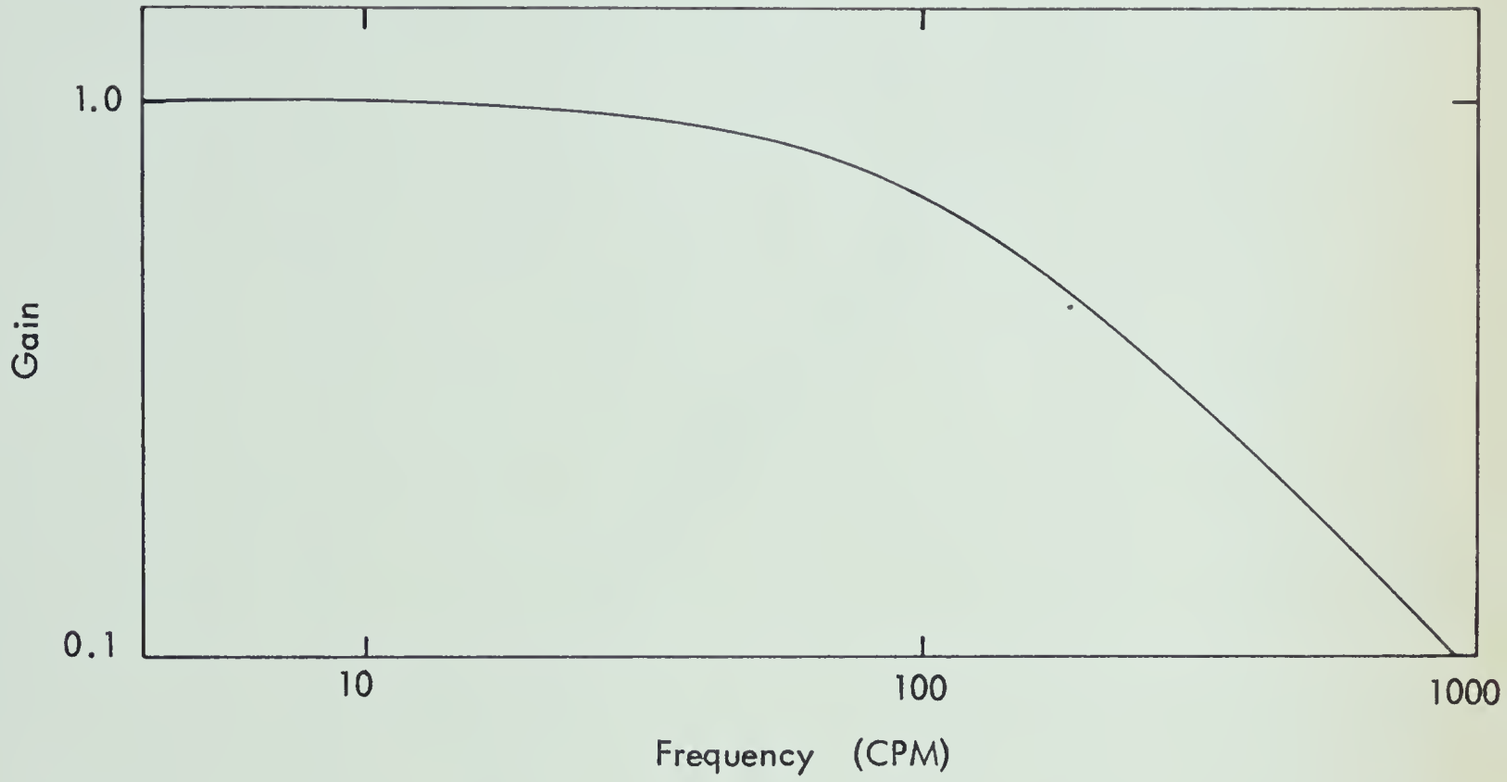

INSTRUMENT TRANSMISSION LINES
GAIN VS FREQUENCY
Figure 20

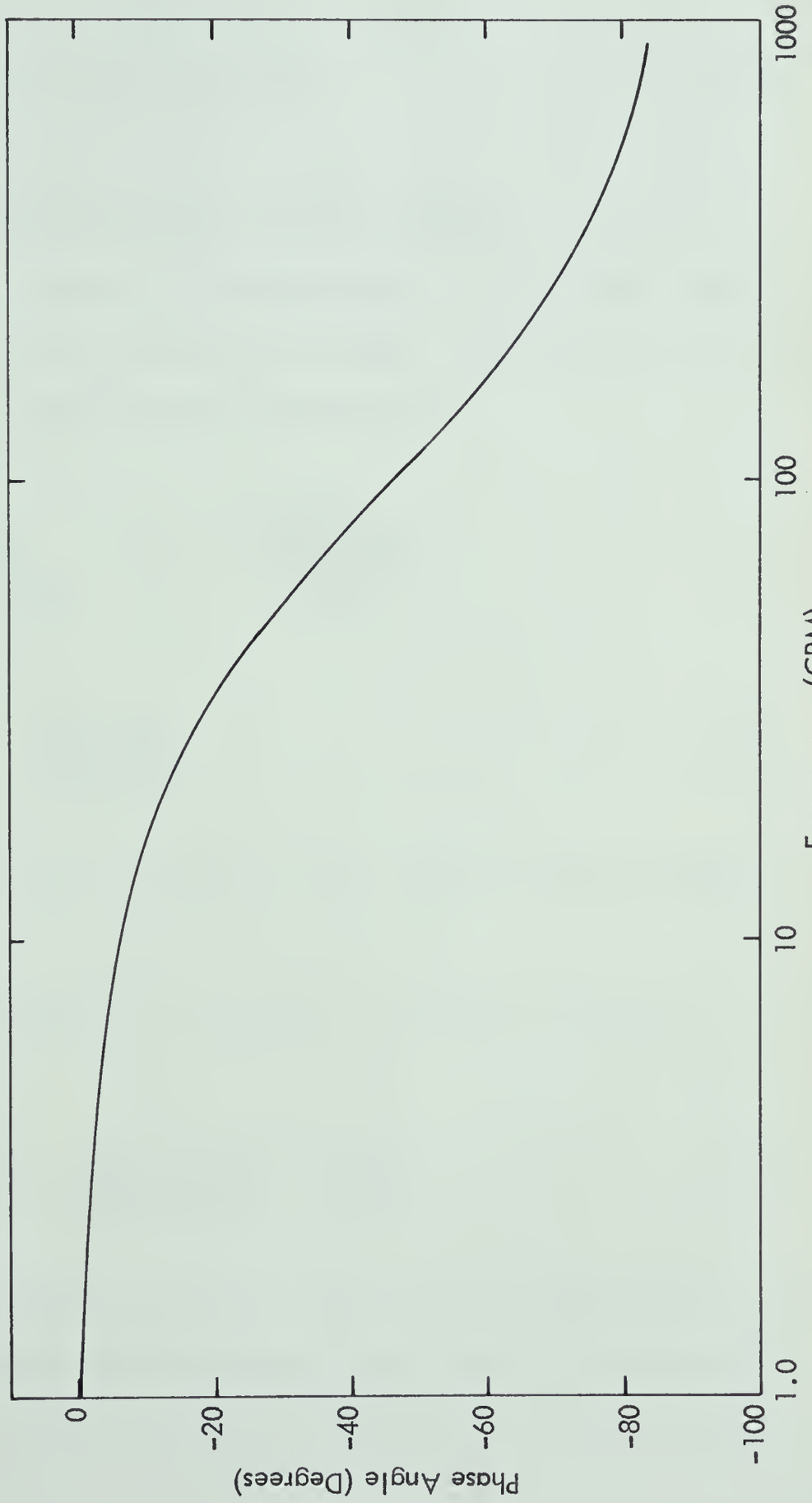

INSTRUMENT TRANSMISSION LINES
PHASE VS FREQUENCY
Figure 21

the controller output pressure. The gain of the valve positioner is

$$\text{Gain} = \frac{dX/X_{max}}{dP_c/(P_{c\ max}-3)} \tag{69}$$

where X is the stem travel of the valve,
P_c is the controller output pressure.

The control valve used was a bevel-disk valve which can be approximated by an equal percentage valve with $\alpha = 10$. The equation that applies is:

$$\frac{X_v}{(X_v)_{max}} = 1 + \frac{\ln \frac{C_v}{(C_v)_{max}}}{\ln \alpha} \tag{70}$$

where

$$\alpha = \frac{(C_v)_{max}}{(C_v)_{min}} \tag{71}$$

The curve of stem travel versus flow is shown in Figure 22.

The gain of the valve is defined using the equation:

$$\text{Gain} = \frac{d\left(Q'/(Q_{max})\right)}{d\left(X/(X_{max})\right)} \quad \frac{Q'_{max}}{Q_{max}} \tag{72}$$

The ratio Q'_{max}/Q_{max} corrects the gain of the valve in the event its maximum flow differs from that of the metering section. In order to determine the gain, a tangent is

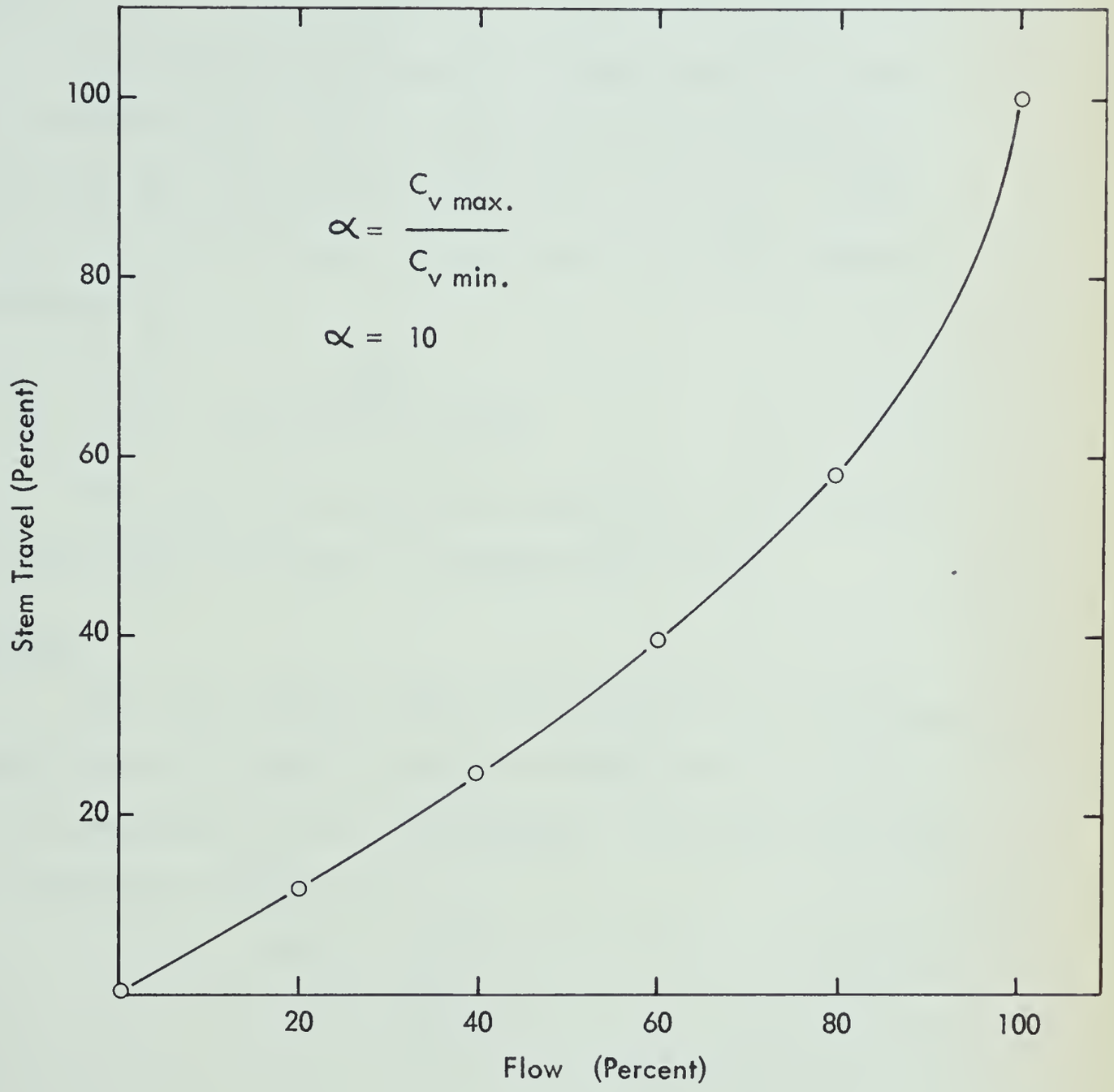

FLOW VS STEM TRAVEL: ΔP = Constant
EQUAL PERCENTAGE VALVE
Figure 22

drawn at the point of expected use. Of course, there is no phase lag associated with the valve stem change and flow change.

The open loop frequency response curve of the valve and positioner can be approximated by a quadratic lag (Figure 29.5, Reference 5) with $M_p = 1.1$, $\zeta = 0.59$, and $W_n = 19.5$ radians/sec. The transfer function can be represented by

$$G_v(S) = \frac{380}{S^2 + 23.0S + 380} \qquad (73)$$

The gain and frequency curves for the valve and valve positioner are shown in Figures 23 and 24.

Simulation

The flow control loop was simulated on the analog computer directly from the transfer functions. A flow rate of 70% of maximum flow was considered. Therefore, the gain of the metering section was

$$\text{Gain} = 2\beta$$
$$= 2(0.7)$$
$$= 1.4$$

The slope of the valve stroke versus flow curve, as shown in Figure 22, equals 1.19 and since this particular valve was sized so that it is wide open when the flow meter indicated 100 percent, the gain is then equal to 1.19.

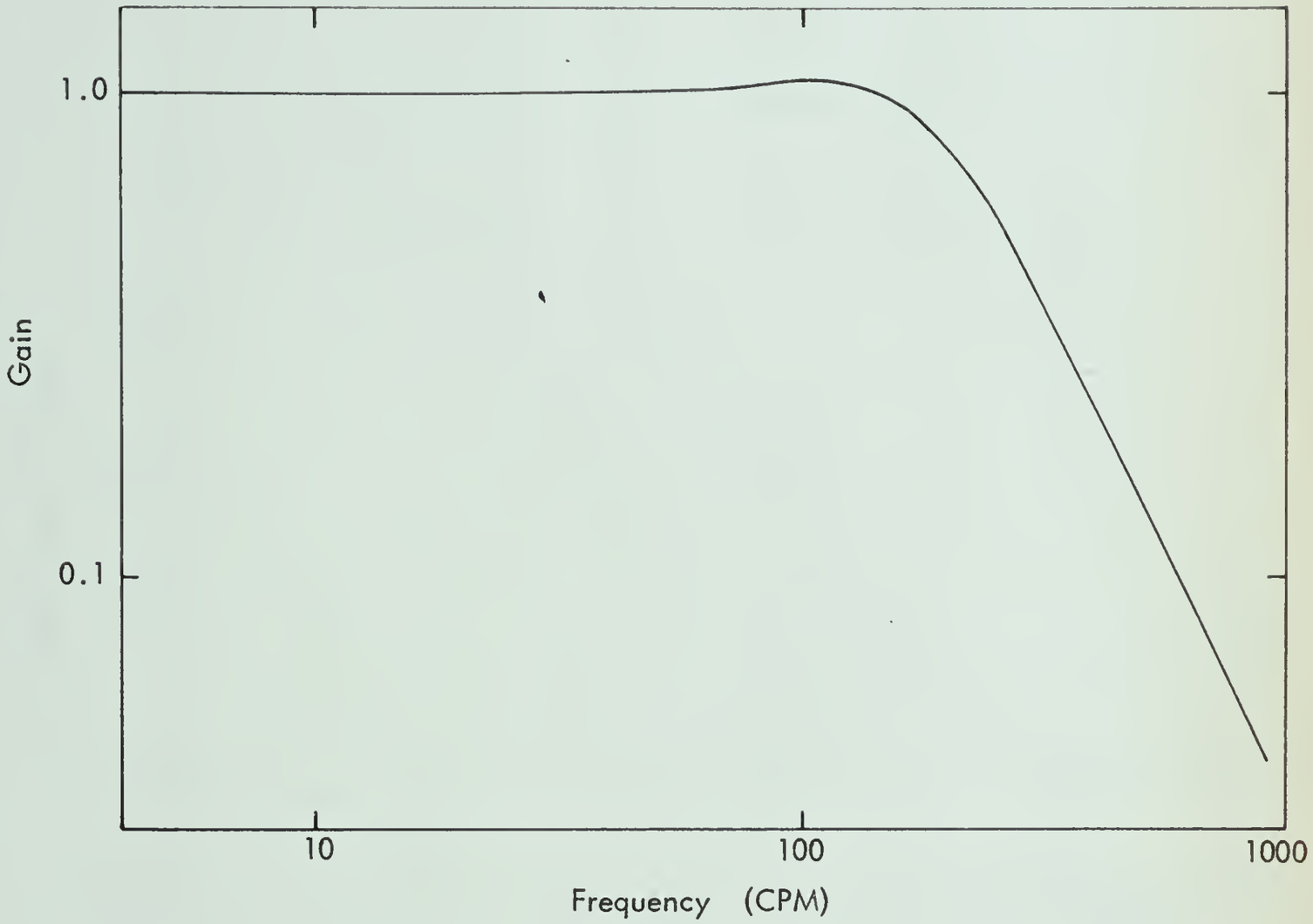

VALVE AND VALVE POSITIONER
GAIN VS FREQUENCY
Figure 23

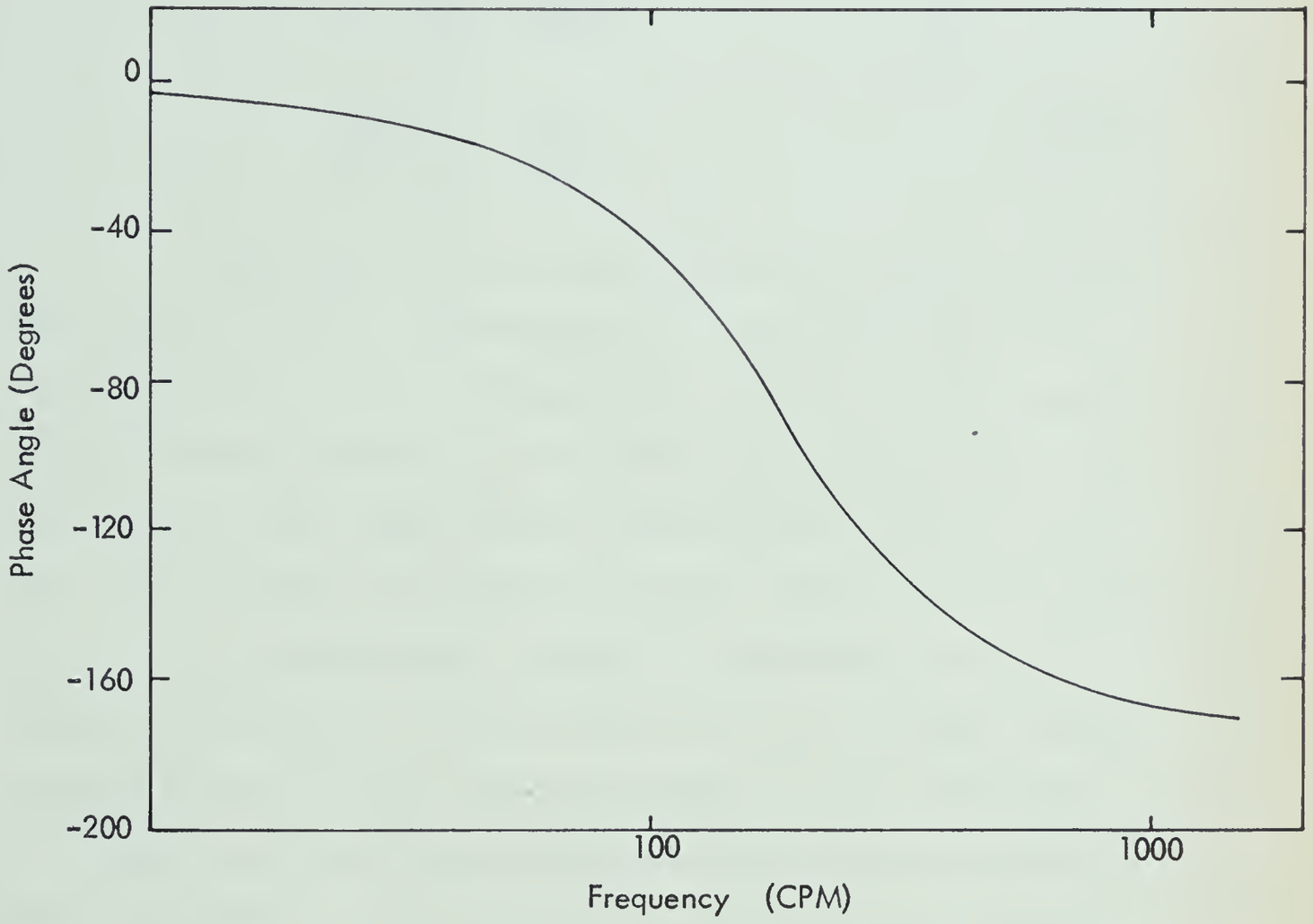

VALVE AND VALVE POSITIONER
PHASE VS FREQUENCY
Figure 24

The value of $\partial Q/\partial (P_1-P_3)$ was chosen in the following manner:

$$Q = C_v\sqrt{\triangle P} \tag{74}$$

$$C_v = \frac{Q}{\sqrt{\triangle P}} \tag{75}$$

$$\frac{\partial Q_v}{\partial \triangle P} = \frac{C_v}{\sqrt{\triangle P}} \tag{76}$$

Reference (5) did not supply the actual size of the control valve. Consequently, it was impossible to determine the value of $\partial Q_v/\partial \triangle P$. However, the value of $\partial Q_v/\partial \triangle P$ was calculated by arbitrarily setting the flow rate equal to 20 IGPM and the pressure drop equal to 30 psi. The value of $\partial Q_v/\partial \triangle P$ for these conditions is 0.667.

A proportional integral controller was used. The gain and reset rate were set to give a $\frac{1}{4}$ decay ratio. Figures 25 and 26 show the Bode plots of the controller. A further discussion concerning the settings is given in the discussion of the transient response of the system. Figure 27 shows the open loop phase versus frequency characteristics of the system.

Figure 28 shows the analog circuit for the simulation of the flow control loop.

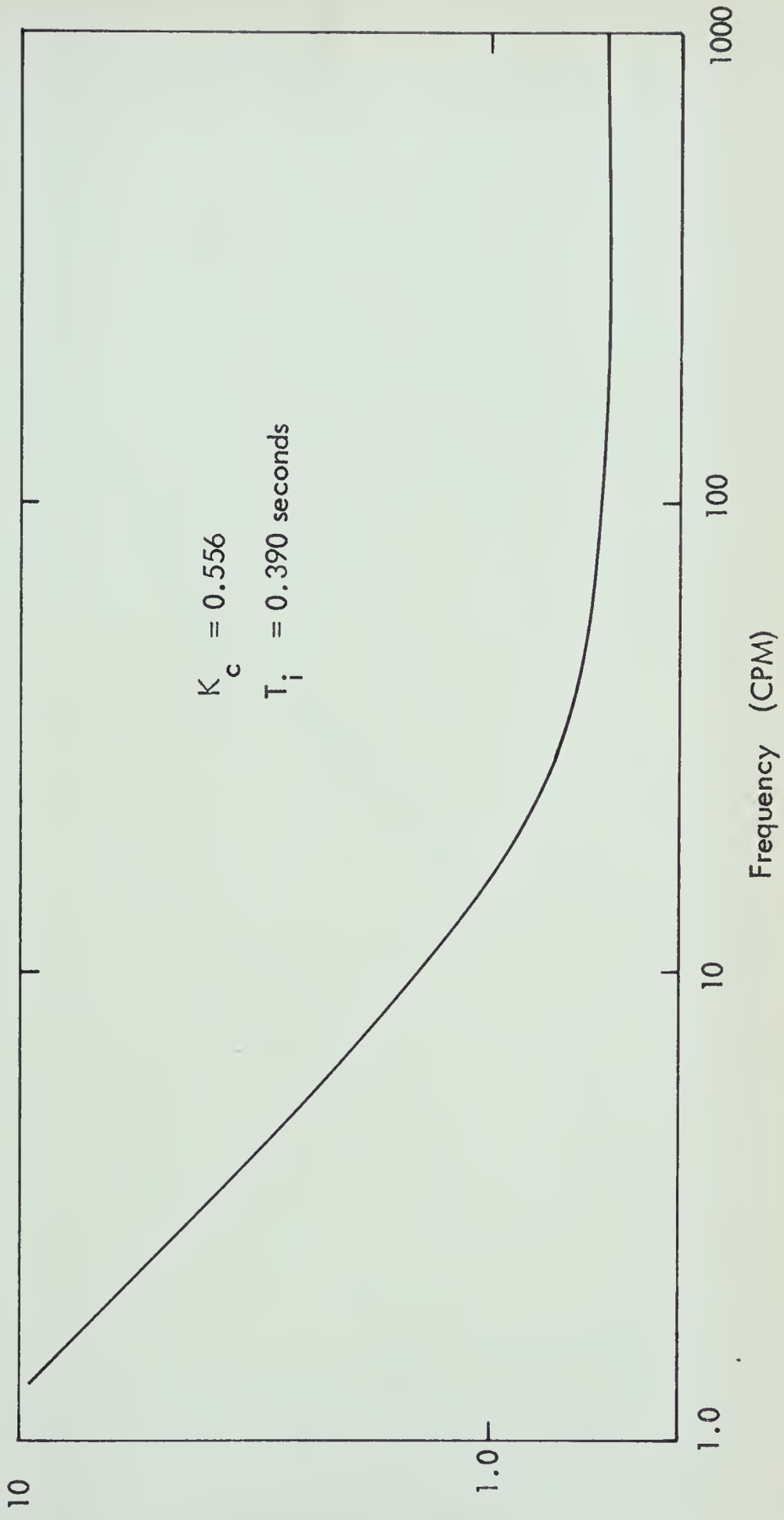

PROPORTIONAL RESET CONTROLLER
GAIN VS FREQUENCY
Figure 25

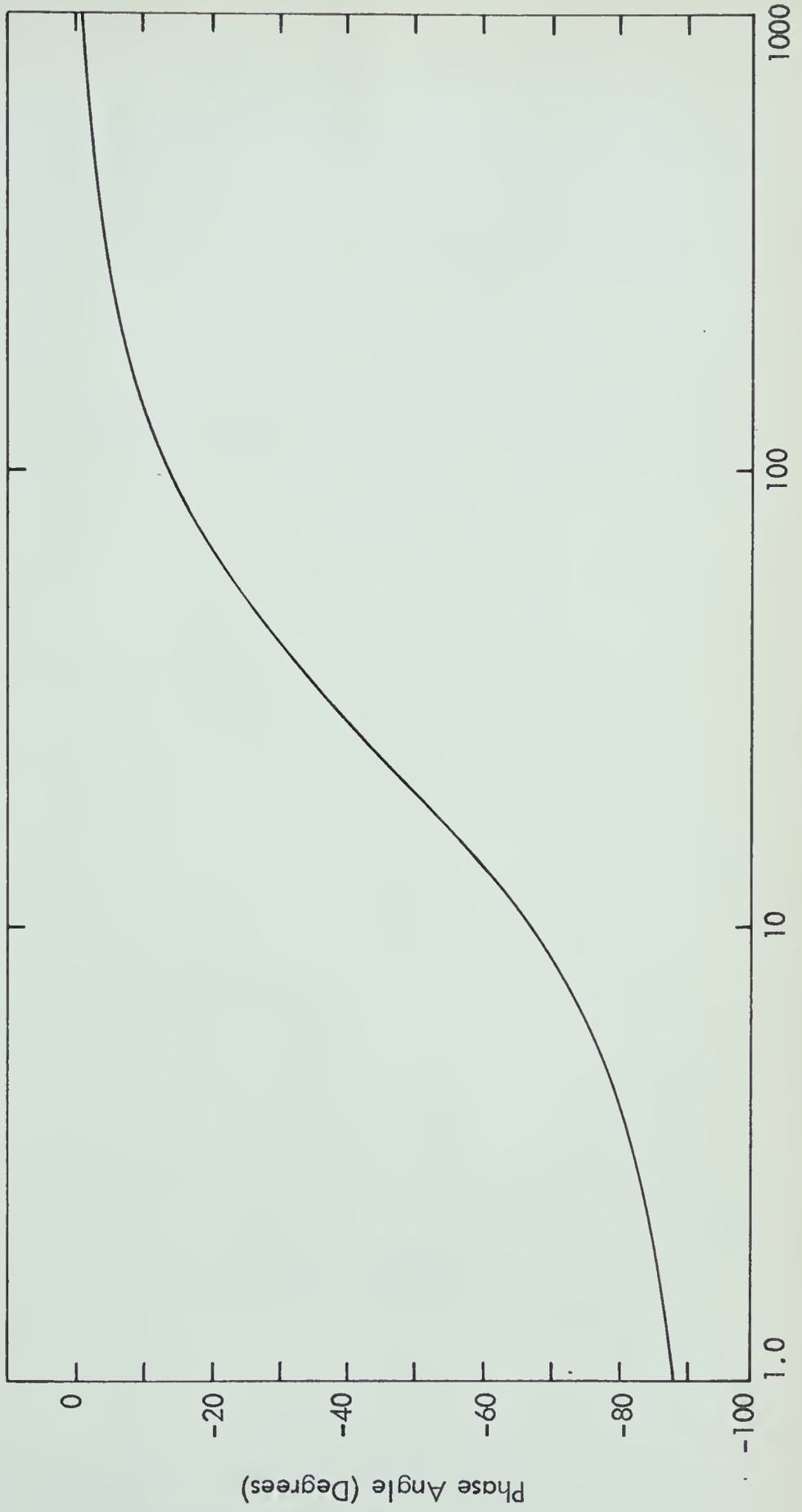

PROPORTIONAL RESET CONTROLLER
PHASE VS FREQUENCY
Figure 26

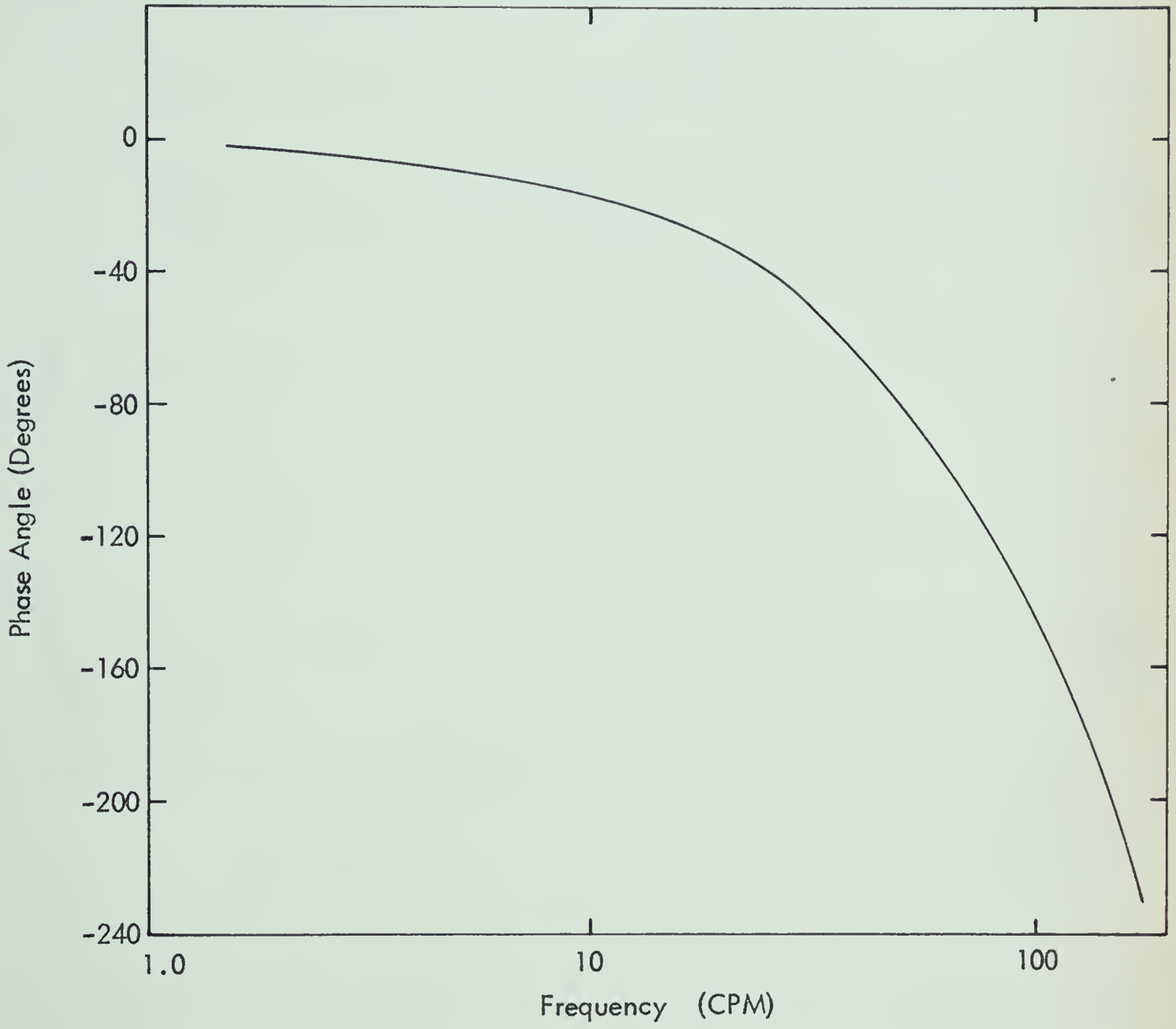

OPEN LOOP: EXCLUDING CONTROLLER
PHASE VS FREQUENCY
Figure 27

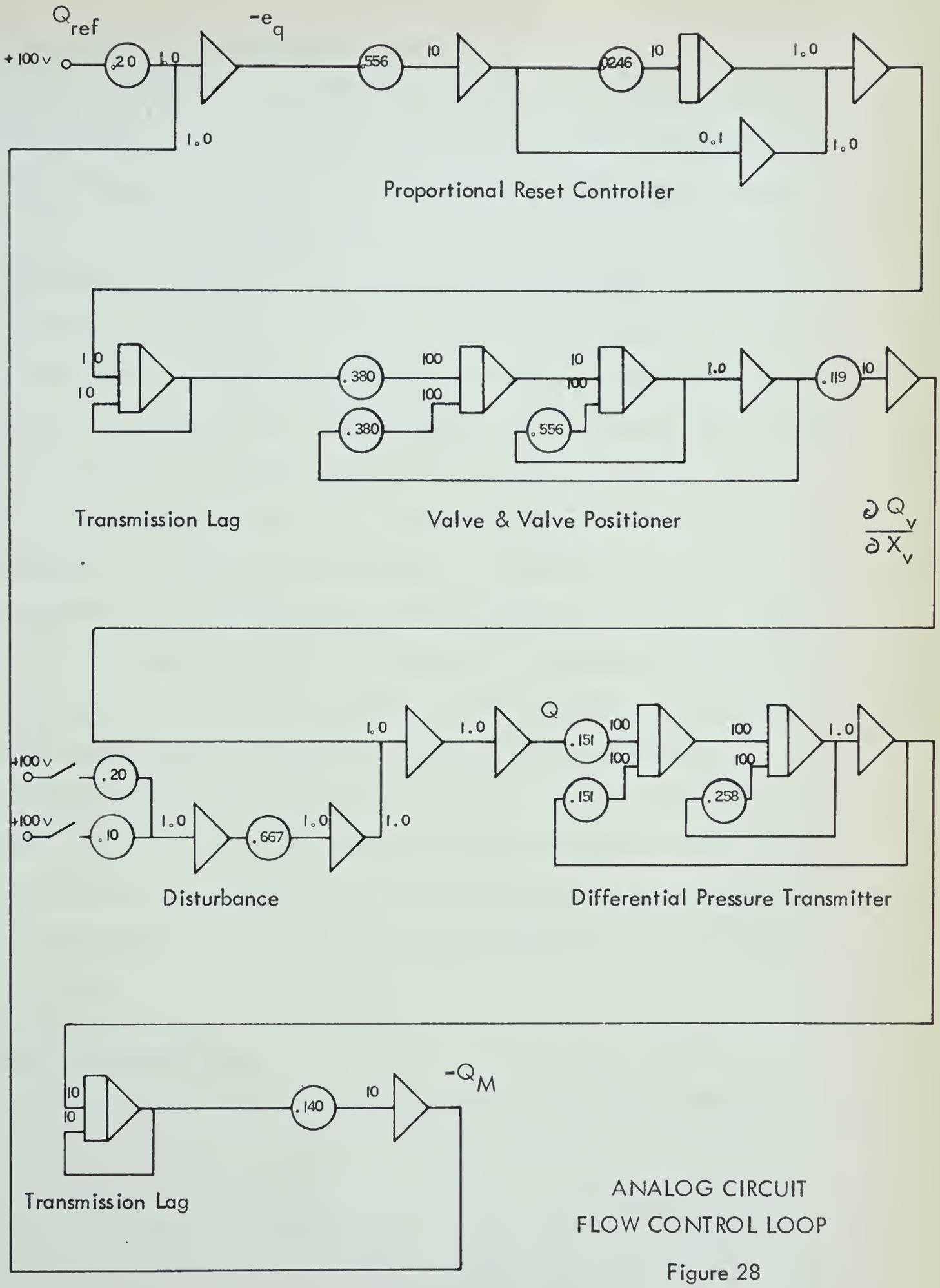

ANALOG CIRCUIT
FLOW CONTROL LOOP

Figure 28

Discussion of Experimental Results

Although a great deal of data was obtained from the experimental testing, only the results of the testing of the final design are shown. Throughout the experimental work, the regulator was tested over wide ranges of flow rates and differential pressures. The accuracy with which the regulator controlled the flow at the set value was a function of the range of the differential pressure and the range of flow rates. In other words, the greater the rangeability of these two variables, the more difficult it was to attain the accuracy specification. It was decided to design the regulator for flow rates between 1.0 IGPM to 10.0 IGPM. It was hoped that the regulator would control the flow within $\pm$1.0% of maximum flow for differential pressure variations of 25 psi to 150 psi. However, at the maximum flow rate, this accuracy was achieved only over the differential pressure range from 50 psi to 150 psi. Figure 29 shows the lower value of the differential pressure range. Below this value, the flow dropped off rather quickly. Also, above 150 psi differential the valve closed excessively and decreased the flow.

Experiment Results

The experimental results are shown in Table 1.

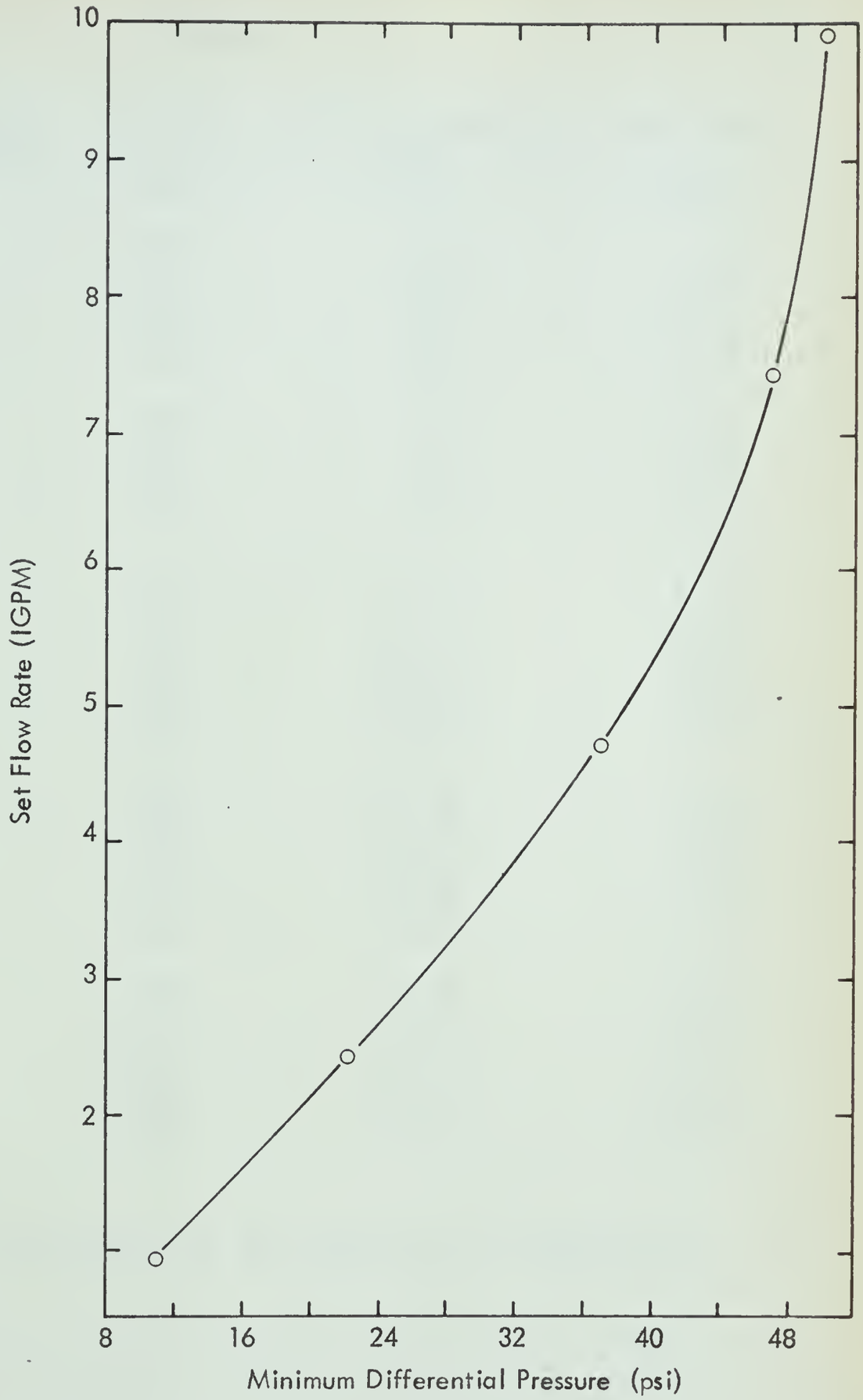

MINIMUM PRESSURE REQUIREMENT CURVE
SET FLOW RATE VS MINIMUM ΔP

Figure 29

TABLE 1

RUN NO.	DIFFERENTIAL PRESSURE (psi)	STROKE (in)	ORIFICE PRESSURE DROP (psi)	FLOW RATE (IGPM)
1	150	0.22	5.90	9.82
2	125	0.19	6.12	9.94
3	100	0.16	6.33	10.04
4	75	0.13	6.80	10.04
5	50	0.09	6.90	9.84
6	150	0.28	8.30	7.34
7	125	0.26	8.73	7.47
8	100	0.22	8.93	7.51
9	75	0.19	8.93	7.45
10	50	0.15	8.62	7.33
11	150	0.34	10.88	4.62
12	125	0.33	11.55	4.72
13	100	0.31	12.10	4.80
14	75	0.28	12.20	4.80
15	50	0.25	11.87	4.74
16	40	0.20	11.33	4.64
17	150	0.40	13.18	2.32
18	125	0.39	14.02	2.40
19	100	0.36	14.92	2.45
20	75	0.35	15.48	2.50
21	50	0.34	15.58	2.50
22	25	0.26	13.93	2.35
23	150	0.43	14.38	0.88
24	125	0.43	15.58	0.92
25	100	0.42	16.45	0.95
26	75	0.41	17.65	0.98
27	50	0.39	18.10	0.98
28	25	0.37	17.43	0.95

The performance of the regulator is summarized in Table 2.

TABLE 2

AVERAGE FLOW RATE (IGPM)	MINIMUM DIFFERENTIAL PRESSURE (psi)	MAXIMUM DIFFERENTIAL PRESSURE (psi)	MAXIMUM FLOW VARIATION (IGPM)	ACCURACY BASED ON A FLOW OF 10.0 IGPM (± %)
9.94	50	150	0.22	1.1
7.42	47	150	0.18	0.9
4.72	37	150	0.18	0.9
2.42	25	150	0.18	0.9
0.94	25	150	0.10	0.5

With the exception of the highest flow rate, the accuracy was within the ±1.0% specification. The measurement of flow was accurate to approximately ±0.1%. Therefore, it can be said that the regulator's accuracy over the above flow range and differential pressure range was approximately ±1.0%.

There was no hysteresis present in the final design. Consequently, it was immaterial whether the results were obtained from increasing or decreasing the differential pressure. The results were also repeatable within the accuracy of the measurement.

The accuracy of the maximum and minimum pressure measurements was ±1.5 psi based on the accuracy of the Marsh gauge. However, the gauges were calibrated prior to taking these measurements.

The accuracy of the orifice pressure drop measurement was ±0.5% of the full range of the differential pressure transmitter. Therefore, the variable was accurate to within 0.10 psi. Again, this instrument was calibrated over its

entire pressure differential pressure range.

The measurement of the stroke was not as accurate as it possibly could have been. The actual value would be within 0.01 inch.

The results are presented in graph form in Figures 30, 31, and 32. Figure 30 shows the plot of flow rate versus differential pressure. All the flow curves pass through a maximum. The flow drops off gradually for high differential pressures and very rapidly for low differential pressures. Figure 31 shows the flow rate versus stroke curves. For each set flow rate, the regulator utilizes approximately $\frac{1}{4}$ of the total stroke. Figure 32 indicates the orifice pressure drop versus stroke. These curves pass through a maximum pressure drop and the maximum becomes more pronounced as the flow rate decreases.

The reason for the maxima in the orifice differential pressure, and hence the flow rate curve arises from the non-linear force exerted by the incoming fluid on the valve stem. That is to say, the term $A_x(P_1-P_2)$ is non-linear. As explained in the design of the valve stem, if P_2 is to remain constant, then from equation (16)

$$\left| \frac{K_c X}{A_b - \phi A_x} \right| = \left| \frac{\phi A_x P_1}{A_b - \phi A_x} \right|$$

Therefore

$$|K_c X| = |\phi A_x P_1| \qquad \text{for } P_2 = \text{constant.}$$

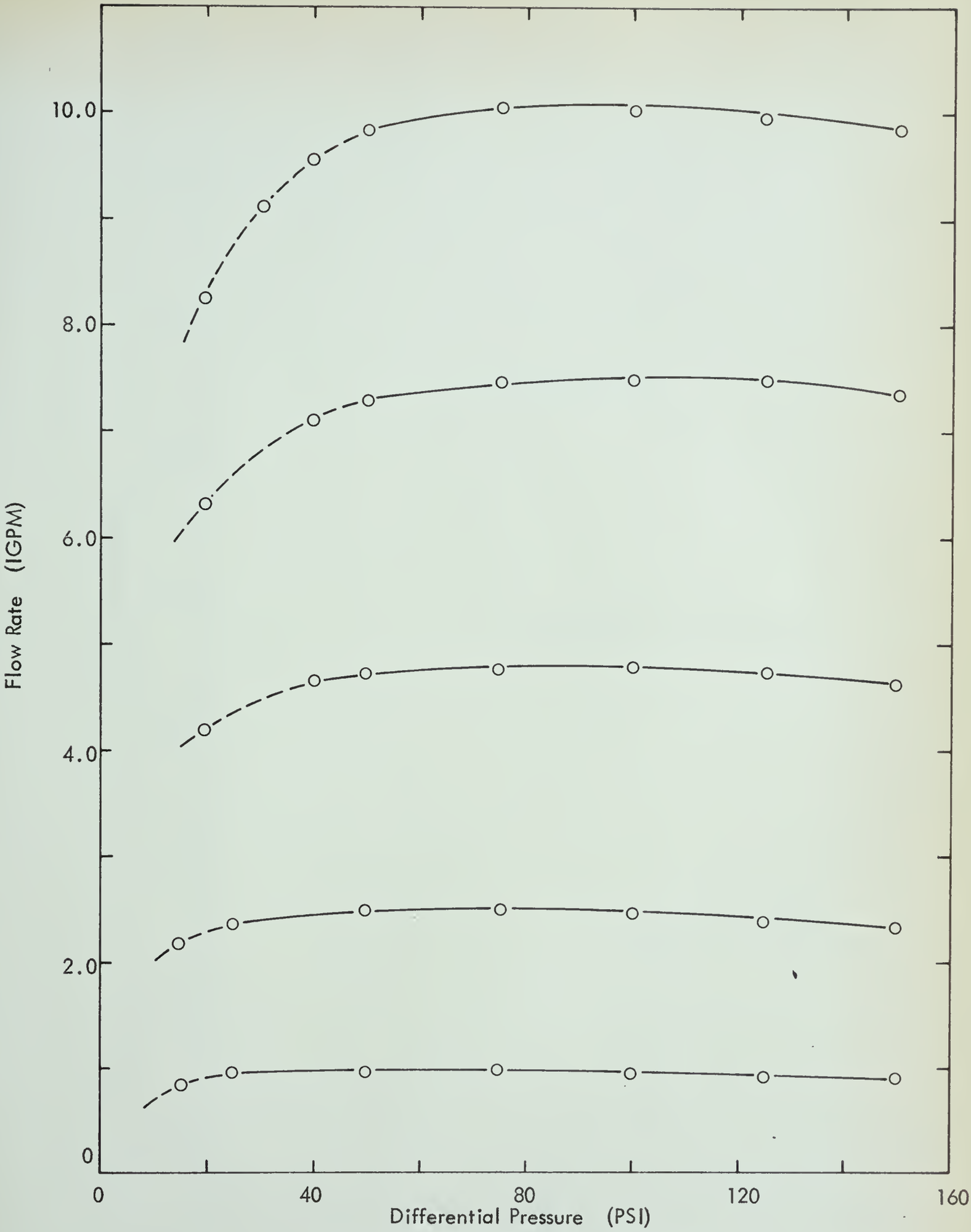

FLOW RATE VS DIFFERENTIAL PRESSURE

Figure 30

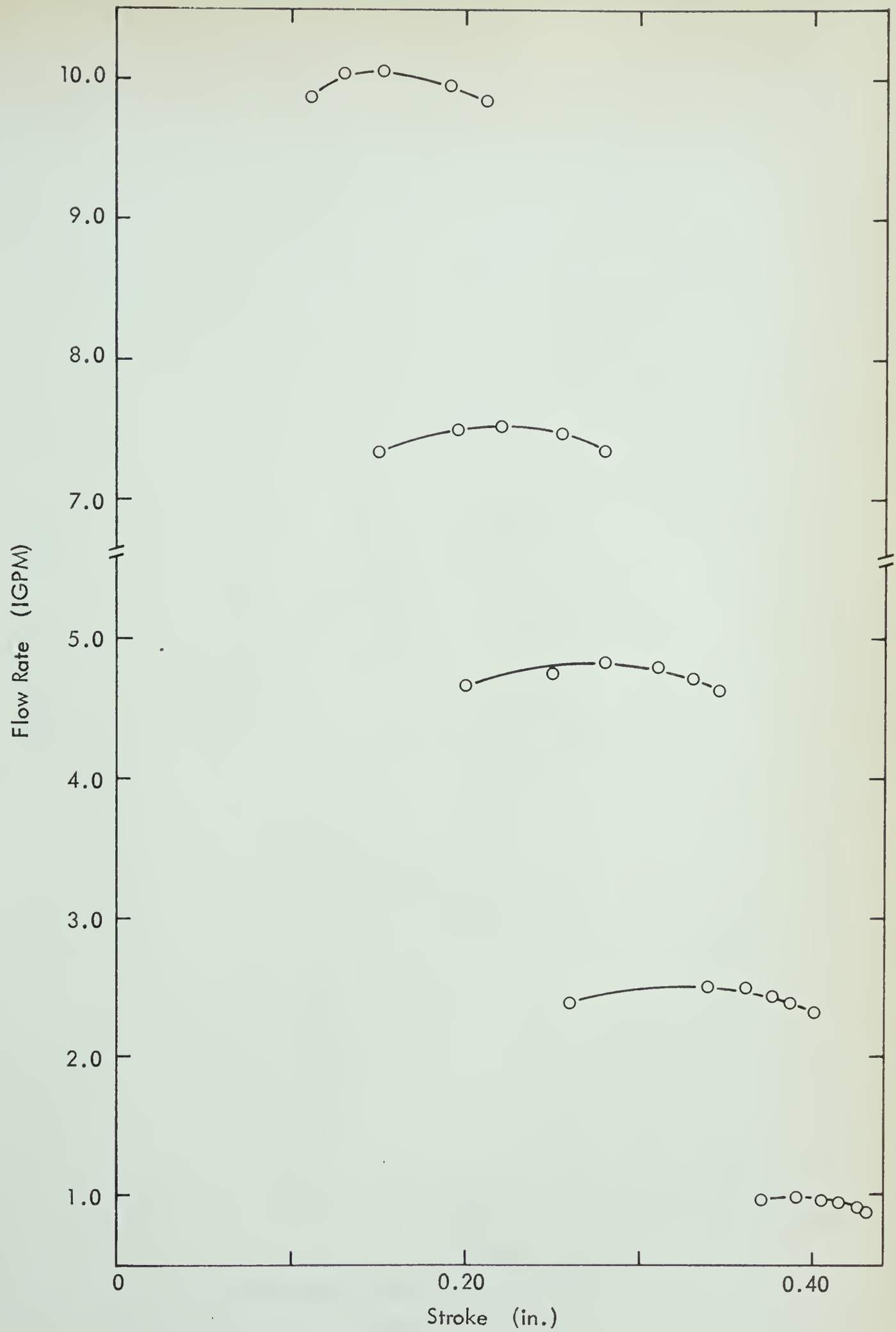

FLOW RATE VS STROKE

Figure 31

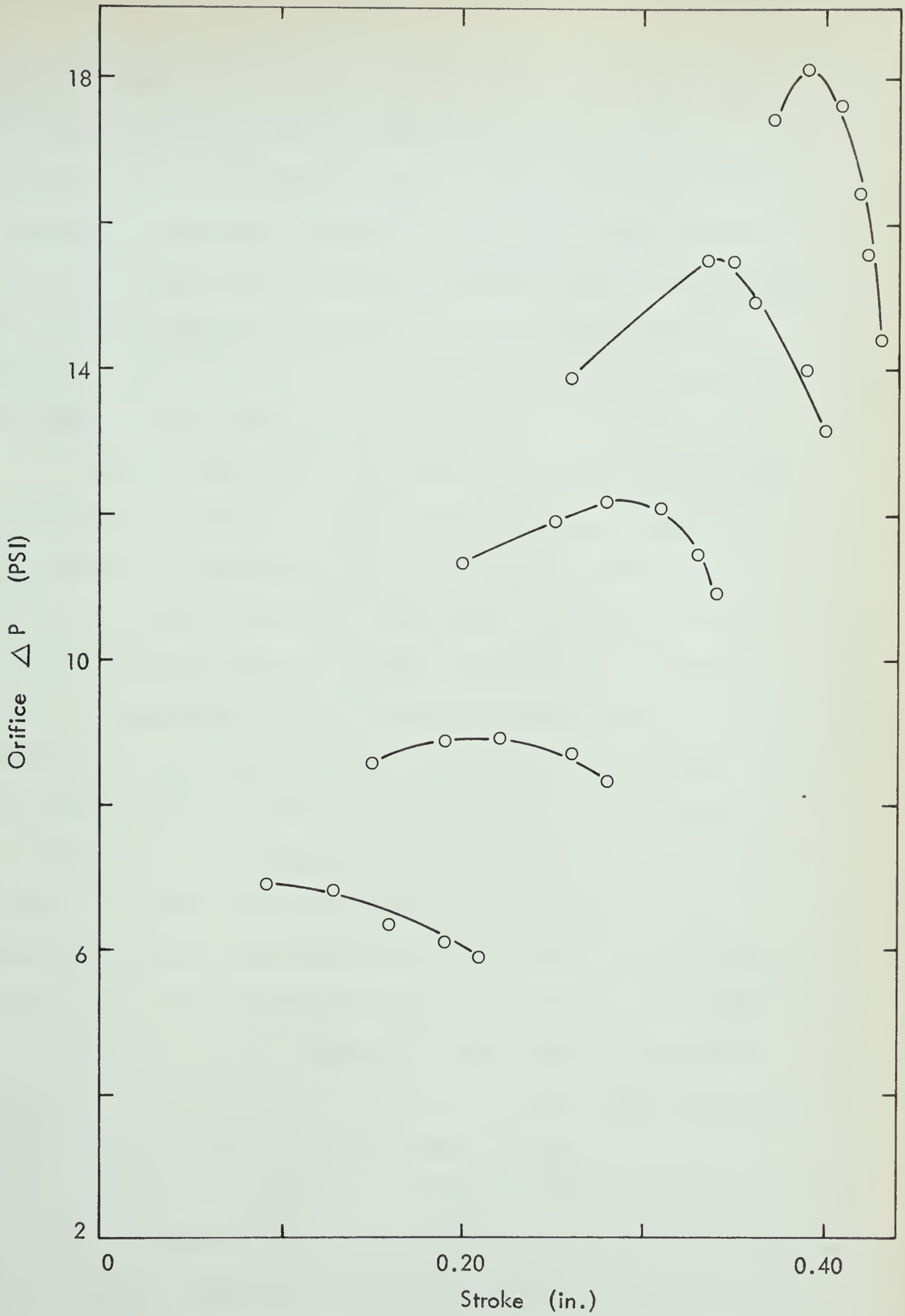

ORIFICE PRESSURE DROP VS STROKE

Figure 32

As P_1 increases, or the differential pressure increases, then the valve must close. Therefore, the term K_cX increases. If X increases, then A_x also increases and ϕ appears to decrease (Table 3). Since at high differential pressures, the term $\phi A_x P_1$ becomes quite significant, the flow rate tends to decrease. At low differential pressures, the flows follow the orifice equation down to zero flow at zero differential pressure.

One of the major limitations in the operation of the regulator is that at high flow rates, a pressure differential of approximately 50 psi is required for regulation within the stated accuracy. Figure 29 shows the minimum differential pressure limitation. In other words, the regulator will maintain the flow within $\pm$1% for differential pressures between this value and 150 psi. The lower pressure drop limitation was hoped to be around 25 psi, which is a reasonable pressure loss in a flow control system. It appears as though the flow range of this regulator has been over-extended since there is a significant pressure drop through the valve at zero stroke. Consequently, with the 3/8 inch port, the valve stem should have been shaped for flow rates up to about 5.0 IGPM. Work is being done in this direction at the present time.

Figure 33 shows the flow rate setting versus orifice area. There appear to be some end effects when the orifice is almost closed. Otherwise, the relationship is essentially

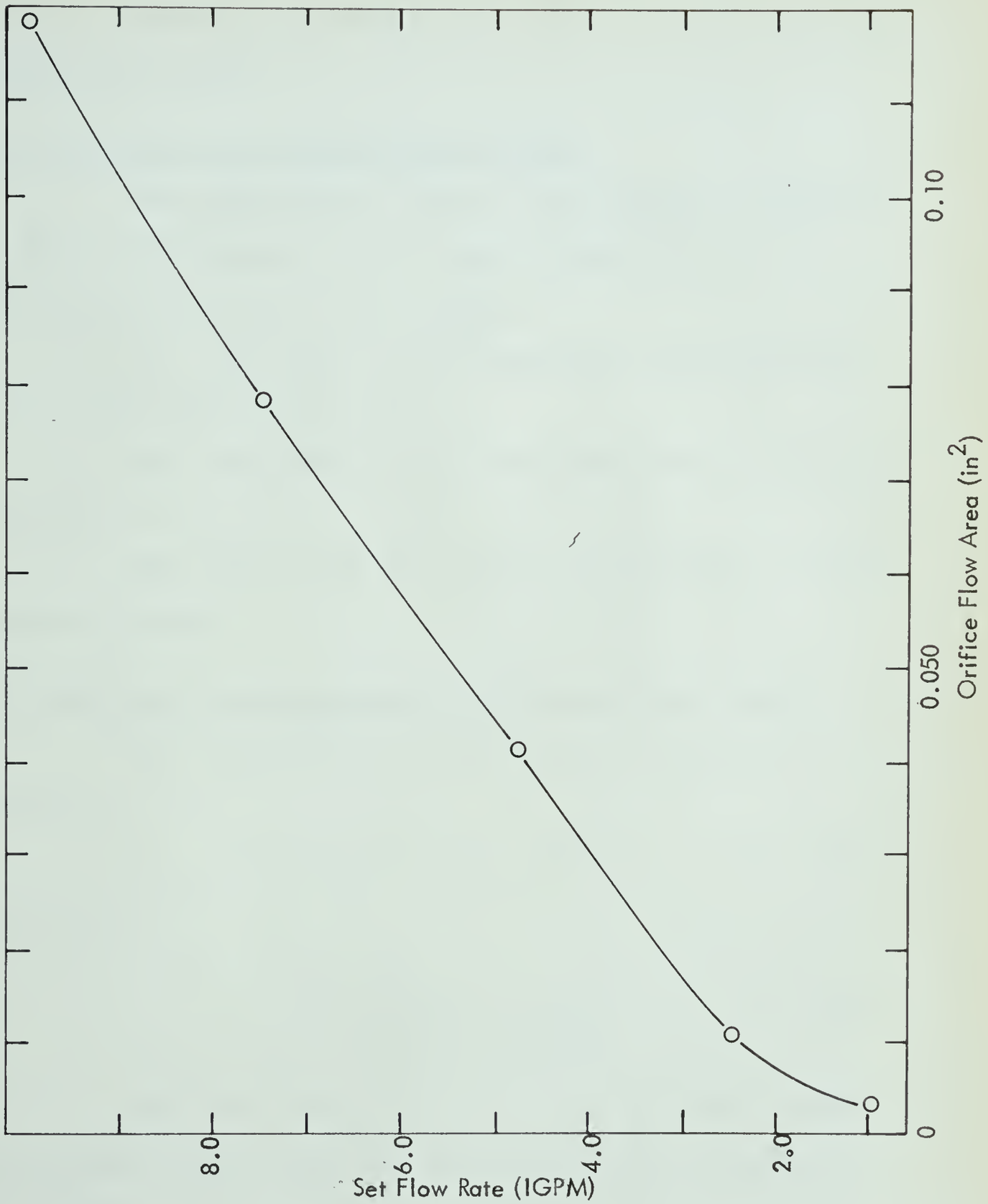

ORIFICE CHARACTERISTICS
SET FLOW RATE VS ORIFICE FLOW AREA
Figure 33

linear. Therefore, the scale for setting the flow rate is essentially linear.

Data Obtained from Experimental Results

The experimental results were analysed primarily to obtain information for the analog simulation. The following information was required:

(1) The value of the discharge coefficient C_{dv} of the main regulating valve.

(2) The value of the flow coefficient C_v of the orifice.

(3) The factor, ϕ , which will satisfy the force balance equation.

(1) Obtaining the discharge coefficient of the valve

This information was obtained by using the equation:

$$Q = C_1(A_p - A_x)\, C_{dv} \sqrt{P_1 - P_2} \qquad (77)$$

therefore

$$C_{dv} = \frac{Q}{C_1(A_p - A_x)\sqrt{P_1 - P_2}} \qquad (78)$$

The value of C_{dv} was calculated for each of the experimental runs, since for each run Q, A_x, P_1, and P_2 are known.

(2) Obtaining the flow coefficient of the orifice

This value was obtained by utilizing the following equation:

$$Q = C_v \sqrt{P_2} \tag{79}$$

therefore

$$C_v = \frac{Q}{\sqrt{P_2}} \tag{80}$$

(3) Determining the factor ϕ

The factor ϕ was inserted into the force balance so that the force balance would be satisfied. If the force balance was a true representation of the system, then ϕ would equal 1.0. The factor was added to the term that represents the force resulting from the inlet pressure. The steady state force balance is

$$A_b P_2 + \phi A_x (P_1 - P_2) - K_c x - F_o = 0 \tag{81}$$

Solving for ϕ

$$\phi = \frac{K_c x + F_o - A_b P_2}{A_x (P_1 - P_2)} \tag{82}$$

The value of these variables is shown in Table 3.

TABLE 3

RUN NO.	DIFFERENTIAL PRESSURE (psi)	FLOW RATE (IGPM)	C_{dv}	C_v	ϕ
1	150	9.82	0.68	4.04	1.32
2	125	9.94	0.69	4.02	1.41
3	100	10.04	0.70	3.99	1.49
4	75	10.04	0.76	3.85	1.54
5	50	9.84	0.76	3.74	1.84
6	150	7.34	0.68	2.55	1.19
7	125	7.47	0.68	2.53	1.22
8	100	7.51	0.66	2.51	1.23
9	75	7.45	0.69	2.49	1.36
10	50	7.33	0.75	2.50	1.64
11	150	4.62	0.69	1.40	1.05
12	125	4.72	0.69	1.39	1.05
13	100	4.80	0.70	1.38	1.07
14	75	4.80	0.67	1.37	1.09
15	50	4.74	0.73	1.38	1.44
16	40	4.64	0.67	1.38	1.03
17	150	2.32	0.72	0.639	1.01
18	125	2.40	0.65	0.641	0.98
19	100	2.45	0.66	0.634	0.48
20	75	2.50	0.66	0.635	0.93
21	50	2.50	0.72	0.633	1.09
22	25	2.35	0.71	0.630	1.56
23	150	0.88	0.68	0.232	0.95
24	125	0.92	0.61	0.233	0.89
25	100	0.95	0.55	0.234	0.85
26	75	0.98	0.53	0.233	0.63
27	50	0.98	0.53	0.230	0.42
28	25	0.95	0.80	0.228	--

The results of this analysis were used in the analog simulation of the flow regulator. Of course, all three quantities vary with the differential pressure for a given flow rate. It is reasonable to assume an average value of the discharge coefficient of the valve, C_{dv}, and

the flow coefficient of the orifice, C_v, for each set flow since these values remain relatively constant. The effect of this approach is considered in the discussion of the analog simulation. It is more difficult to justify averaging the value of the factor ϕ for each set flow. The effect of averaging ϕ will be considered in the discussion of the analog simulation.

Table 4 summarizes the above results.

TABLE 4

AVERAGE FLOW RATE (IGPM)	AVERAGE C_{dv}	AVERAGE C_v	AVERAGE ϕ
9.94	0.72	3.93	1.52
7.42	0.69	2.52	1.33
4.72	0.69	1.38	1.12
2.42	0.69	0.635	1.01
0.94	0.62	0.232	0.75

Discussion of Analog Simulation of Flow Regulator

The simulation of the flow regulator on the analog computer was done to study the dynamic characteristics of the device. In order to ensure that the model was a reasonable representation of the regulator, the steady state values of the model were compared with the experimental results.

When the problem was set up on the analog computer, problems were encountered. At a certain differential pressure and flow rate, a high frequency sinusoidal voltage was generated by the program which, of course, made the recording of the variables impossible. The frequency was about 5000 CPS, computer time, or 5000 CPM, actual time. At the point where this began, these voltages would tend to build up and die out. However, if the differential pressure was increased, the sinusoidal signals started to affect the program. The program being run on an Applied Dynamics Analog Computer was checked on a Pace Analog Computer. The same problem was encountered. Initially, the problem appeared to be associated with the scaling. However, rescaling the program did not eliminate the difficulty. The problem was eventually overcome by installing a low time constant first order component at an appropriate point in the computer network. The time constant was 10^{-4} seconds which gave a cut-off frequency of about 1600 CPM, actual time. Therefore, the filter would not affect the dynamic response of the

system over the frequency range of interest. When this component was inserted into the analog network, the simulation was completed.

In the simulation, the constants such as the spring constants, the initial spring force, the bellows area, and the port area were set equal to their actual values. The shape of the valve stem was simulated on the function generator. The experimental results used were the average values of C_{dv}, C_v, and ϕ that are shown in Table 4.

It was very difficult to calculate the value of K_d, the damping coefficient in the force balance equation. The displacement of the bellows was observed when only the bellows was stroked and released. The bellows returned to its original position with very little overshoot. Consequently, a damping factor of 1.0 was used and the value of the corresponding damping coefficient was calculated.

The same variables that were plotted from the experimental results were plotted from the analog computer. Figure 34 shows the flow rate versus differential pressure plot for each of the set flow rates. The circles indicate the experimental points and the comparison of the analog and experimental results is quite evident.

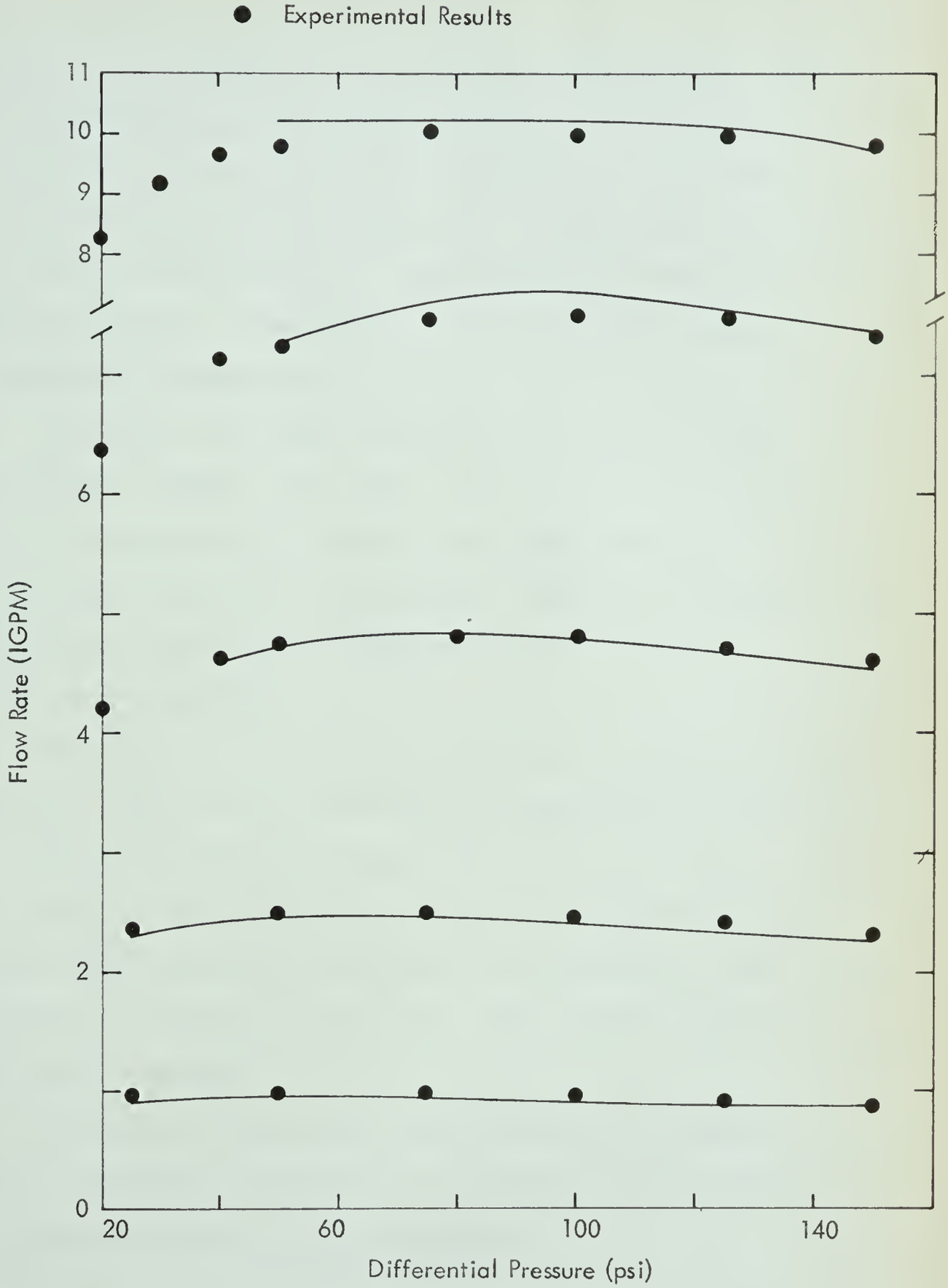

FLOW RATE VS DIFFERENTIAL PRESSURE

Figure 34

A study was made on the analog to determine the sensitivity of the results to varying C_{dv}, C_v, and ϕ. The effect of changing C_{dv} and C_v from their average values, as shown in Table 4, was quite small. Increasing C_{dv} caused the flow rate to increase slightly, and increasing C_v caused the flow rate to increase also. Increasing ϕ resulted in a decreased flow rate. From Table 3, it is evident that at high differential pressures, the value of ϕ is below the average. Therefore, at these conditions the analog would have predicted a higher flow rate. This is one reason why the analog curves tend to decrease more than the actual results at high differential pressures. However, putting the factor ϕ on the function generator for each flow setting was not justified.

The analog plot of flow rate versus stroke is shown in Figure 35. The circles indicate the experimental results.

The relationship between the orifice pressure drop and stroke predicted from the model is essentially the same as the experimentally determined relationship. The model results are shown on Figure 36. The circles indicate the experimental results.

The shape of the valve stem is shown in Figure 37. The area of the stem is plotted as a function of the stroke and corresponds with the actual stem shape.

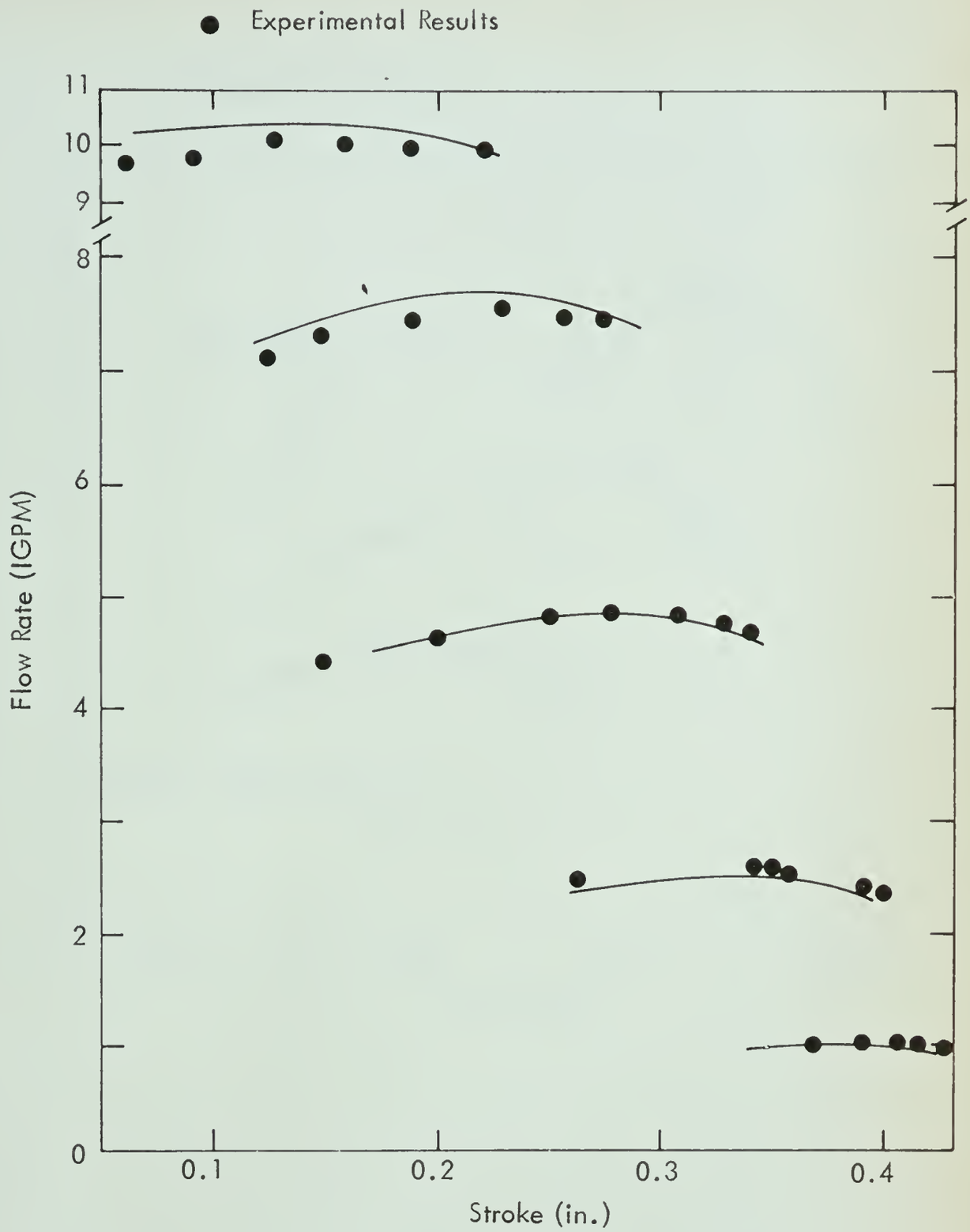

ANALOG SIMULATION RESULTS
FLOW RATE VS STROKE
Figure 35

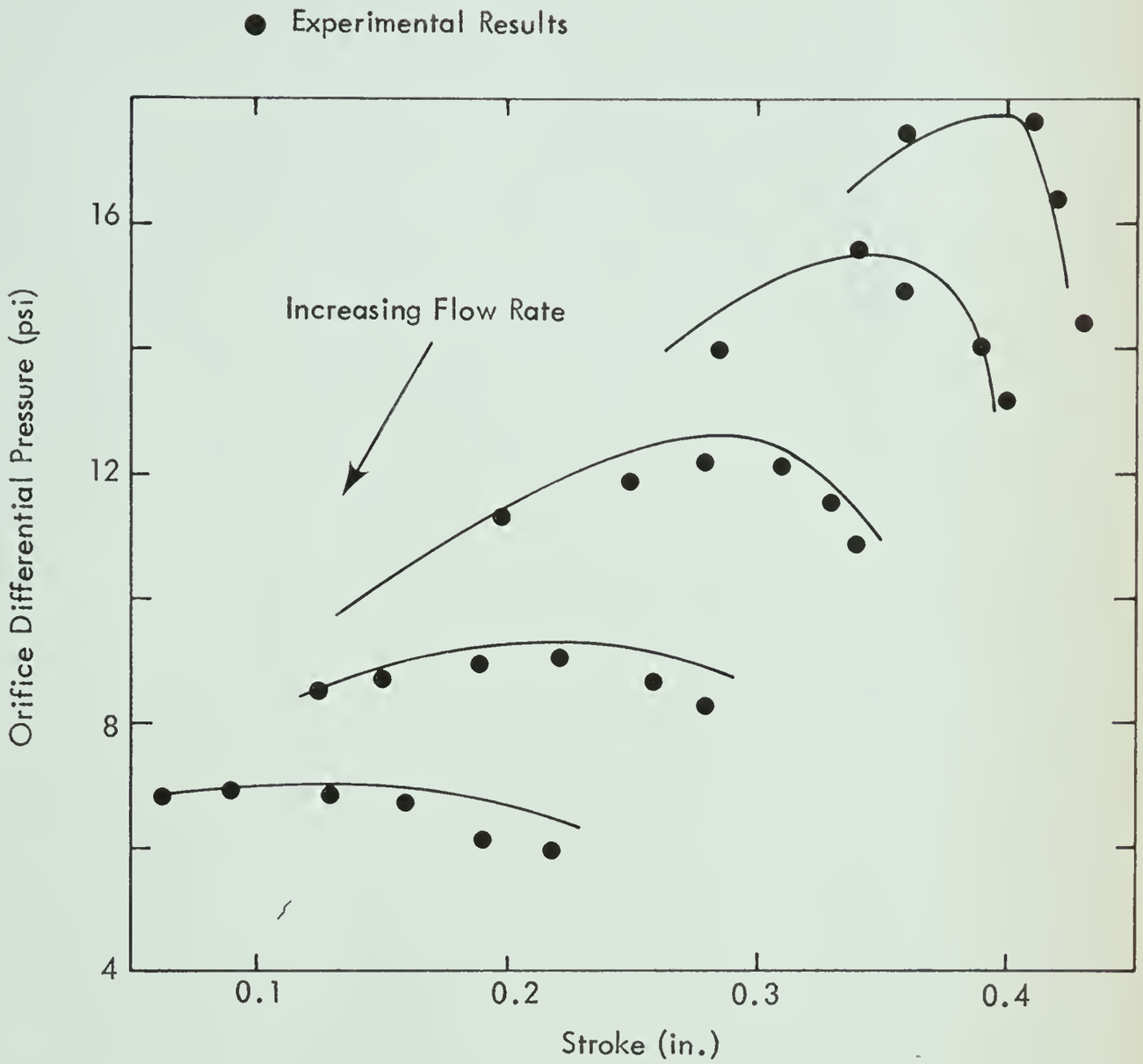

ANALOG SIMULATION RESULTS
ORIFICE DIFFERENTIAL PRESSURE VS STROKE
Figure 36

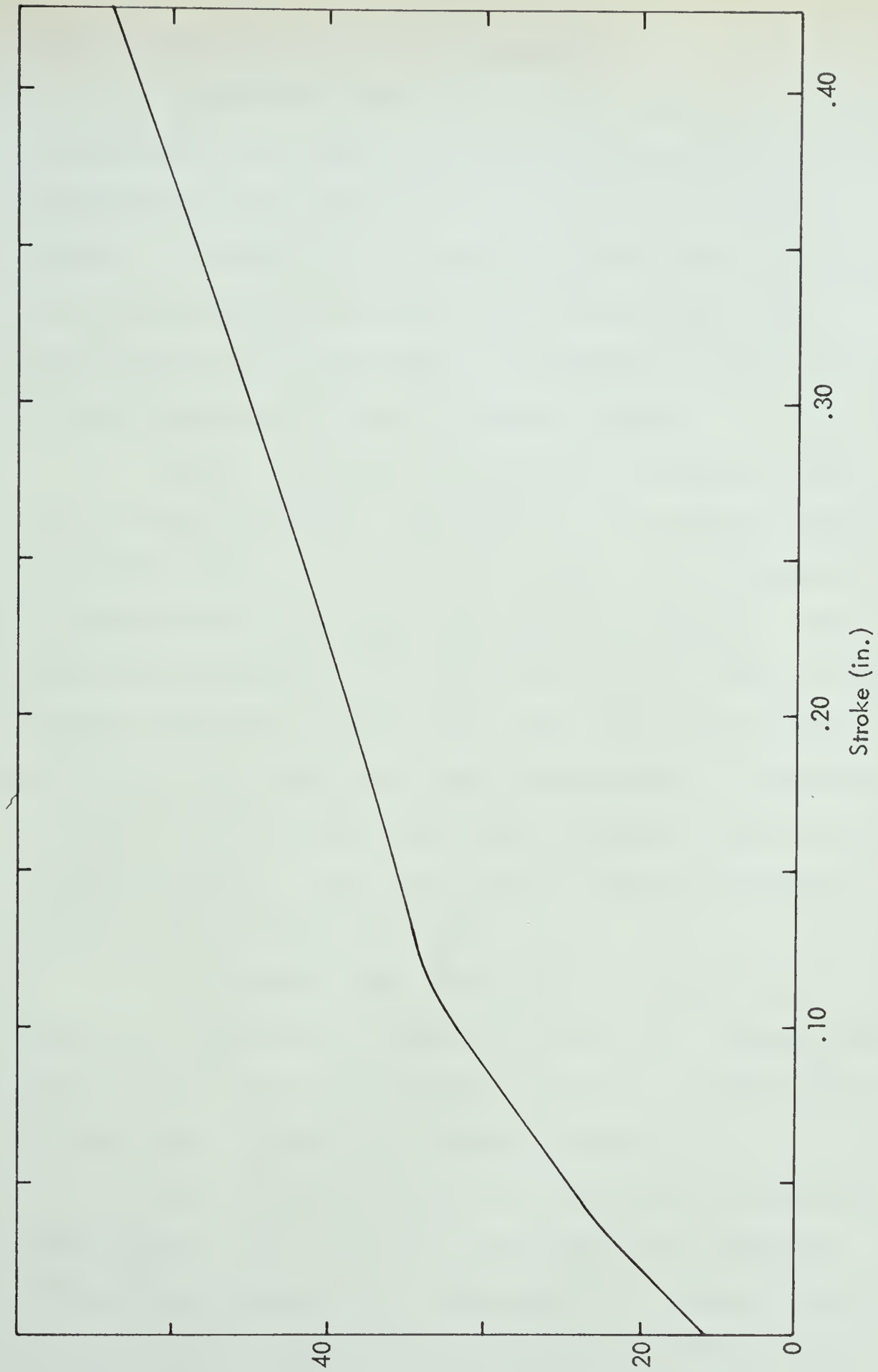

AREA OF STEM VS STROKE

Figure 37

Frequency Response of Flow Regulator

The analog model of the flow regulator was used to determine its frequency response characteristics. The performance of the regulator to changes in load were studied. Its ability to control the flow rate for changes in the differential pressure were of interest. The performance of the regulator is compared to the performance of the flow control loop in a later section.

Since the model is non-linear, special care was taken in the analysis. The size of the pressure disturbance was varied from 5 psi to 30 psi to see if the magnitude of the input signal affected the frequency response. The output signal was essentially a sine wave for this range of input signals. However, for an input sine wave disturbance of 30 psi, the output flow rate signal was slightly distorted, but it did not affect the actual gain and phase angle plots to any great extent. The final results were obtained for pressure disturbances of 5 psi.

The results were obtained for a set flow of 4.72 IGPM and a differential pressure of 80 psi. These steady state values were chosen because they are in the middle of the flow and differential pressure ranges.

The input sine wave was generated by a Hewlett-Packard Model 203 A Variable Phase Function Generator. The gain and phase angle were measured by utilizing an oscilloscope. The device was tested from a frequency of about 1 cycle per

minute to 1500 cycles per minute.

The Bode plot of gain versus frequency is shown in Figure 38. The results were normalized through the following manipulation:

$$Q^2 = C_v^2(P_1-P_2) \tag{83}$$

Consider P_2 as essentially constant and suppose it operates around a mean value, $P_{2\ m}$, then

$$Q_o^2 = C_v^2(P_1-P_{2\ m}) \tag{84}$$

also

$$Q_{o\ m}^2 = C_{v\ m}^2(P_{1\ m}-P_{2\ m}) \tag{85}$$

where the subscript m refers to the mean value of that variable.

If C_v is relatively constant, then

$$\frac{Q_o^2}{Q_{o\ m}^2} = \frac{P_1-P_{2\ m}}{P_{1\ m}-P_{2\ m}} \tag{86}$$

or

$$\frac{Q_o^2}{P_1-P_{2\ m}} = \frac{Q_{o\ m}^2}{P_{1\ m}-P_{2\ m}} \tag{87}$$

The gain is then defined by the equation:

$$\text{Gain} = \left(\frac{P_{1\ m}-P_{2\ m}}{Q_{o\ m}^2}\right)\ \frac{Q_o^2}{P_1-P_{2\ m}} \tag{88}$$

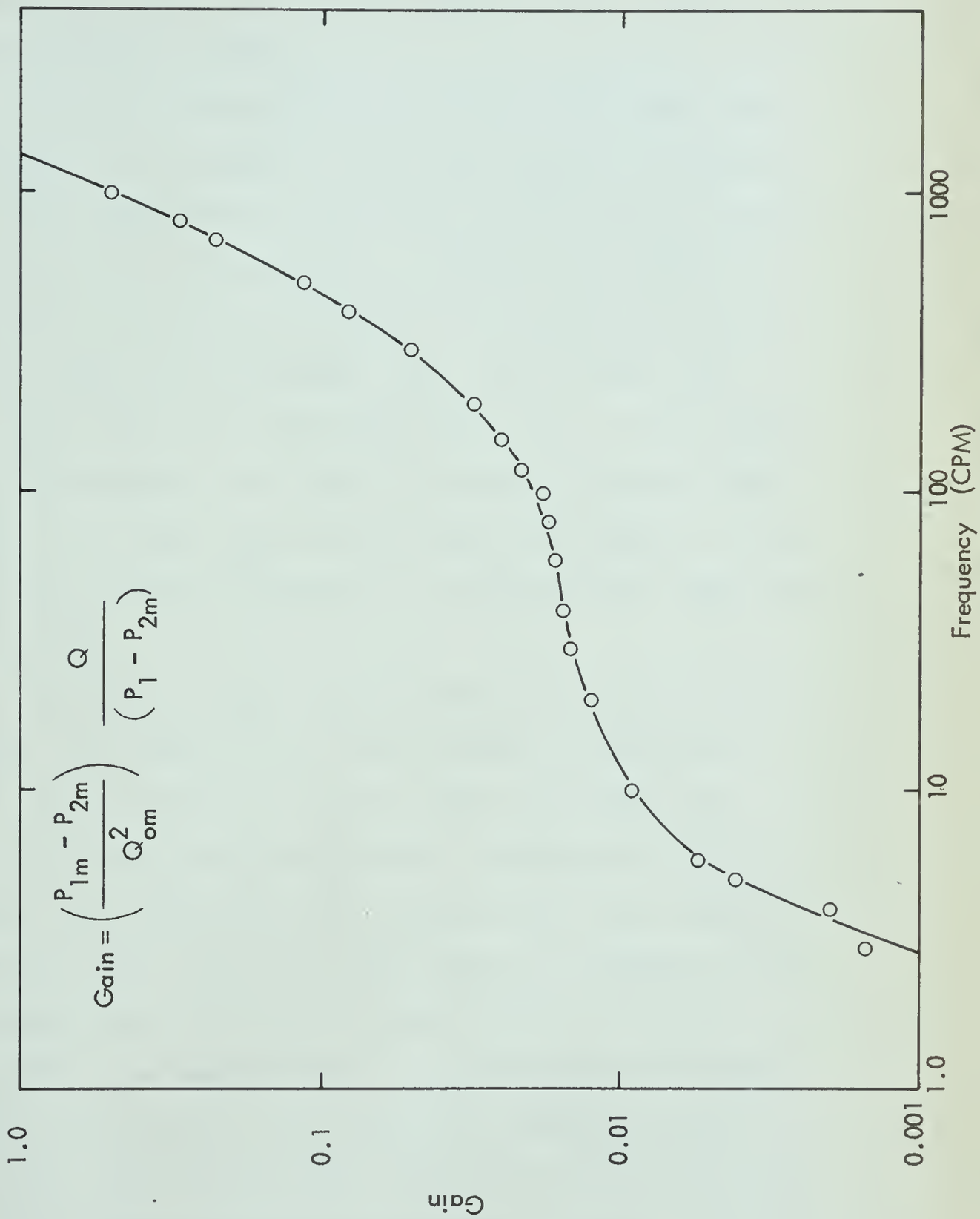

FREQUENCY RESPONSE OF FLOW REGULATOR

GAIN VS FREQUENCY

Figure 38

The steady state values of $P_{1\ m}$, $P_{2\ m}$, and $Q_{o\ m}^{2}$ are 80 psi, 12.2 psi, and $(4.80)^{2}$ respectively. The constant is equal to 2.94.

The ideal regulator is one that maintains the flow constant for changes in the load variable. Therefore for good flow regulation, the ratio of $Q_o^2/(P_1-P_{2\ m})$ should be as close to zero as possible. The Bode plot indicates that the ratio is extremely small for frequencies up to 1000 CPM. Above this frequency, the curve rises very rapidly which means that the flow would vary a great deal for load disturbances that have a frequency greater than 1000 CPM. In a later section the curve is compared to the closed loop frequency response of a proportional reset flow control system.

The phase angle versus frequency is plotted in Figure 39. The shape of the curve cannot be explained. However, it is interesting to note that the phase lag appears to be increasing rapidly for frequencies above 1000 CPM. The combination of a large phase lag, possibly 360 degrees, and a large gain that could be present at say 5000 CPM may shed some light on the trouble that was encountered in the generation of high frequency voltages. The system would react like a positive feedback system. If there is any small disturbance, then the high gain of the system would tend to generate a sinusoidal signal. However, since the system is quite non-linear, it is difficult to

FREQUENCY RESPONSE OF FLOW REGULATOR
PHASE VS FREQUENCY
Figure 39

analyse this phenomenon. This problem was not studied any further because the frequency that it occurs at is well beyond the frequency of interest in a flow control system.

Transient Response of the Flow Regulator

The transient response analysis of the flow regulator was performed on the model with the analog computer. These results were not checked experimentally because the response of the regulator was too fast. The solution was time scaled by a factor of 60.

Step changes in the load variable were made for a set flow of 4.72 IGPM and a steady-state differential pressure of 80 psi. Two different sized step changes were inserted in both the negative and positive directions.

Figures 40 and 41 show the result of a step change of +15 psi and -15 psi respectively. The transient response of the inlet flow, Q_i, and the outlet flow, Q_o, are shown. When the step change is inserted, Q_i increases immediately and then decreases to its steady-state value. The outlet flow is damped considerably since as soon as P_2 increases, the valve will begin to close. The inlet flow returns to steady state in about 0.06 seconds, and the outlet flow transient lasts for about 0.002 seconds. The response to load changes is extremely fast.

The results of step changes in differential pressure of +30 psi and -30 psi are shown in Figure 42 and Figure 43. The curves are of the same general shape, and again, the transient period is extremely short. The inlet flow returns to its steady-state value in about 0.08 seconds, and the outlet flow in about 0.003 seconds. The

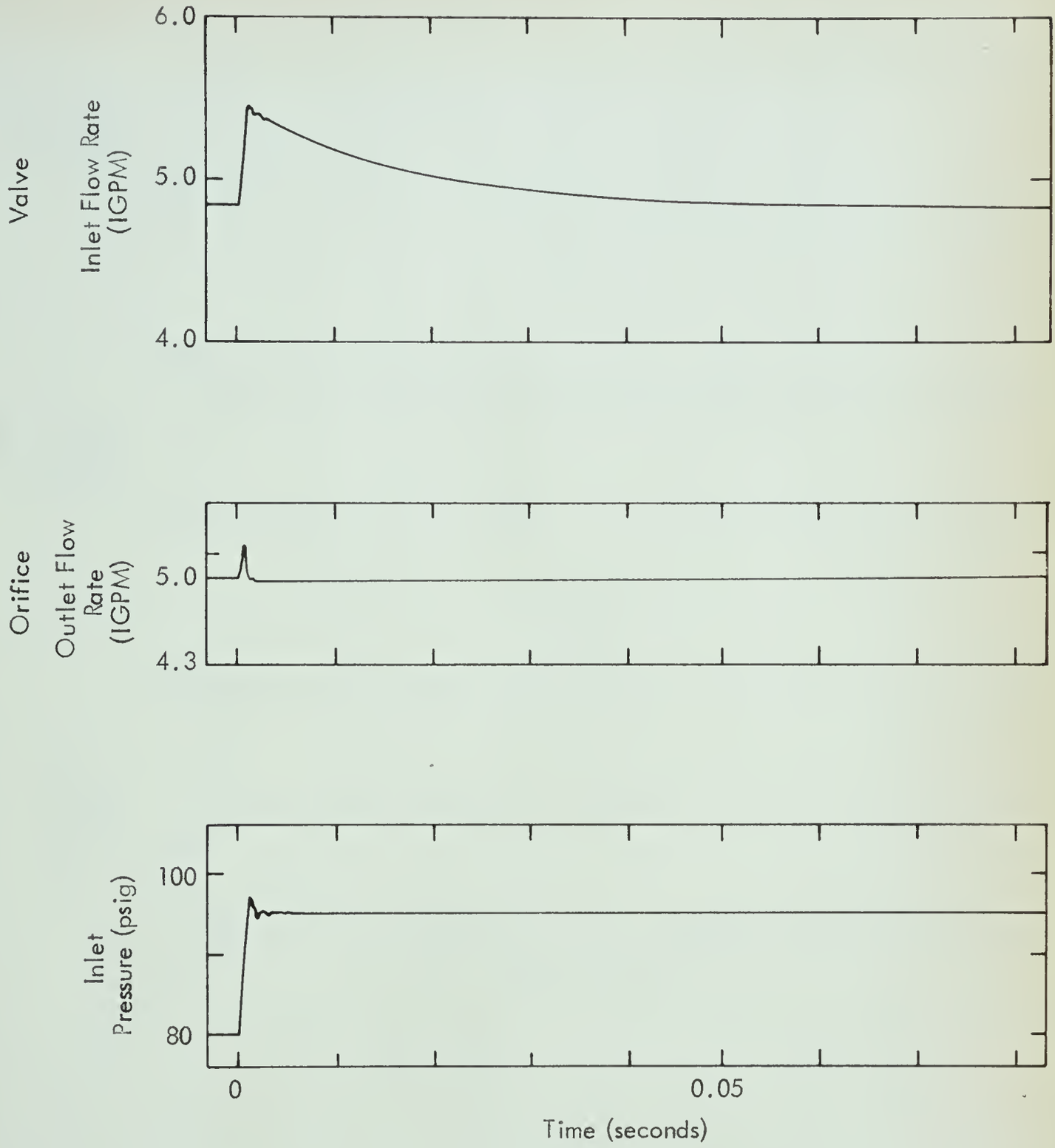

TRANSIENT RESPONSE OF FLOW REGULATOR

INLET PRESSURE STEP: +15 psi

Q_i, Q_o vs Time

Figure 40

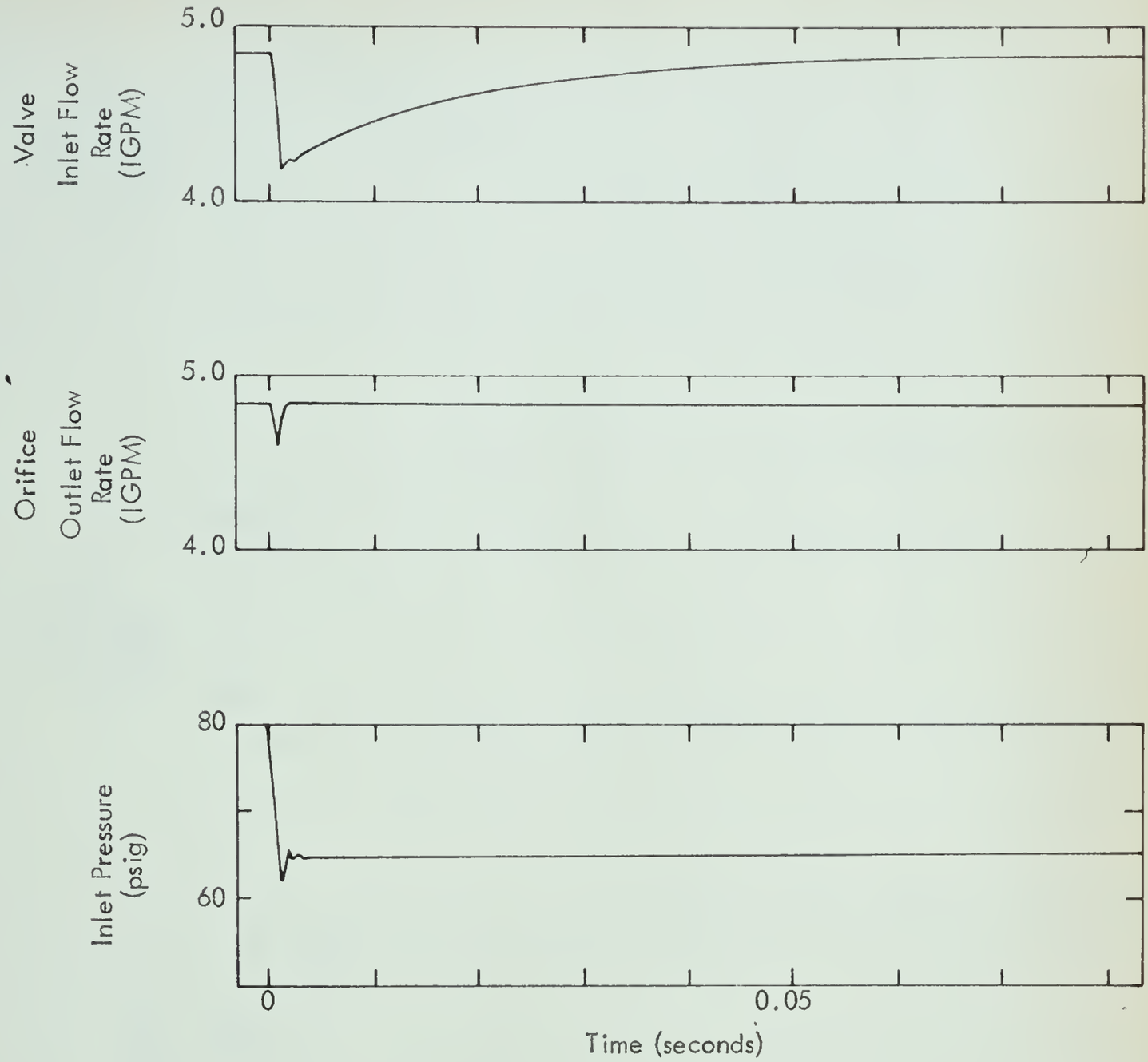

TRANSIENT RESPONSE OF FLOW REGULATOR
INLET PRESSURE STEP: -15 psi
Q_i, Q_o vs Time

Figure 41

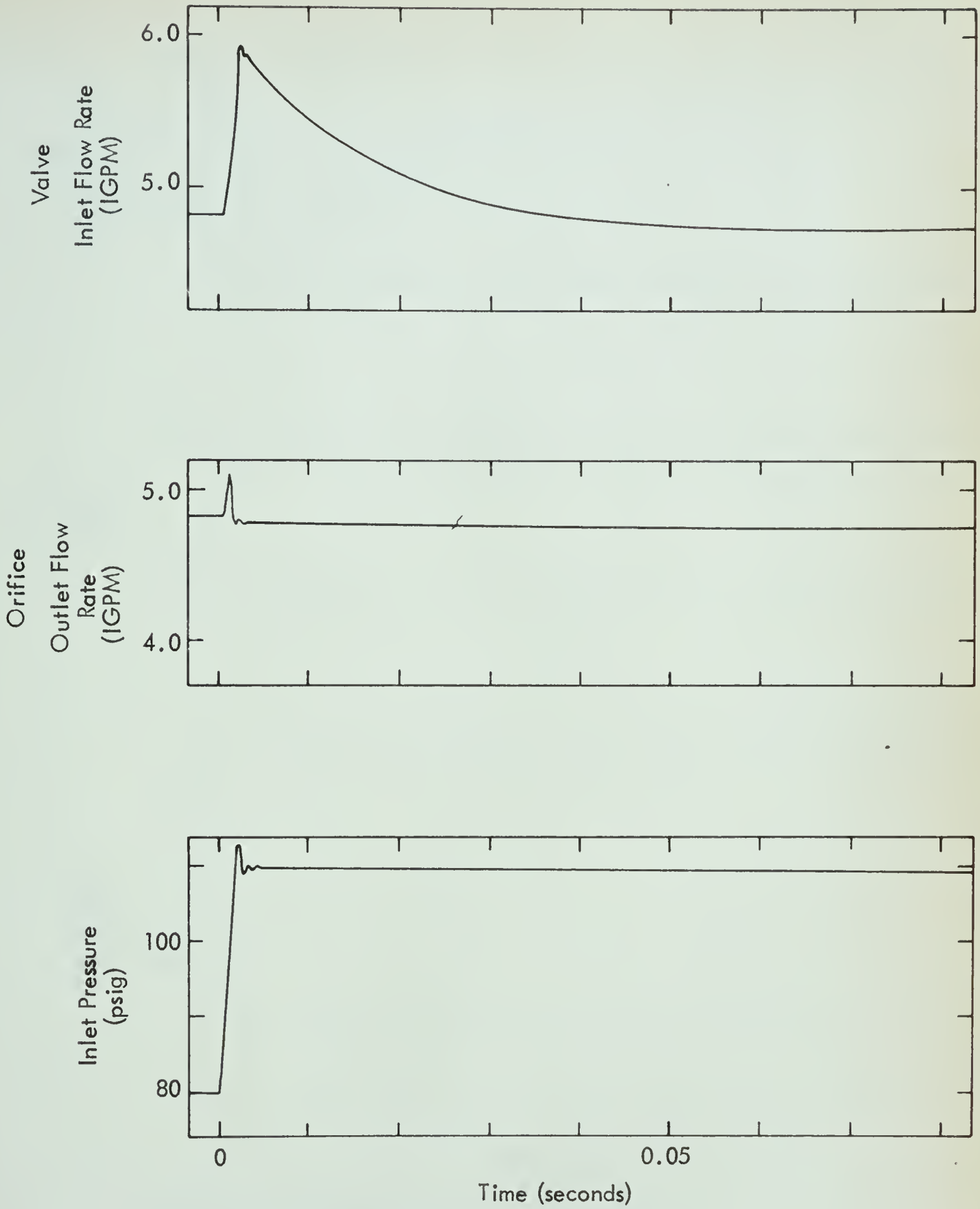

TRANSIENT RESPONSE OF FLOW REGULATOR

INLET PRESSURE STEP: +30psi

Q_i, Q_o vs Time

Figure 42

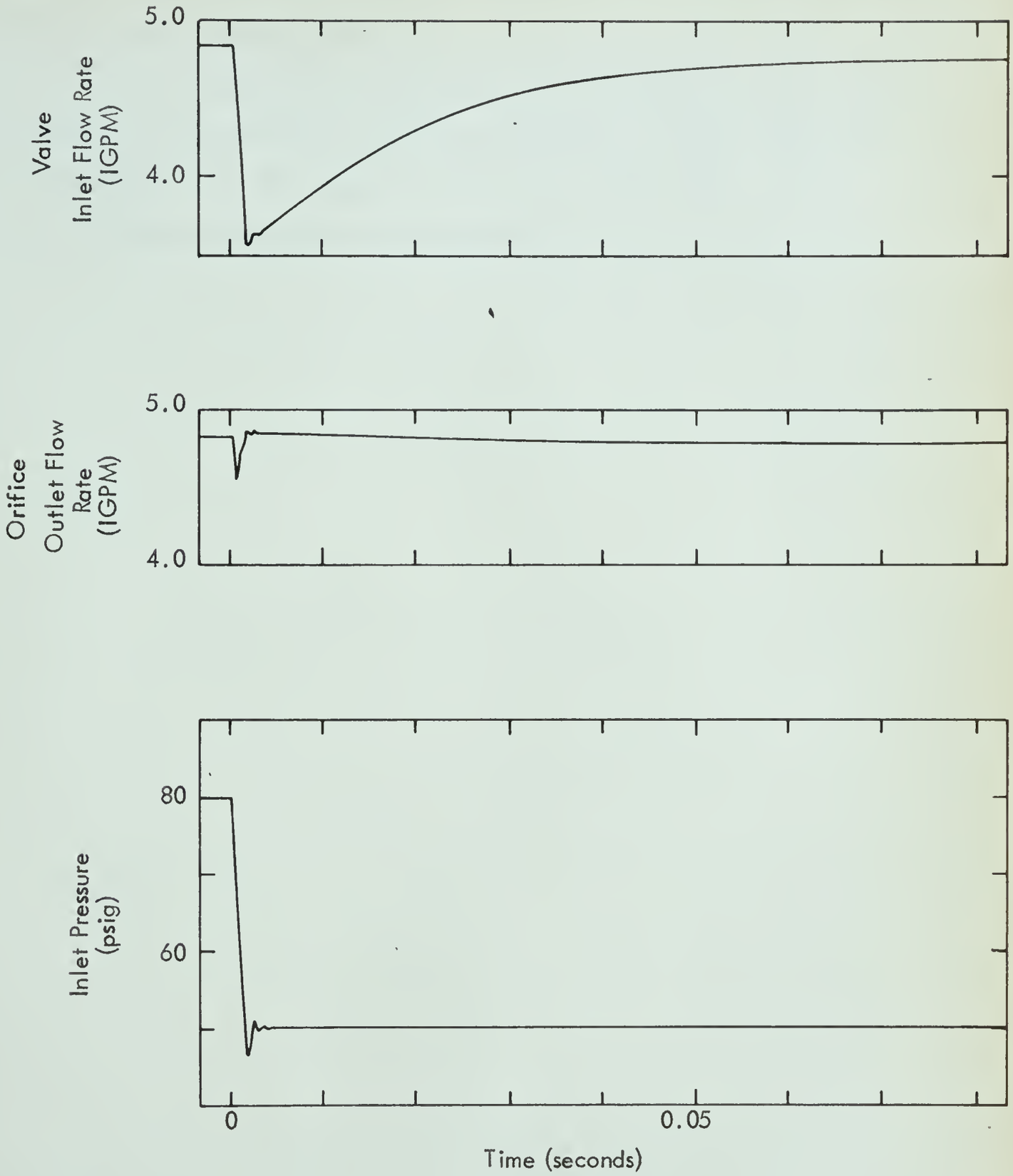

TRANSIENT RESPONSE OF FLOW REGULATOR

INLET PRESSURE STEP: -30psi

Q_i, Q_o vs Time

Figure 43

+30 psi step transient period was slightly shorter than the -30 psi transient period.

The frequency response of the regulator, as shown in Figure 38, predicted the fast response. Since the gain is extremely low for frequencies up to 1000 CPM, a very short transient period was expected.

Frequency Response of a Flow Control Loop

The closed loop frequency response of a proportional reset flow control system was determined. The open loop frequency response of the various components of the flow loop are shown in a previous section.

The performance of the control loop to a varying load was studied. A steady-state flow rate of 20 IGPM and a load of 30 psi were used. The value of $\partial Q_v / \partial (P_1 - P_3)$ was set equal to 0.667 for these particular conditions.

The closed loop transfer function is of the form (see equation 51)

$$\left[\frac{1}{\frac{\partial Q_v}{\partial (P_1 - P_3)}}\right] \frac{Q}{(P_1 - P_3)} (S) = \frac{1}{1 - \frac{G_1(S)}{G_2(S)}} \qquad (89)$$

$$= \frac{G_2(S)}{G_2(S) - G_1(S)}$$

The open loop transfer functions were reduced to the form

$$T(S) = \frac{G_2(S)}{G_3(S)} \qquad (90)$$

The gain and phase angle of the closed loop transfer function were calculated on the digital computer. Figure 44 shows the gain versus frequency of proportional-reset flow control loop. The phase angle versus frequency

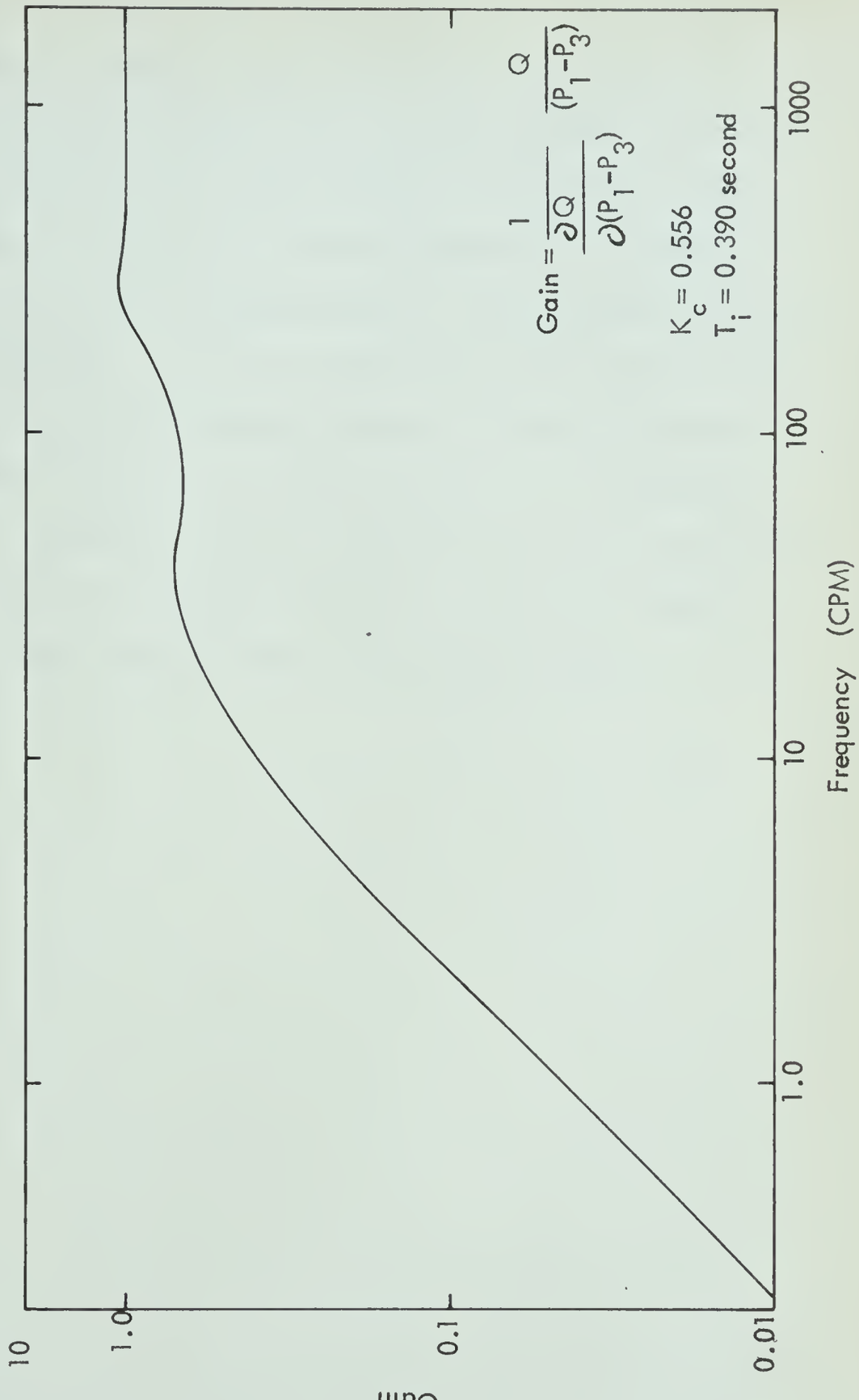

FLOW CONTROL LOOP: LOOP CLOSED

GAIN VS FREQUENCY

Figure 44

plot is shown in Figure 45. These plots can be compared to the frequency response curves for the flow regulator. The gain of the flow control loop is much higher than that of the flow regulator for the frequency range of interest. The phase angle of the flow control system is -90 degrees for low frequencies and asymptotically approaches 0 degrees at high frequencies. At high frequencies the deviation in flow is simply the disturbance because of the filtering action of other components in the network. In comparing the frequency response plot of the regulator and the control loop, the transient response period of the flow regulator will be less than that of the flow control system.

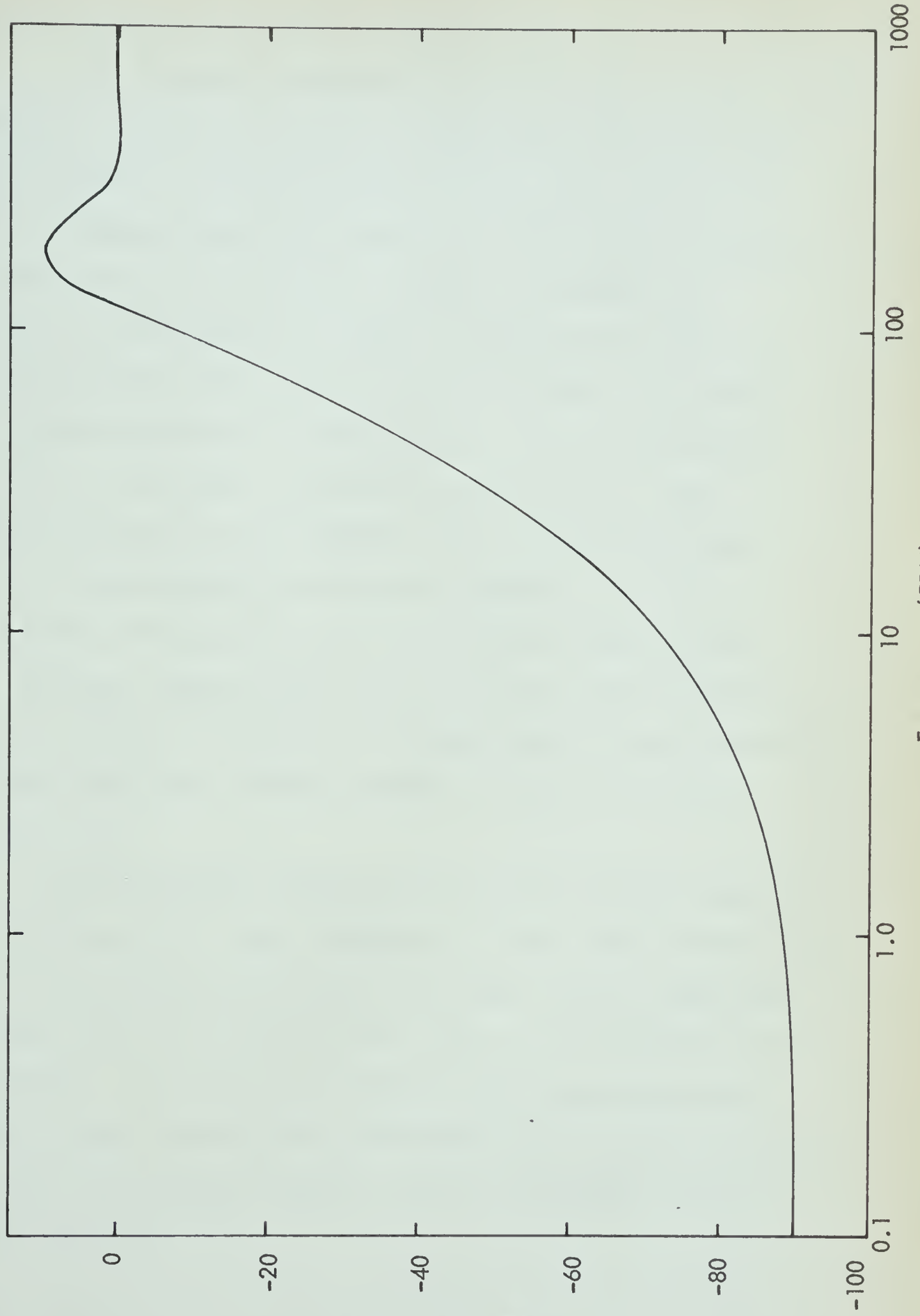

FLOW CONTROL LOOP: LOOP CLOSED
PHASE VS FREQUENCY

Figure 45

Transient Response of the Flow Control Loop

The transient response characteristics of the proportional-reset flow control system were studied on the analog computer. The controller settings were determined in the following manner (Reference 5). The sum of the open loop phase lags of the control system, excluding the controller, were plotted as shown in Figure 27. The frequency at 180 degree phase lag was 128 CPM. The reset rate was approximated by multiplying by 1.2. Converting this value to seconds, the reset rate was set at 2.56 repeats per second or an integral time is 0.390 seconds. The gain was adjusted on the analog computer to give a quarter decay ratio of the flow for a step change in the load. Although these values may not be the actual optimum values, it should not affect the comparison of the transient response of the flow control system to that of the flow regulator.

The transient response of the flow control loop is shown in Figure 46. Step changes of +10 psi and -10 psi were added to the steady-state load of 30 psi, and the resulting flow change from its steady-state value of 20 IGPM flow rate was recorded. The transient period lasted approximately 1 second. As was expected from observing the frequency response plots, this is somewhat longer than the transient period of the flow regulator.

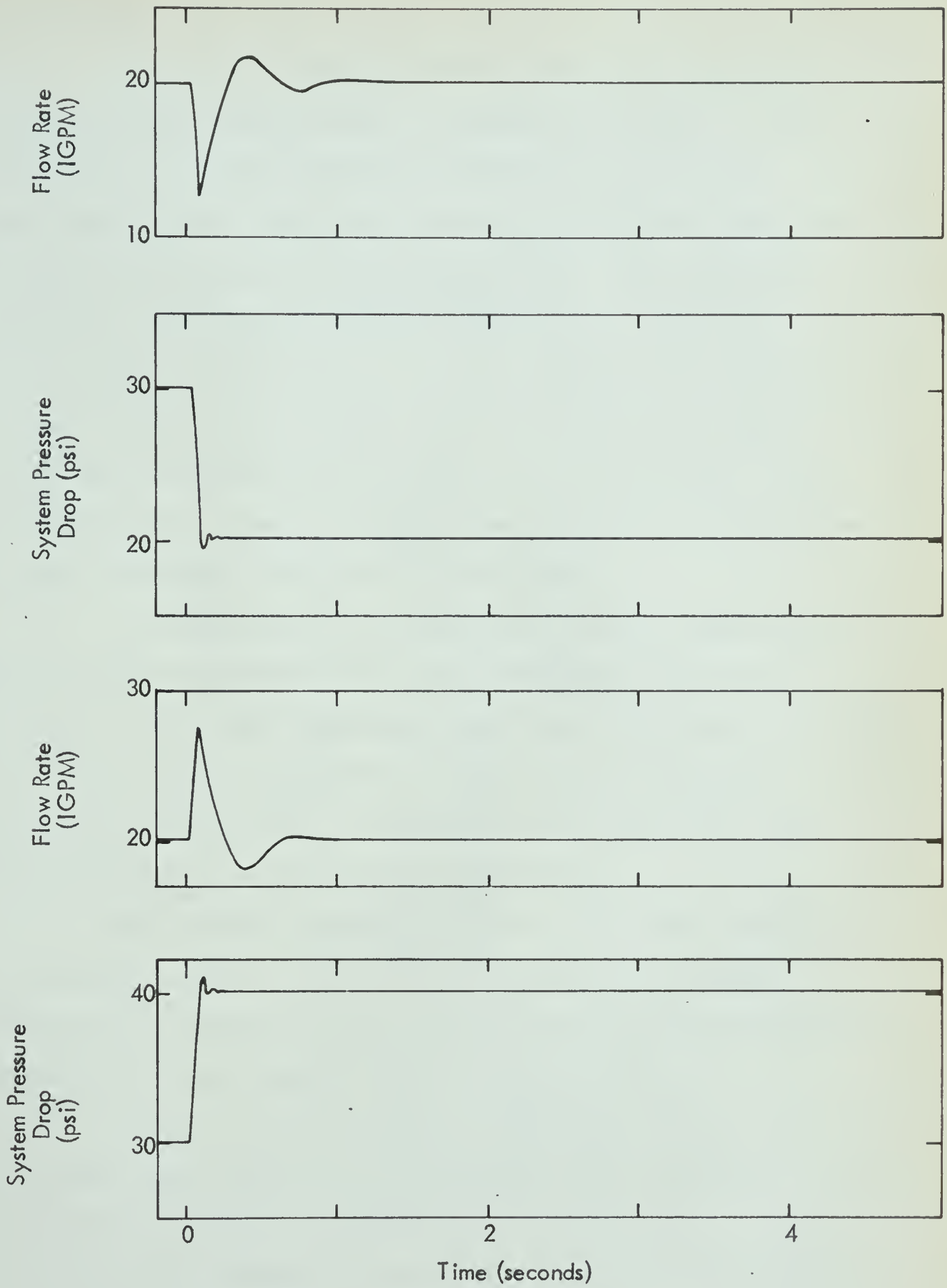

TRANSIENT RESPONSE OF FLOW CONTROL LOOP

LOAD PRESSURE CHANGE: ± 10 psi

FLOW RATE VS TIME

Figure 46

Conclusions

The initial goals regarding the flow regulator design and performance were, in general, realized. The design has no sliding parts and exhibits none of the hysteresis effects that are present in the Kates Regulator. The major criticism of the design is that the regulator requires a significant minimum differential pressure. However, this problem can be at least partially solved. For flow rates of 10.0 IGPM, the size of the valve port should be increased from 3/8 inch to say 7/16 inch. This would cause the pressure drop across the port to be reduced by about 50% when the valve is wide open.

In comparing the accuracy of the two regulators based on their maximum flow rate, the Kates Regulator is inferior. The Kates Regulator exhibits a flow deviation from $\pm$1.8% to $\pm$11.3% as compared to $\pm$1.0% for the regulator developed in this study. Because of its simplicity, the economics of this device appear favorable.

The dynamic characteristics of the flow regulator are extremely good. The transient response to changes in differential pressure is very fast compared to the transient response of a flow control system.

Some preliminary design work was done on a regulator that uses these principles. The mechanical design was altered to facilitate economic machining and construction. Figures 48 and 49 show the design of a regulator that could be produced commercially.

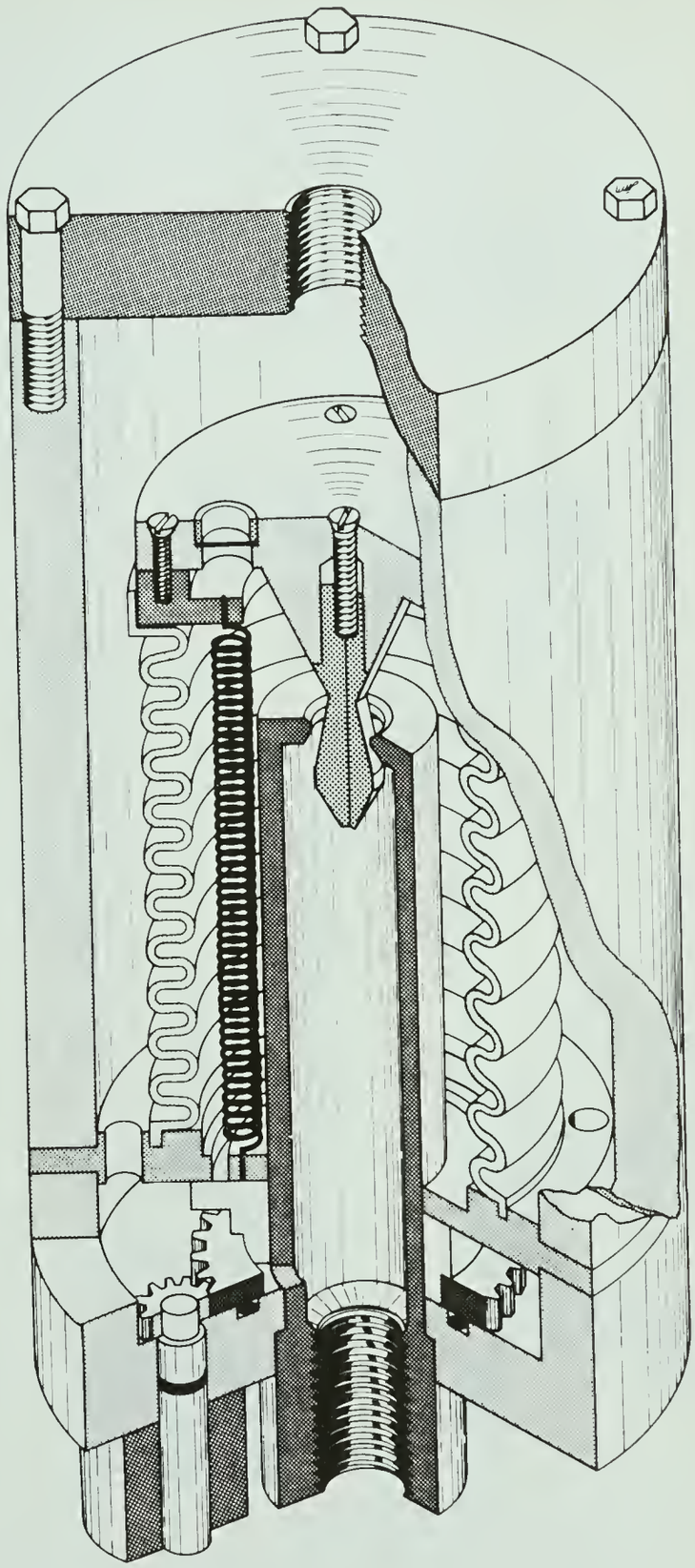

FIGURE 47

TECHNICAL ILLUSTRATION OF CONTROL VALVE

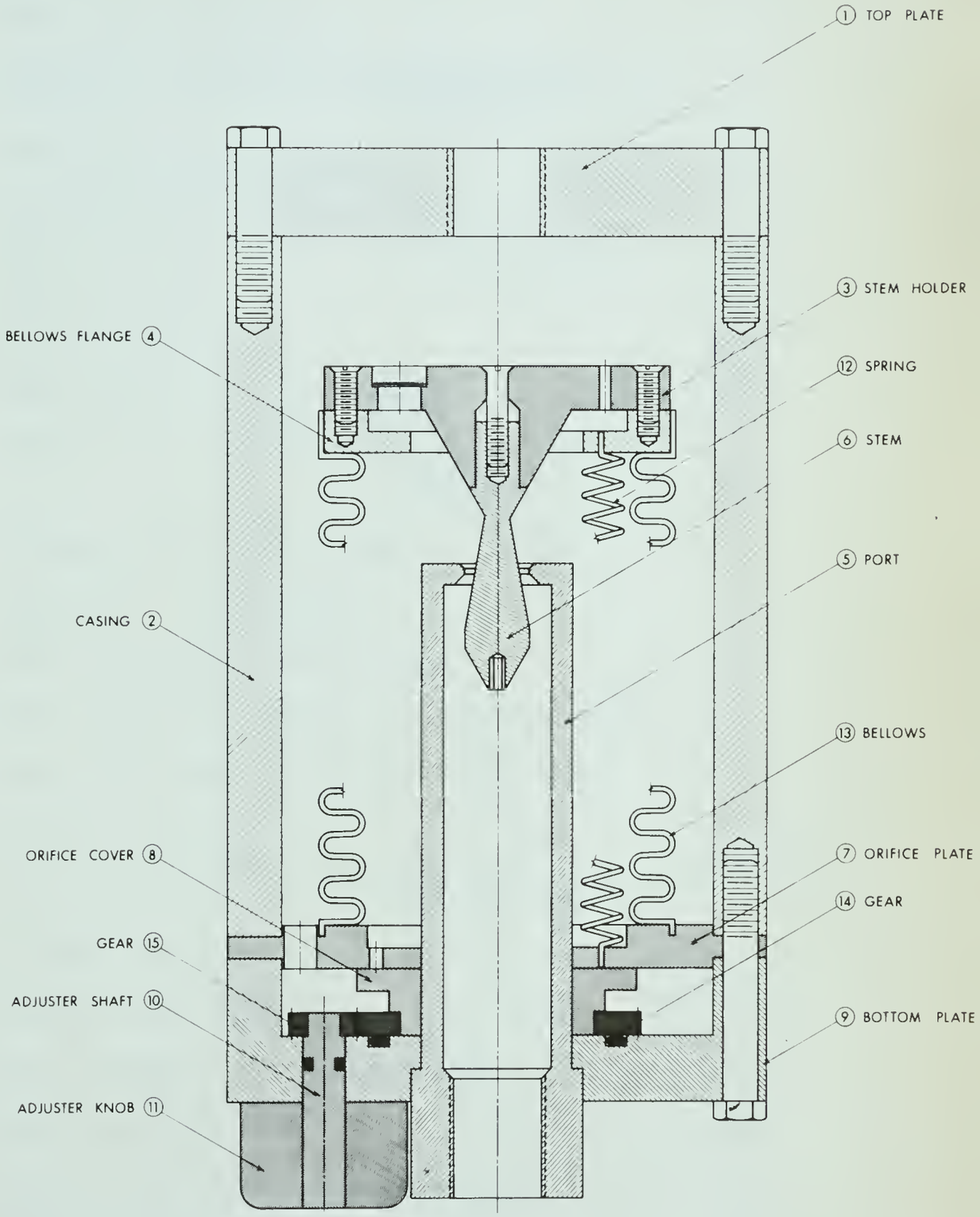

FIGURE 48

ASSEMBLY OF CONTROL VALVE

Nomenclature

Symbol		Units
A	area (as defined)	in^2
A_b	effective cross-sectional area of bellows	in^2
A_{eff}	effective area of flow	in^2
A_o	area of neck of stem at X = 0	in^2
A_p	area of port	in^2
A_{pist}	area of piston	in^2
A_x	area of stem at a stroke X	in^2
a_b	effective cross-sectional area of bellows	ft^2
C_1	constant in flow equation (38.1)	-
C_2	constant (as defined)	-
C_d	flow discharge coefficient	-
C_{do}	flow discharge coefficient of orifice	-
C_{dv}	flow discharge coefficient of valve	-
C_v	flow coefficient $C_v = \frac{Q}{C_1}\sqrt{\frac{\rho}{62.4\Delta P}}$	IGPM/psi
CPM	cycles per minute	-
CPS	cycles per second	-
D	mean diameter of orifice slot	in
e_q	error in flow rate	IGPM
F_o	initial force exerted by spring	lb_f
f	resonant frequency	CPM
f_c	corner frequency	CPM

f_n	undamped natural frequency	CPM
g	acceleration of gravity	ft/sec^2
g_c	Newton's Law conversion factor	$\frac{lb_f\text{-}sec^2}{lb_m\text{-}ft}$
K	constant (defined)	-
K_c	combined spring rate constant of bellows and springs	lb_f/in
K_d	damping coefficient in force balance equation	-
K_s	spring rate constant	lb_f/in
L_i	length of spring at X = 0	in
L_f	free length of spring	in
M	mass of moving parts of regulator	lb_m
M_p	height of resonant peak	-
m	subscript for mean value	-
P_1	inlet pressure	psig
P_2	pressure downstream of valve (or orifice)	psig
P_3	outlet pressure	psig
P_c	output pressure of controller	psig
P_t	differential pressure transmitter outlet pressure	psig
$\triangle P_o$	pressure drop due to initial spring tension	psi
$\triangle P_{or}$	pressure drop across the orifice	psi
Q	flow rate	GPM
Q_i	flow rate into regulator	IGPM
Q_m	measured flow rate	IGPM

Q_{max}	maximum flow rate through orifice	IGPM
Q'_{max}	maximum flow rate of control valve at 100% stroke	IGPM
Q_o	flow rate out of regulator	IGPM
$R_v(X_v)$	resistance of valve	psi/IGPM
S	complex frequency	radians/sec
T	time	min
T_L	time constant of transmission lag	sec
t	time	sec
V	volumetric flow rate	ft^3/min
V_o	volume of bellows assembly at X = 0	ft^3
V_b	volume of bellows at time t	ft^3
W	width of orifice slot	in
W_i	mass flow rate of fluid into regulator	lb_m/min
W_o	mass flow rate of fluid out of regulator	lb_m/min
w	frequency	radians/sec
w_n	undamped natural frequency	radians/sec
X, x	stroke of regulator	as defined
X_v	stroke of control valve	in
σ, β, γ	variables as defined in the section on the analysis of a flow control loop	-
ζ	damping constant for quadratic lag	-
ϕ	experimental constant that satisfies the force balance	-
ρ	weight density of fluid	lb_m/ft^3

BIBLIOGRAPHY

1. Anderson, N., Instrumentation for Process Measurement and Control, Instruments Publishing Company, Pittsburgh (1964).

2. Beard, C. S., Control Valves, Instruments Publishing Company, Pittsburgh (1957).

3. Berry, W. R., Spring Design, Emmott & Company, Limited, London (1961).

4. Buckley, P. S., Techniques of Process Control, John Wiley & Sons, Inc., New York (1964).

5. Caldwell, W. I., Coon, G. A., and Zoss, M. Z., Frequency Response for Process Control, McGraw - Hill Book Company, Inc., New York (1959).

6. Campbell, D. P., Process Dynamics, John Wiley & Sons, Inc., New York (1958).

7. Cleaglske, N. H., Automatic Process Control for Chemical Engineers, John Wiley & Sons, Inc., New York (1956).

8. Considine, D. M., Process Instruments and Controls Handbook, McGraw - Hill Book Company, Inc., New York (1957).

9. Del Toro, V. and Parker, S. R., Principles of Control Systems Engineering, McGraw - Hill Book Company, Inc., New York (1960).

10. Oberg, E. and Jones, F. D., Machinery's Handbook, The Industrial Press, New York (1959).

11. Oldenburger, R., Frequency Response, The MacMillan Company, New York (1956).

12. Truxal, J. G., Control Engineers' Handbook, McGraw - Hill Company, Inc., New York (1958).

13. Young, A. J., An Introduction to Process Control System Design, Longmans, Green and Company, London (1955).

ANALOG SYMBOLS

Figure 49

INTEGRATING AMPLIFIER

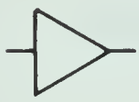

SUMMING AMPLIFIER

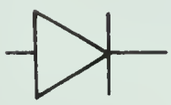

DIODE

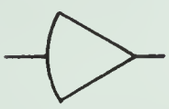

AMPLIFIER

RESISTOR

POTENTIOMETER

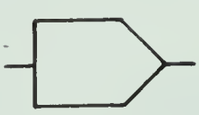

MULTIPLIER

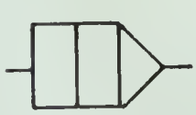

FUNCTION GENERATOR

SWITCH

APPENDIX A

List of Equipment

ITEM	MANUFACTURER	SERIAL NO.	REMARKS
Pump	-	-	Capacity 10 IGPM @ 160 psig
Differential Pressure Transmitter	Foxboro Co. Limited	M 71973	Range: 0 - 600" H_2O Accuracy: $\pm$0.5% of full scale
Pressure Indicators	Jas. J. Marsh Corp.	-	
PI-1			0 - 160 psig
PI-2			0 - 30 psig
PI-3			0 - 10 psig Accuracy: $\pm$1.0% of full scale
Recorder	Foxboro Co. Limited	-	-
Small Rotameter, R1	Fischer & Porter Ltd.	M6-1718/2	Range: 0.2 - 1.6 IGPM
Larger Rotameter R2	Fischer & Porter Ltd.	-	Range: 1.0 - 8 IGPM
Weigh Scale	Fairbanks	C 70898	Capacity: 500 lbs.
Timer	Precision Scientific Company	-	Accuracy: 0.01 minutes